THE EVALUATION OF POTENTIAL IMPROVEMENTS OF BARTON POT OXIDES FOR LEAD ACID BATTERIES

BY

LAURENCE THOMAS GEYER

STUDENT NUMBER : 20140150

A dissertation submitted to the Faculty of Applied Science,

Port Elizabeth Technikon, in partial fulfilment of the requirements

for the degree of

MASTER OF TECHNOLOGY
(CHEMISTRY)

Promoter : Mr E. E. Ferg

Abstract

Lead Oxide (PbO) is the main material used for the preparation of the active material for the positive and negative electrodes in the lead acid battery where the electrochemical reaction that provides the electrical energy of the battery takes place. The particle size distribution and surface area characteristics of the lead oxide play a major role in the electrical performance of the completed battery. The two most commonly used processes to manufacture PbO in the lead acid battery industry are the Barton pot and the Ball mill processes. These two processes produce oxides that differ in particle size distribution, particle shape and surface area. It is generally accepted that the Ball mill process produces an oxide with a smaller mean particle size with a higher surface area and better initial electrical performance than the Barton pot process to the detriment of an initial higher capital and running cost.

The study showed that it is possible to improve the surface area and particle size distribution characteristics of Barton pot oxide, by subsequently hammer milling the oxide particles before the paste manufacturing process.
The results showed that there was an initial reduction in the particle size with an increase in the surface area. This increased the electrochemical performance in terms of the high rate discharge. However, further hammering of the oxide reduced the average particle size only slightly with little change in the surface area and a reduction in the electrochemical performance.

The study showed that an improvement in Barton pot oxide can be achieved with a hammering of the oxide in order to obtain a uniform particle size with improved surface area and an improved high rate performance of the electrochemical cells made with such an oxide.

As a comparison, the particle size and surface area characteristics of Ball mill lead oxide subjected to the hammer milling process was also studied. The results showed a similar effect to the Barton pot oxide on the particle size distribution. However, there was no appreciable change in the surface area due to the hammer milling process.

Acknowledgments

The Author would like to thank the PETMRC and the NRF for the financial support for this project. The support received from the PE Technikon Chemistry department and from my promoter Mr E Ferg is appreciated.

Thanks to Willard Batteries and SABAT batteries for the supply of oxide samples and battery assembly materials.

Related publications by the Author

Part of this work was presented as a poster at the 36th Convention of the South African Chemical Institute in Port Elizabeth from 1-5 July 2002

L.T. Geyer, E.E. Ferg, Improvement of Barton pot lead oxide for automotive lead acid batteries, J. Power Sources, submitted.

Declaration

I hereby declare that this dissertation is my own, unaided work. It is being submitted for the degree of Master of Technology (Chemistry) at the Port Elizabeth Technikon. It has not been submitted before for any degree or examination in any other University or Technikon.

L. T. Geyer

Table of contents

List of abbreviations

SLI	Starting, lighting and ignition
T3	Tri-basic lead sulphate
T4	Tetra-basic lead sulphate
MBS	Mono-basic lead sulphate
PE	Polyethylene
PVC	Polyvinylchloride
UPS	Uninterrupted power supply
MCL	Miners cap lamp
AGM	Absorptive glass mat
VRLA	Valve regulated lead acid
A	Amps
h	Hours
Ah	Ampere hours
V	Volts
C_{20}	Twenty hour capacity
^{o}C	Degrees Celsius
%	Percentage
DOD	Depth of discharge
RSL	Refined soft lead
MMD	Mass mean diameter
BET	Brunauer, Emmett and Teller
SSA	Specific surface area
SEM	Scanning electron microscope

Chapter 1
Overview

1.1 Introduction

Lead oxide (PbO) is the main starting material for the manufacture of the active material in the lead acid battery. The active material is where the chemical reaction with sulphuric acid takes place to produce electrical energy. Lead oxide is made by reacting molten lead with the oxygen that is present in air, as shown in equation 1.

$$2Pb + O_2 \;?\; 2PbO \qquad (1)$$

In a typical medium sized battery manufacturing facility that produces 6000 to 7000 automotive batteries per day, PbO is produced at a rate of 800 – 1000 kg per hour using 3 - 4 lead oxide mills that are capable of producing between 50 - 70 tons of PbO per day. Since the quality of the electrode depends on the PbO produced, this process is extremely critical in the battery manufacturing process and often limits the consistency of producing a high quality battery.

The two most common manufacturing methods used to produce lead oxide powder in the lead acid battery industry are the Barton pot process and the Ball mill process[1]. In the Barton pot process, molten lead is poured into a reactor vessel. A rotating paddle agitates the lead to maximise the exposure of the lead to the air. The lead reacts with the oxygen in the air to form lead oxide. The lead oxide powder is removed from the reactor vessel using an air extraction system into a cone shaped silo where it is stored before further processing.

In the Ball mill process, solid balls of lead are fed into a rotating reactor vessel. As the balls of lead rub against each other, friction causes the lead balls to heat up. The lead reacts with oxygen to form lead oxide, which is removed from the reactor vessel using air suction.

The lead oxide powder produced by these two processes differs in their shape, reactivity, particle size, surface area and phase composition. In general the lead acid battery industry would aim at maximising the oxide production rate while maintaining a consistent oxide quality that has a small particle size with a high surface area. This, in turn, will produce an electrode with repeatable electrical performance.

In general the Ball mill process produces lead oxide that has a smaller particle size and higher surface area than that of the Barton pot process[1,2,3]. However; the Barton pot process has a lower initial capital cost for the company. The process is also more energy efficient and is cheaper to operate[1]. If an industry had initially started with the Barton pot process, it would be extremely costly and impractical to change to the Ball mill process if only a finer oxide is required. Other factors such as the increased running costs of the Ball mill process would also have to be taken into account.

1.2 Aim

The aim of this study was to investigate the possibility of improving the physical characteristics of lead oxide produced by the Barton pot process. It is desirable to produce an oxide with a consistent smaller particle size and a higher surface area. This was done by passing the lead oxide through an additional grinding step, before being used for further manufacturing. The study considered the following:

1. The change in particle size and surface area of the standard Barton pot oxide by repetitive grinding through a laboratory scale hammer

mill. As a comparison the effect of this hammering process on Ball mill oxide was also investigated.

2. A comparison of the physical and chemical characteristics of the Barton pot and Ball mill oxide after subjecting it to repetitive grinding in a hammer mill.
3. The electrochemical performance of a flat plate positive electrode made with the Barton pot oxide that was subjected to different degrees of grinding.

1.3 The basic process of lead - acid battery manufacturing

The electrochemical principles of the lead-acid battery system was discovered more than one hundred years ago by Planté[4]. Since then, many developments in the manufacturing technology, covering a range of materials, have occurred that have made the lead acid battery one of the most versatile and cost effective energy storage devices available.

The lead acid battery derives its name from the fact that the basic components making up the battery are lead and sulphuric acid. When compared with other energy storage devices, the cost of the raw materials used to manufacture lead acid batteries is relatively low. This has allowed the lead acid battery to remain competitive against other battery technologies in terms of cost per unit of energy. On the environmental side, the lead acid battery industry has over the years developed one of the best recycling systems to recover the lead from spent batteries. There is presently an efficient recycling system in place whereby spent batteries are returned to the manufacturer when they are replaced with a new one. From these spent batteries, approximately 95% of the lead can be recovered, where the lead is purified, and then reused to manufacture lead for the battery industry[5,6]. This has resulted in there being very little contamination of the environment from spent batteries, and in particular, lead.

The basic manufacturing process of the lead acid battery is given pictorially in figure 1

Figure 1 : Pictorial overview of the lead acid battery process

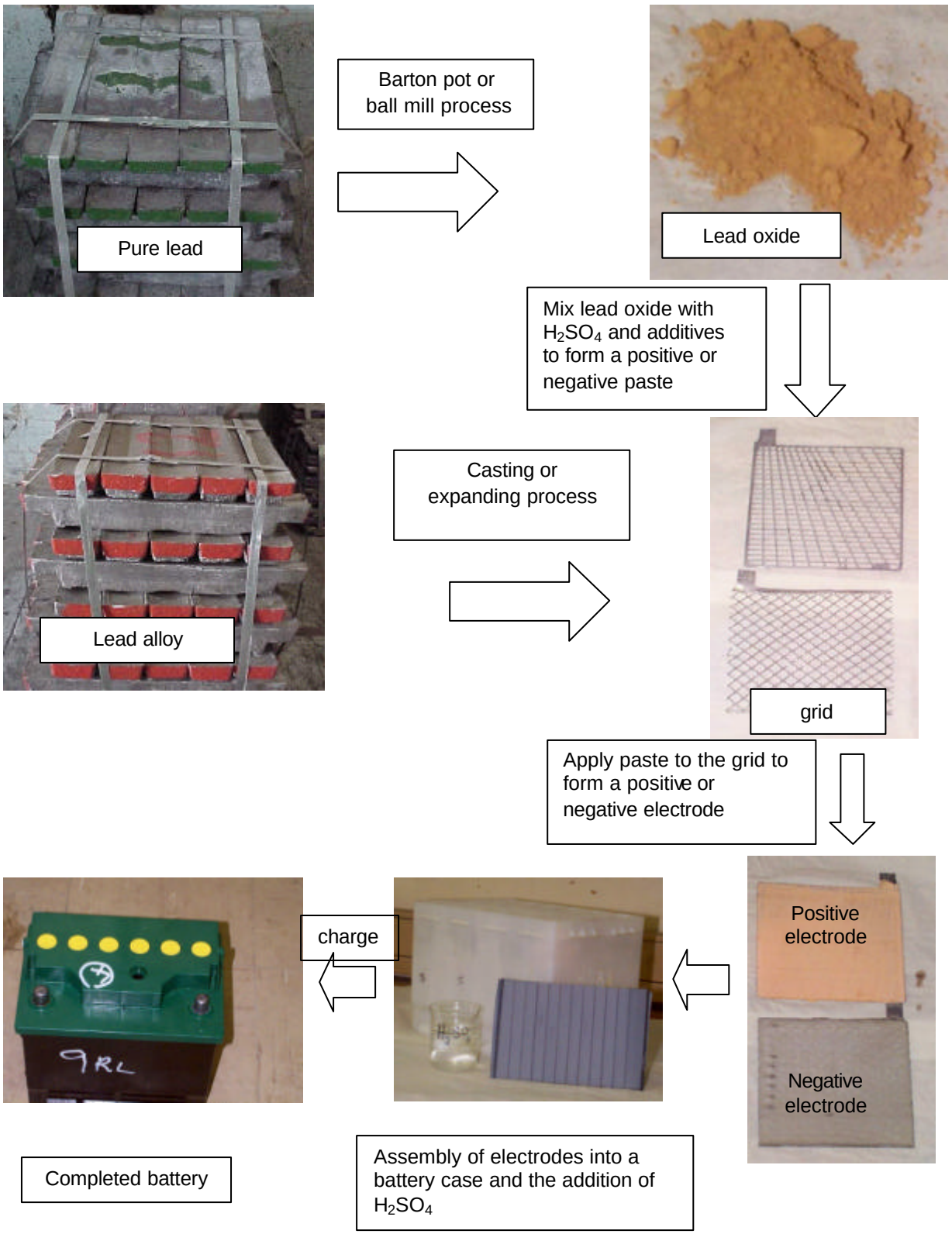

A brief description of the various processes is outlined below.

1.3.1 Lead oxide manufacturing

Pure Lead at various purity levels (99.97%, 99.99% or 99.999%) is converted into lead oxide powder in the presence of air in a reactor vessel that uses either the Barton pot process or the Ball mill process (equation 1). The lead used is either recycled lead from spent batteries or virgin lead obtained from a mining process. A more detailed explanation of this process is provided in chapter 3.

1.3.2 Grid manufacturing

A lead alloy is used to form the positive and negative electrode supporting current collector called a grid. This is done by using, either, a grid casting, continuous casting, or an expanded metal process. The lead alloy usually contains small amounts of either antimony or calcium and tin to provide hardness to the grid structure. Additional alloying elements like Cu, Se, S, As, Ag are often added to improve grid castability and to provide the necessary characteristics for extending the grid's durability. The main function of the grid is to support the active material and to act as a current carrier for the electrical energy when the battery is charged and discharged.

1.3.3 Plate manufacturing

The lead oxide powder is mixed with dilute sulphuric acid and various additives to form either a positive or negative paste. This active material is then pressed into the grid to form the positive or negative electrode or plate. The electrodes are then placed into a high humidity curing chamber where the active material develops the correct crystal structure, surface area and porosity. The active material also develops the necessary strength during the curing process to enable them to be

handled in the battery assembly process. The chemical equations that occur during the curing process are as follows[7].

$$PbO + H_2SO_4 \rightarrow PbSO_4 + H_2O \quad (2)$$

$$PbSO_4 + 3PbO \rightarrow 3PbO.\ PbSO_4 \quad (3)$$

$$PbSO_4 + 4PbO \rightarrow 4PbO.\ PbSO_4 \quad (4)$$

$$2Pb + O_2 \rightarrow 2PbO \quad (5)$$

$3PbO.\ PbSO_4$ = Tri-basic lead sulphate also known as T3
$4PbO.\ PbSO_4$ = Tetra-basic lead sulphate also known as T4

In general battery manufacturers would prefer the formation of tri-basic lead sulphate (T3) crystals for automotive battery applications. The properties of T3 crystals are that they form the skeletal structure of the final formed active material and are smaller and are easily converted to the formed PbO_2 phase[8]. In certain applications the formation of T4 crystals are preferred which are larger and create a much stronger electrode that has better capacity cycling ability[9].
The final cured material gives the skeletal structure that gives the mechanical strength for the electrode to be handled during battery assembly and during its electrochemical application.

1.3.4 Battery assembly

The positive and negative electrodes are assembled into cells and are separated by using porous separators made from polyethylene (PE), paper, polyvinylchloride (PVC) or rubber. The positive and negative electrodes are connected in parallel to form a cell group. The electrode's thickness, size and their numbers per cell depend on the energy and power specifications and application of the battery. This is usually calculated by considering the theoretical energy density of the

active material present. By increasing the number of plates in the battery an increase in the energy output is achieved. By increasing the number of cells in series, the power output of the battery is increased. The lead acid battery cell has a nominal voltage of 2V and, in a typical automotive battery, six cells are connected in series to produce a 12 volt battery. Polypropylene or polycarbonate plastic is usually used for the housing container of the battery.

1.3.5 Battery formation

Dilute sulphuric acid is added to the cells followed by an electrical charge in order to polarize the electrodes. During this process lead dioxide is formed at the positive electrode and lead, also known as sponge lead is formed at the negative electrode.

The formation reaction equations are as follows[7]:

Positive electrode

$$3PbO.\,PbSO_4 + 3\,H_2SO_4 \rightleftharpoons 4\,PbSO_4 + 3\,H_2O \quad (5)$$

$$PbSO_4 + 2H_2O \rightleftharpoons PbO_2 + H_2SO_4 + 2e^- + 2H^+ \quad (6)$$

Negative electrode

$$3PbO.\,PbSO_4 + 3\,H_2SO_4 \rightleftharpoons 4\,PbSO_4 + 3\,H_2O \quad (7)$$

$$PbSO_4 + 2e^- + 2H^+ \rightleftharpoons Pb + H_2SO_4 \quad (8)$$

The final stage of the battery manufacturing process involves the cleaning, labelling and an electrochemical performance test.

1.4 The lead-acid battery as a preferred motor vehicle battery

The lead acid battery is still considered as the preferred battery technology for automotive battery applications even though it has a number of disadvantages.

- Lead is a very heavy metal, which makes the final product's mass comparatively high.
- Another disadvantage is that approximately one third of the battery mass is made up of non energy producing parts such as the grids, posts and connectors that are also made of lead. These are merely current carrying conductors that have about 16 times the resistivity of copper[5]. Attempts have been made to replace the current collectors with other types, but none have proven to be commercially successful.
- Lead is also toxic which means that costly environmental control measures are needed to ensure a safe manufacturing and supply environment.
- The lead acid battery contains corrosive sulphuric acid that can cause damage or injury if the battery housing leaks or breaks.
- The lead acid battery produces an explosive mixture of hydrogen and oxygen gas during charging which can lead to an explosion when exposed to a naked flame or spark.

However the advantages of the lead acid battery system outweigh the disadvantages.

- Lead is relatively inexpensive when compared with other metals used for battery manufacturing[5].
- Lead is easily smelted (the melting point of lead is about 330^{o}C) [4].
- Lead is easily recyclable[5].
- The lead acid battery has one of the highest cell voltages when compared with other battery types.

In terms of the cost/unit energy, there is currently no other battery type that can compete with the lead acid battery[10]. The lead acid battery can also be used in many diverse applications, from small portable miners cap lamp batteries to large UPS cells that are able to deliver large amounts of capacity and power.

This has resulted in the continued competitiveness of the lead acid battery as a renewable source of energy in the global market today.

Chapter 2

Technological advances in the lead acid industry

Advances in the lead acid battery used in automotive applications are to a large extent driven by the manufacturers of new motor vehicles. As the electrical requirements for new motor vehicles change, greater demands are required from the battery in terms of performance at a competitive cost per unit. This requires the battery manufacturer to continually improve the manufacturing processes and to use advanced materials to make a battery.

An example is the requirement to decrease the size of the engine compartment in modern vehicles. This resulted in the need for smaller sized batteries to deliver the same performance with a lower mass. However, the more compact engine compartment has resulted in a rise in the battery operating temperature, and in some cases specialised insulation of the battery from the heat generated by the engine is used.

There has also been an increase in the service intervals for motor vehicle owners. This has introduced the need for a low maintenance or maintenance free battery. The hazards associated with the corrosive electrolyte in a normal flooded type battery has led to the development of the valve regulated lead acid (VRLA) battery, where the electrolyte is immobilised in absorptive glass mat separators (AGM) or a silica gel[11]. Further developments in vehicle electric traction technology have led to the development of batteries that have an improved energy to weight ratio.

The following areas are considered by battery manufacturers to improve the performance of the application of the lead-acid battery. These are the energy and power density, life cycle ability, maintenance reduction,

VRLA technology, and materials and manufacturing process optimisation. Each of these points will be briefly discussed.

2.1 Improvement in energy density

The energy density of a battery can be classified as the number of amperes (A) that a battery can deliver over a period of time (h). In an automotive battery this is usually measured over a 20 h period at relatively low currents to a lower voltage limit of 10.5 V. For example, a 100 Ah battery should be able to deliver a current of 5 A for 20 h. This is referred to as the amp hour (Ah), or C_{20} capacity of a battery.

This test simulates low current applications in the vehicle like alarm systems, interior lights, parking lamps or radios when the engine is turned off. Since the discharge period is long and the current draw is low, the kinetics of the discharge reaction is relatively slow, and there is enough time for the acid to diffuse into the pores of the active material for the energy producing reaction to occur. In these types of applications a large percentage of the available active material on the electrodes can be utilised to deliver the required capacity.

According to Faraday's law, the theoretical amount of positive and negative active material required to produce 1 Ah of energy can be calculated. 4.463 g of positive active material (PbO_2) and 3.866 g of negative active material (Pb) is required to produce 1 Ah of electrical energy[4]. However, in practice only 45 to 55 % of the theoretical energy value is achieved in a battery. This implies that about twice the theoretical amount of active material is required to achieve a given capacity value.

Over the past few years, improvements in the energy density without compromising the battery's life cycle ability has been limited, and is largely governed by the equipment available to manufacture the battery. One example of improving the energy density was the use of thinner

electrodes. In order to do this, specialised equipment was needed to manufacture thinner grids and automated handling systems were developed to handle the more delicate electrodes without causing damage to them. The result was that less lead was used for the grids and that the energy to mass ratio of the battery (Ah/kg) was improved.

2.2 Improvement in Power density

The power density of a battery is defined as the maximum current that a battery can deliver over short periods of time at a given temperature. This simulates the starting or cranking of the vehicle engine. It is also called the crankability of the battery. Various international and specific customer specifications are used to evaluate the cranking ability of a battery (appendix II). It is normally done at low temperatures e.g. 0^{o}C, -18^{o}C, or -29^{o}C and high currents (150 – 500 A) to a specified cut-off voltage (6 V, 7.2 V, or 8.4 V) over a period of seconds (30 s, 60 s or 150 s). Due to the short duration and high current involved, the kinetics of the discharge reaction is largely dependent on the surface reaction of the acid with the electrodes and is limited by the diffusion rate of the acid into the active material[4]. Only a small portion of the active material is utilised in order to deliver the required power.

Improvements in the power density require an increase in the surface area and porosity of the active material in contact with the acid and a reduction in the internal resistance of the battery according to Ohm's law (V = IR)[11]. The increase in the surface area of the electrodes is achieved by reducing the thickness of the electrodes by using better manufacturing processes. This allows for more plates to be packed in the same cell space, thus increasing the overall surface area exposed to the sulphuric acid. For example, the thickness of the electrodes that was commonly used in automotive batteries in the 1950's was 5 mm compared with the 0.9 mm that is presently being used[13]. This was accomplished by improvements in grid casting and plate pasting technology.

The internal resistance of the battery was reduced by improving the separator material that is used between the positive and negative electrode. In the past, wooden, rubber, paper, or PVC separators were used[4]. The most common material that is currently being used for separators is microporous polyethylene. It has a very low electrical resistance and improvements in separator technology has enabled the production of thinner separator sheets with a high puncture resistance[14].

2.3 Improvement in life cycle capacity

The three main factors that determine the battery's life cycle capabilities are:

1) The operating temperatures (higher temperatures reduce life cycle).
2) The cycle duty (how many repeated discharges and charges the battery underwent at a certain depth of the discharge (DOD)).
3) The quality of the materials and manufacturing processes used to assemble the battery.

1) An increase in the battery's operating temperature results in an increase in the kinetics of the chemical reactions in the battery. This results in an increase in the corrosion of the lead components (grids and connectors), an increase in the water-loss due to electrolysis and an increase in the shedding of the active material. It is beneficial to ensure that the battery's operating environment is kept at a relatively low temperature. Some motor manufacturers have opted to place the battery in the boot of the car rather than under the bonnet. However; this requires the additional cost of longer high power cables. All energy-consuming devices in a car are rated in terms of power (watts). Since the battery voltage is fixed at 12 V, the use of high currents for starting would require thicker cables in order to sustain the load

Another method used by motor vehicle manufacturers to reduce the battery operating temperature is to install heat shielding devices around the battery.

2) The cycle duty of the battery was improved by the addition of special additives such as glass fibres to the positive electrode and to include the use of glass mat separators so that the active material adhesion to the grid is increased. State of health indicators on batteries were introduced to allow consumers to check the level of charge of the battery ensuring that the battery is kept at a maximum charge condition.

3) The improvement in manufacturing processes was achieved through the implementation of quality systems, improvement in the process technology and automation that has resulted in batteries of consistent quality. This has reduced the number of premature battery failures and increased the supply of a consistent product that would supply the capacity for a number of years.

2.4 Maintenance reduction

The water-loss or gassing of the battery occurs during the charging of the battery at a sufficiently high potential where water is electrolysed to produce oxygen at the positive electrode and hydrogen at the negative electrode. This requires that the water lost during operation would have to be replenished in the battery at various service intervals. The service was normally done outside the control of the battery manufacturer where there was little control over the purity of the water used, and the correct service interval chosen.

The water-loss in a lead acid battery increases when there is an increase in foreign metal species (that are not Pb) in the battery[12]. For example, Fe, Ni, Cu may come from impure water, and Sb from the grid alloy used to manufacture the positive electrode. Since the Sb content

in lead-acid battery grids can vary between 1 - 10% depending on the battery application, it plays a major role in the water-loss properties of the battery[15]. The Sb can dissolve into the acid electrolyte and migrate to the negative electrode where it would be electrochemically plated and contribute to the increase in hydrogen gassing. Improvements in grid casting and lead alloy technology has allowed battery manufacturers to reduce the antimony content in the lead alloy to below 1% in recent years.

The development of calcium lead alloys that uses calcium and tin eliminates the use of antimony completely. Today a car battery using a calcium lead alloy can operate without the need for replenishing the water for a number of years[16].

2.5 Valve regulated lead-acid batteries (VRLA)

The need for a completely maintenance-free battery in terms of having to replenish the lost water has led to the development of the valve regulated battery (VRLA). In this battery technology the H_2SO_4 is immobilised by containing it in an absorptive glass mat (AGM) separator or in a gelled silica system[17]. During battery charging the oxygen generated at the positive electrode passes through pores or cracks in the glass mat or gel and is consumed at the negative electrode (called recombination)[11].

The gases inside the battery are maintained at a relatively high pressure with the excess gas vented via a pressure valve. The immobilised electrolyte allows for the battery to be placed near sensitive electronic equipment without the problems of acid spills or the emission of dangerous gases.

However, due to the high cost of this type of battery in comparison to the conventional flooded type and the reduced ability to work under high temperatures, the use of this technology has been limited in motor vehicle (SLI) applications[18].

2.6 Materials and manufacturing process improvements

The global energy demand for storage devices with a high performance to mass ratio (lighter batteries with better performance) has forced battery manufacturers to look for improvements in every aspect of their business, in particular the use of raw materials. For example, the battery housings that were previously made from hard rubber were replaced by polypropylene. Besides the reduction in mass and cost, polypropylene has the additional advantage of being recyclable.

Expanded metal or continuous casting processes in the manufacturing of electrode grids are replacing the gravity cast process, where very thin electrodes can be produced at a much faster rate.

There is a legal requirement to monitor the concentration of Pb in the employee's blood and to maintain it below set levels. This has resulted in the improvement of the dust extraction systems in battery factories to provide a more environmentally friendly area for the employees.

The formation process of the battery is amongst one of the longest stages in battery manufacturing. It may take between 15 and 100 h to form an automotive battery depending on its size and capacity. In order to reduce the formation time, modern formation rooms use water-bath cooling processes combined with high charging currents.

This study will investigate the improvement of manufacturing the lead oxide in order to produce improved electrodes with better electrical performance.

Chapter 3

The lead oxide manufacturing process

The consistency of making a lead oxide with well defined physical properties is important in terms of obtaining the quality of the electrodes that will produce the necessary electrical performance in the battery. During the oxide manufacturing process, various properties of the oxide are carefully monitored to ensure that they comply within pre-determined specifications. These specifications include particle size, density, reactivity, surface area and free lead. The objective is to produce an oxide that has a relatively small average particle size within a narrow range of particle size distribution with a high surface area to provide the best reactivity with H_2SO_4.

The Barton pot and Ball mill processes manufacture a lead oxide that differs in their respective physical properties, and therefore also influence the characteristics of their final application differently. The differences between these two processes and their properties are explained as follows:

3.1 Barton pot process

The schematic in figure 2 shows the various components in the Barton pot process[19]. In the Barton pot process, pure lead ingots are fed into a lead melt pot [A] where the lead is liquefied. The molten lead is fed into the reaction vessel [B] through an opening in the top of the reaction pot [C]. This opening also allows for the air to enter the reaction vessel for the oxygen to react with the lead. The molten lead is agitated in the reaction pot using the stirring paddle [D] to increase the exposure of the lead to the air, and is oxidised to lead oxide (equation 1). To remove the lead oxide from the reaction pot, a suction air draft is created using the exhaust fan [E]. The force of the air draft is usually controlled by

opening or closing the vents in the system. This also allows for a steady stream of oxygen to flow into the reaction vessel and a suction force to remove the oxide powder from the reactor.

The oxide particles have to travel up the almost vertical exhaust duct [J] against the gravitational force in order to exit the reaction pot. This process acts as a particle size classification system [F]. Particles of certain sizes will have enough velocity to get to the top of the duct leaving the reaction vessel, whereas the larger size particles will return to the reaction vessel until they are small enough to be removed.

Figure 2: Schematic of a typical Barton pot process

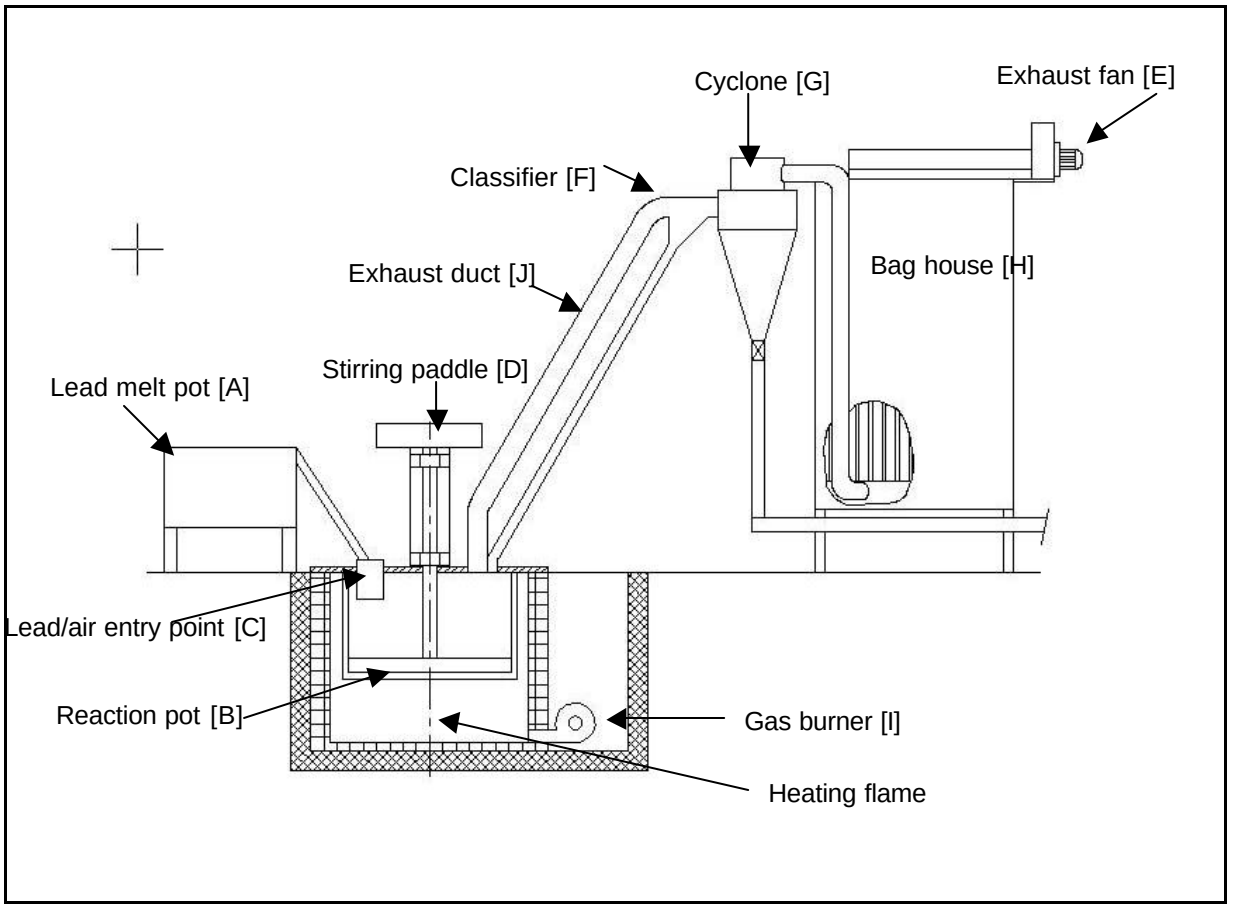

The cone shaped cyclone [G] causes a swirling action on the oxide. As the oxide hits against the walls of the cyclone it falls down into a screw conveyer which moves the oxide into silos where the final product is stored. The bag-house [H] acts as a filter to prevent any of the oxide from exiting the system and polluting the environment.

Initially, heat has to be applied to the reaction vessel using a gas burner [I], but once the exothermic oxidation reaction progresses, enough heat is normally generated to maintain a relatively consistent reaction temperature. The temperature of the reaction vessel can be controlled by adjusting the flow rate of Pb and air flow, or by the addition of water to the reaction vessel.

Since molten lead is added to the reactor vessel, this process is often called a high temperature process.

3.2 Ball mill process

The schematic in figure 3 shows the typical components of the Ball mill process[3].

In this process solid balls or slugs of lead are first cast using a ball caster [A]. The solid balls of lead are fed into a rotating reactor vessel [B]. As the balls of lead rub against each other, friction causes the temperature to rise. Air is introduced into the reactor vessel by creating a draft through the system by using an extractor fan [C] in a similar way as is done with the Barton pot process. The lead reacts with the oxygen in the air to form lead oxide, which is then removed from the reactor vessel using the extraction draft into a storage system.

Since solid lead balls are added to the reactor vessel, this process is often referred to as a low temperature process.

Figure 3: Schematic of a typical Ball mill process

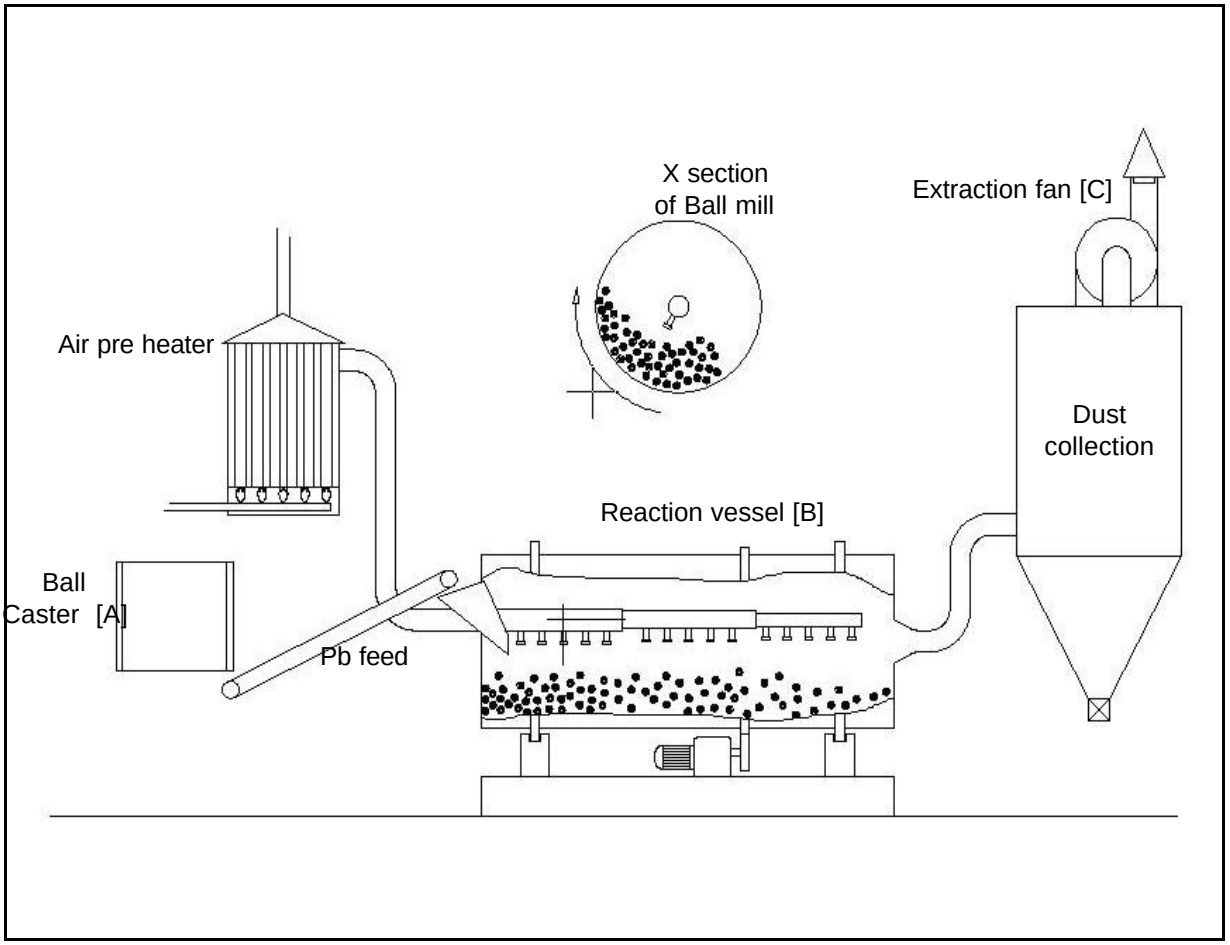

3.3 Lead resources for the production of lead oxide

The quality of lead used in the manufacturing of lead oxide is referred to as three nines (99.97%), four nines (99.99%) or five nines (99.999%). This depends on the level of purity that the manufacturer requires, which will influence the water-loss characteristics of the final battery. There are two main sources of pure lead also known as refined soft lead (RSL), available in the battery industry. The sources of lead are known as primary lead and secondary lead.

Primary lead is also referred to as virgin lead. This is lead that is mined as a Galena ore[4]. There are no lead mines in South Africa and all

primary lead has to be imported. The major source of primary lead in South Africa comes from China and Australia where the purity of the lead is normally 99.99% or 99.999%.

Secondary lead is also referred to as recycled lead and comes from the recycling of spent or used batteries. The lead is usually purified to a purity level of 99.97% by South African lead smelters. Improving the lead purity level further, required additional processes, which are more costly.

3.4 Typical pure lead specifications

Various independent bodies like ASTM and DIN have produced standards for lead to be used for the production of lead oxide. Due to the high cost of very pure standards, the lead smelting and battery industries have also developed lead specifications with a greater emphasis on the final product application. Table 1 shows a typical comparison of these lead standards[19].

Table 1: Comparison of pure lead standards

Chemical impurities in Pb (max allowed)			
	ASTM Wt %	**Flooded Battery Wt %**	**VRLA battery Wt %**
Antimony (Sb)	0.0005	0.001	0.0005
Arsenic (As)	0.0005	0.001	0.0005
Tin (Sn)	0.0005	0.001	0.001
Copper (Cu)	0.0010	0.0015	0.001
Silver (Ag)	0.0025	0.005	0.0025
Bismuth (Bi)	0.025	0.03	0.025
Zinc (Zn)	0.0005	0.001	0.001
Tellurium (Te)	0.0001	0.0005	0.00010
Nickel (Ni)	0.0002	0.0005	0.0002
Iron (Fe)	0.001	0.001	0.001
Cadmium (Cd)	-	0.001	0.001
Manganese (Mn)	-	0.0005	0.0001
Selenium (Se)	-	0.0005	0.001
Thallium (Tl)	-	0.01	0.01
Lead (Pb) By difference	99.97	99.97 – 99.99	99.99

One example of the lead smelting industry's initiative was the study of the effect of bismuth on battery performance. Bismuth is a naturally occurring element in mined lead and is often found in concentrations higher than the required standards. However, it is costly to remove in the lead purification process. Studies carried out on the effect of bismuth revealed that a certain level of bismuth is beneficial to battery performance[20]. This allowed the lead smelter to propose a product for the battery industry that had higher bismuth levels than what was previously tolerated[20].

3.5 The phases of lead oxide produced

The lead oxide produced by either of the two processes described previously consists of three components in varying proportions. They are α-PbO, β-PbO and free lead.

a) a-PbO

The crystals of α-PbO are tetragonal in shape and are often referred to as Litharge or as the red modification due to its reddish colour[4].
This is the preferred form of the oxide due to its smaller crystal size and its ease of conversion to the sulphate phase[1]. It is formed at temperatures below 480^{o}C[1] .

b) b-PbO

The crystals of β-PbO are orthorhombic in shape and are often referred to as Massicot or the yellow modification due to its yellowish colour[1].
This phase is formed at temperatures above 480^{o}C and tends to promote the formation of larger crystals in the cured plate which may lead to reduced battery performance[1,26].
Even though the reaction vessel is usually kept below 480^{o}C, localized temperature effects may cause the formation of β-PbO especially in the Barton pot process. It is generally accepted in the battery industry that a maximum of 15% of β-PbO is allowed[1]. Only very small amounts of β-PbO are produced in the Ball mill process where the friction process has minimal localized high temperature effects.

c) Free lead

This is some of the finely divided un-oxidised lead that remains in the lead oxide powder. About 25 – 35% of the oxide is “free lead” and is an important component for the subsequent curing process in which the

lead is then oxidized into PbO and the formation of either T3 or T4 crystals in the high humidity curing process[21]. The curing process is an important process in developing the “cementing” properties of the active material to the grid to form a physically strong electrode.

3.6 Lead oxide Characteristics

Since lead oxide is the main starting material in the manufacturing process of the lead acid battery, variations in lead oxide quality could result in variations in the electrical performance of the final product. It is therefore important for a manufacturing process to consistently produce a good quality lead oxide within specified physical parameters.

During the lead oxide manufacturing process, certain tests are performed to determine its characteristics, and are often specific to the lead acid battery industry. All these tests usually relate to the particle size, surface area and reactivity of the oxide. These characteristics are the free lead, the apparent density, the acid absorption number, the particle size distribution and the surface area.

3.6.1 Free lead (%)

The free lead is an important element that is used to control the lead oxide manufacturing process. The free lead percentage is usually determined by the mill operator on an hourly basis, and adjustments are made to the oxide mill controls accordingly. A simple wet chemistry technique is used whereby a sample of lead oxide is dissolved in a 5 % solution of boiling acetic acid[22]. The residual free lead is removed, dried, and determined as a percentage of the original lead oxide sample. The detailed test method is provided in appendix II.

3.6.2 Apparent density (g/ inch^3)

This test gives an indication of the particle size of the oxide and is also known as the Scott number[22]. A sample of lead oxide is allowed to fall into a 1 inch^3 cup along successive angled glass slides that are mounted in a cylindrical box. Small particles will give a lower value than larger particles[22]. This technique was developed uniquely for the battery industry as a cheap and quick method of achieving particle size information. This test is often carried out at the lead oxide mill by the operator. Variations in apparent density will have an impact on the paste mixing and curing reaction. The apparatus used to determine the apparent density is shown in appendix II (fig 38).

3.6.3 Acid absorption number (mg H_2SO_4/g PbO)

The acid absorption test is done to determine how fast the oxide will react with dilute sulphuric acid. The results are expressed in milligrams of acid per gram of oxide[22].

The acid absorption number relates to the particle size and surface area of the oxide. The larger the number, the more reactive the lead oxide will be. If there are large variations in the acid absorption number during lead oxide manufacturing, the paste mixing process would become inconsistent. The rate of acid addition in the paste mixing process is usually pre-determined according to the system's ability to control the temperature rise during paste mixing. If the oxide quality is not consistent, variations in the paste quality and final electrode quality would result.

3.6.4 Particle size analysis (μm)

There are a number of methods to determine the particle size distribution of dry powders. Some methods are relatively quick and simple to use in a production environment, while others are more complex and require expensive equipment.

Some of the techniques are:

a) Fisher particle size analysis
b) Retention on a 45 μm mesh
c) Laser diffraction particle size distribution

a) Fisher particle size

This is a relatively simple method that measures the average particle size of a sample of oxide using the air-permeability principle. This principle employs the fact that particles in the path of a regulated air flow will affect that air flow in relationship to their size. The lead oxide sample is placed into a sample tube, compacted with a set torque and placed in the path of a regulated air flow. The flow of air through the oxide sample is measured by means of a calibrated manometer and the average particle size is determined. A typical lead oxide would have a Fischer particle size of 2 μm. The apparatus used for this determination is pictorially shown in appendix II (fig 39).

b) Retention on a 45 μm mesh

This method measures how many lead oxide particles are larger than 45 μm. This is a simple and quick method where a value of less than 5% is desired in the manufacturing process.

c) Laser diffraction particle size distribution

This is a more sophisticated method using laser diffraction to determine the particle size distribution over a wide range of particle size. A sample of lead oxide is usually dispersed in water as the medium and the particle size distribution is calculated using an algorithm that assumes that all particles are spherical in shape and a distribution of size is obtained. The results of the mass median diameter (MMD), the volume mean diameter and the surface area mean diameter (Sauter mean) are calculated.

3.6.5 Surface area analysis

The most widely used method to determine the surface area of lead oxide in the battery industry is the BET surface area nitrogen adsorption method. In this method the sample of lead oxide is cooled to liquid nitrogen temperatures. Nitrogen gas is passed through the sample and the amount of nitrogen that adsorbs onto the surface of the lead oxide is measured. The BET surface area is determined by measuring the monolayer amount of nitrogen adsorbed on the surface of the particles.

3.7 Comparison of Barton pot and Ball mill lead oxide

The Barton pot and Ball mill processes produce an oxide that differs in particle size, shape and physical properties. A narrow particle size distribution is preferred since this allows for a consistent reaction of the oxide with H_2SO_4 in the paste mixing process to develop the required crystal structure in the active material. The particle size distribution range does not only depend on the process used, but also on the process control that is exercised during the lead oxide manufacturing. Older oxide mills tend to have less sensitive controls and as a result an oxide with a wider particle size distribution range is often produced.

During the manufacturing process, in order to obtain a consistent particle size, a slower production rate is often required. This in turn reduces the amount of material produced and the number of batteries that can be built in a particular day.

Table 2 shows a comparison of some of the properties of oxide made using the Barton pot and Ball mill oxide processes [1,2,19,23,24,25].

Table 2: Comparison of Barton pot and Ball mill oxide

	Barton pot	Ball Mill
Particle shape	Rounded	Flatter
Average BET surface area (m^2/g)	0.7	2.5
Acid absorption No (mg H_2SO_4 / g PbO)	150 – 200	200 – 250
Average particle size (µm)	3 – 4	2 – 3
Free lead (%)	18 – 28	25 – 35
Oxide crystal structures (wt%)	5 – 30 % ß-PbO Balance a-PbO	100% a-PbO
Paste mixing Characteristics	Makes a softer paste that is easier to paste	Makes a stiffer paste that may require careful control
Paste curing	Average curing rate	Slightly faster curing rate
Batter performance	Lower initial capacity	Good initial capacity
Deep cycle ability	Usually good	Sometimes good
Investment considerations	Lower initial and operating and maintenance costs, compact in size, relatively quiet to run	Higher initial, operating and maintenance costs. Requires more space and is noisier

3.8 Hammer milling Barton pot oxide

The objective of this study was to investigate the possibility of improving the physical properties of Barton pot oxide by increasing its surface area and reducing its particle size. This was done by passing the oxide through a hammer mill after it was made by the Barton pot process and before it was transported to the paste mixer.

The process of hammer milling Barton Pot oxide is not new. Early Barton pot oxide mills produced a very course oxide which resulted in electrode manufacturing problems and excessive active material shedding[22]. To solve this problem the oxide was passed through a hammer mill in order to make it more usable. This practice was later discontinued as technology improvements such as more sensitive

detection and control devices as well as computer aided control systems in the Barton Pot process allowed for the production of a finer oxide[22].

With the ever increasing requirement for improved battery performance and the need for greater production output, this hammer milling process can offer a solution to further improving the consistency of oxide particles with a higher production rate.

Chapter 4
Experimental

4.1 Hammer milling of oxide

A laboratory size hammer mill (micro hammer mill “Culatti” type 5) was used to grind the lead oxide. The specifications of the hammer mill are given in appendix I.

Lead oxide, made by using the Barton Pot process was received from a local battery manufacturer and ground by repeatedly passing it through the hammer mill. This was done about 20 times, with samples taken at selected intervals to determine the change in the following characteristics:

a) Particle size distribution analysis by laser diffraction using a Malvern particle size analyzer (model MSS).
b) BET surface area analysis by nitrogen adsorption using a Micrometrics BET analyser (model Gemini).
c) Free lead analysis by using a standard wet chemistry method used in the battery industry (appendix II).
d) Acid absorption number by using a standard method used in the battery industry (appendix II).
e) The particle size and shape were studied using an Olympus optical microscope (model PMG3) and a Phillips scanning electron microscope (SEM) model (XL30).
f) Phase composition analysis by XRD using a Brucker model (D8 advance) diffractometer.

These experimental techniques were discussed in section 3.6.

As a comparison, oxide made by a Ball mill process was acquired from a different battery manufacturer and was also milled 20 times and evaluated in the same way as the Barton pot oxide.

4.2 Evaluation of positive electrode electrical performance

Positive electrodes were made with the milled oxide taken at selected intervals and the electrical performance of the cell was evaluated. The lead oxide (300 g) and a binder (0.3 g supplied by a local battery manufacturer) were mixed with water (35 ml) in a container using a bench top stirrer. Sulphuric acid (24 ml, 1.4 S.G.) was slowly added to the mixture over a 15-20 min period using a burette while the mixture was continually stirred to form a stiff paste. This paste was pressed onto a lead alloy grid to form a pasted positive electrode. The grid size used was the XLTP type Pb-Ca alloy which had a Ca composition of 0.05%.

The electrodes were cured by placing them into a high humidity chamber set at 22^{o}C and a humidity of 85% for 24 hours. The plates were then allowed to air dry to develop the optimum strength for a further 24 hours. The active material mass of the cured plate was determined and found to be between 65 and 70 g per single plate. The rated C_{20} capacity of 9 Ah per positive plate was used as specified by the local battery manufacturer for this plate type. Single battery cells were assembled using one positive plate and two negative plates, which were separated by a polyethylene envelope separator. The negative plates were supplied by the local battery manufacturer and were the XLTN expanded metal Pb-Ca alloy negatives with a Ca composition of 0.1%.

The formation process was done by filling the cells with 1.240 S.G. sulphuric acid which was supplied by the local battery manufacturer and formed at ambient temperature using 44 Ah ($5C_{20}$) of energy. Since the positive plate was rated at 9 Ah, a total Ah input of $5C_{20}$ was used to form the cells as is commonly used in the battery industry.
The theoretical number of Ah required to form a cell is 227 Ah/kg[7]. On average, the positive plates contained 70 g of active material which

meant that 632 Ah/kg (2.8 times the theoretical value) was used to form the cells in practice.

All formation and electrochemical evaluation tests were done using the Maccor series 2000 battery tester.

The formation profile was done using the steps shown in table 3:

Table 3: Formation program for 9 Ah cells

Mode	Current	Hours	Ah
Rest	0	0.33	0
Charge	1.75	20	35
Charge	1.2	7.75	9.3
Total		**28.08**	**44.3**

After the formation process the electrical performance of the cells was evaluated by determining the energy density. The cells were discharged at 0.45 A until the voltage reached 1.75 V. The Ah capacity measured was converted to Ah/kg by dividing by the mass of the active material. The cells were then charged at a voltage of 2.67 V with a current maximum of 2 A for 24 h. Five of these capacity tests were done.

The power density was determined by discharging the cells at 10 A, 20 A and 40 A at ambient temperature until the voltage reached 1.2 V. The result in Ah was converted to Ah/kg by dividing by the cured active material mass. The cells were then recharged at 2.67 V with a current maximum of 2 A for 20 h.

Chapter 5
Results and discussion

5.1 XRD phase analysis of lead oxide

The XRD phase analysis results of the lead oxide from the Barton pot and Ball mill processes before the hammer milling process is shown in table 4.

Table 4: XRD phase analysis results

	Barton pot	Ball mill
a- PbO (%)	79	100
ß- PbO (%)	21	-

The results showed that the Ball mill oxide contained no ß-PbO. The reason for this is the lower temperature at which the Ball mill operates and is in line with what was reported in the literature[2].

5.2 Particle size distribution by laser diffraction

5.2.1 Barton pot process

The effect of repeatedly passing a sample of PbO made using the Barton pot process through the hammer mill and its influence on the particle size distribution is shown in figure 4.

Figure 4: Particle size distribution of Barton pot oxide

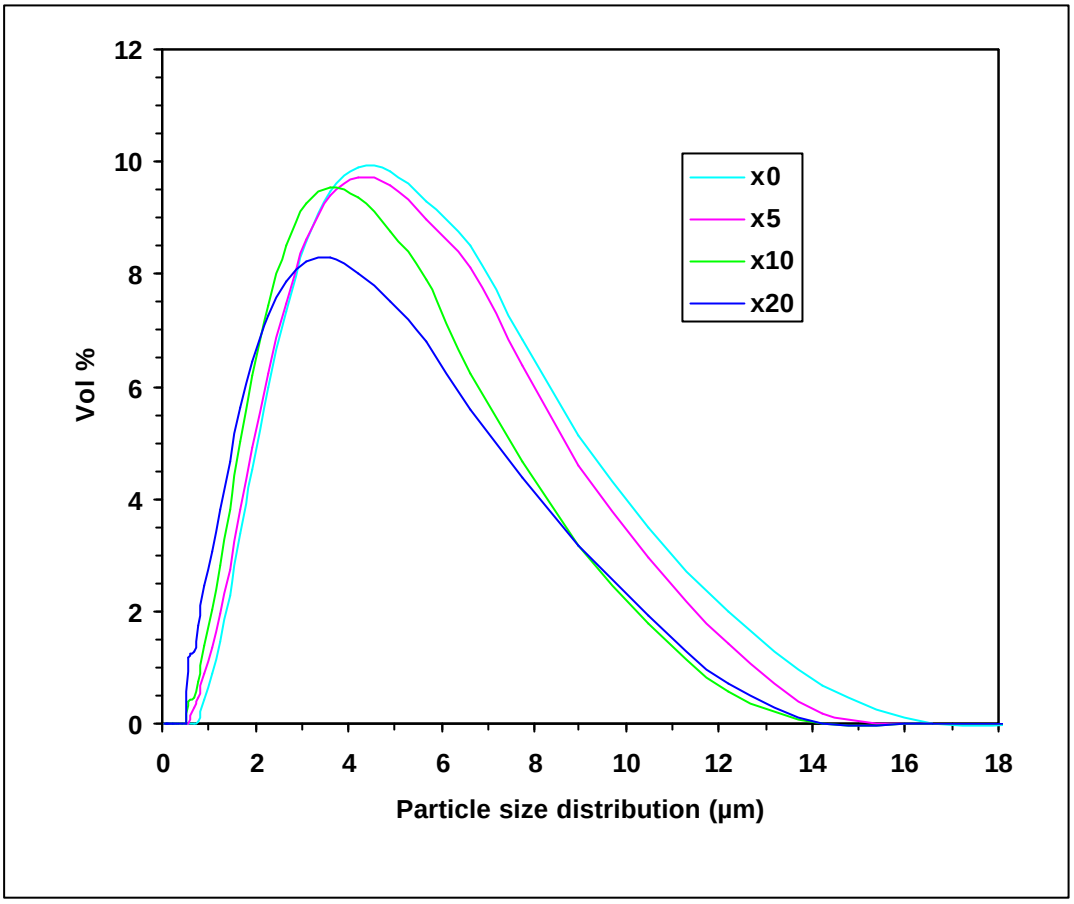

x0 :Not passed through the hammer mill
x20 :Passed 20 times through the hammer mill

The oxide, as received from the manufacturer, before being subjected to the hammering process showed a modal diameter (most commonly occurring particle size) of 5 µm. The effect of repeatedly passing the oxide through the hammer mill resulted in a reduction of the modal diameter from 5 µm to 3 µm. There was also a decrease in the frequency of the modal diameter as the sample was hammered. This was due to the fact that as the larger particles were reduced in size and the particle size distribution curve shifted towards the finer particle size. During the first 5 passes through the hammer mill, the particle size distribution range shifted from 0.8-17 µm to 0.7-15 µm. However, from 10-20 passes through the hammer mill, the overall particle size range remained between 0.5-14 µm.

The biggest change in the particle size distribution range occurred during the first few passes through the hammer mill. There was no significant change in the particle size distribution range after 10 passes through the hammer mill. Only a change in the frequency within the particle size distribution range was observed. This would imply that there is an initial reduction in the particle size range after which a limit is approached and the rate of change becomes slower.
Additional graphs of repeated experiments are shown in Appendix III (figures 40 and 42) and showed very similar trends.

The 3D view of the particle size distribution curve is shown in figure 5 where the shift in the modal diameter is more clearly visible.

Figure 5: Particle size distribution – 3D view

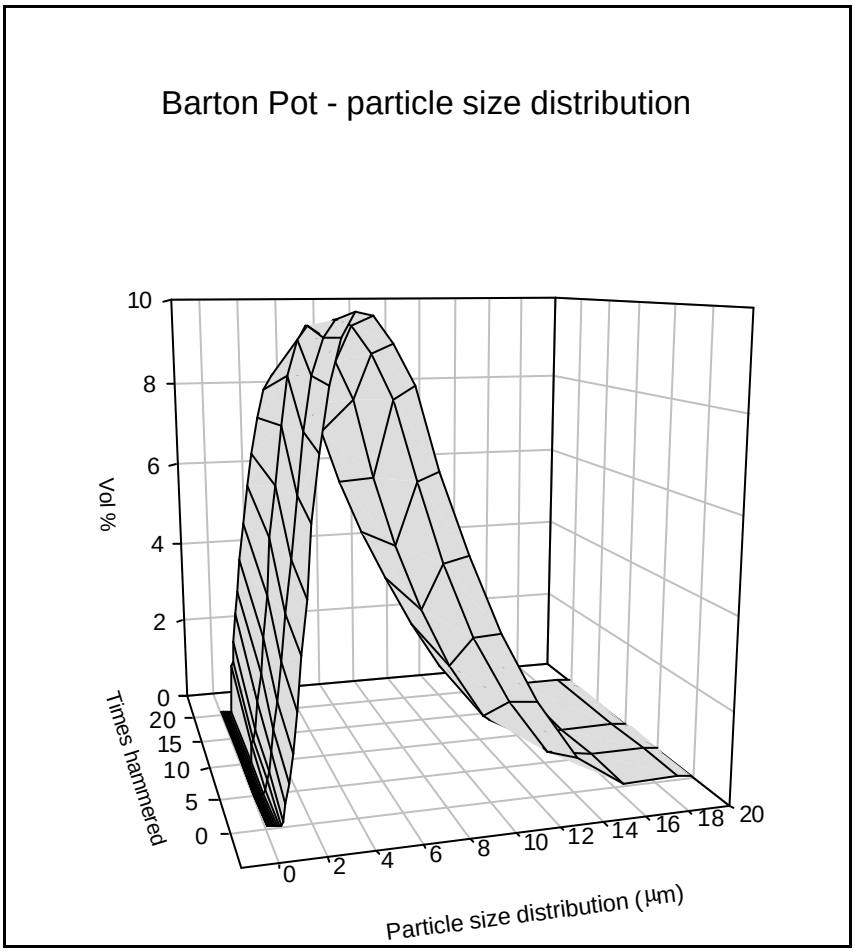

The statistics of the particle size distribution are calculated by the instrumental software using international method (BS2955:1993)[27]. The results are shown in table 5 where:

D[4,3] is the volume mean diameter

D[3,2] is the surface area mean diameter or Sauter mean

D(v,0.5) is the mass mean diameter (MMD) – the particle size at which 50% of the sample is larger and 50% is smaller than this size

D(v,0.1) is the particle size for which 10% of the sample is below this size

D(v,0.9) is the particle size for which 90% of the sample is below this size

Span is the measure of the width of the particle size distribution. The smaller the value, the narrower the distribution, and is calculated as {d(0.9)-d(0.1)}/d(0.5)}.

Table 5: Calculated statistics of the particle size distribution

	No of times through the hammer mill			
	0	**5**	**10**	**20**
Volume mean diameter D[4,3] (µm)	4.47	4.20	3.72	3.46
Surface area mean diameter D[3,2] (µm)	3.24	2.96	2.57	2.19
Mass mean diameter (MMD) D(v,0.5) (µm)	3.93	3.71	3.25	2.91
10% of particles < this size D(v,0.1) (µm)	1.77	1.59	1.37	1.07
90% of particles < this size D(v,0.1) (µm)	7.99	7.54	6.79	6.70
Specific surface area SSA (m^2/g)	0.185	0.203	0.234	0.275
Span (µm)	1.58	1.60	1.66	1.93

The results showed that there was a decrease in the mean diameters of the particle size distribution as the sample was repeatedly passed through the hammer mill. The particle size at which 10% and 90% of the sample was smaller than this size also decreased. There was an increase in the specific surface area and the span as the sample was repeatedly hammered. The result of the hammering process decreased the particle size mean diameters with an increase in the specific surface area. The cumulative % of the particles that are smaller than a given size is shown in figure 6. The % on the y-axis corresponds to the % of particles smaller than the corresponding µm value on the x-axis. A statistical analysis of the variance (ANOVA) of the various means is shown in appendix V.

Figure 6: Effect on cumulative % of passing oxide through the hammer mill

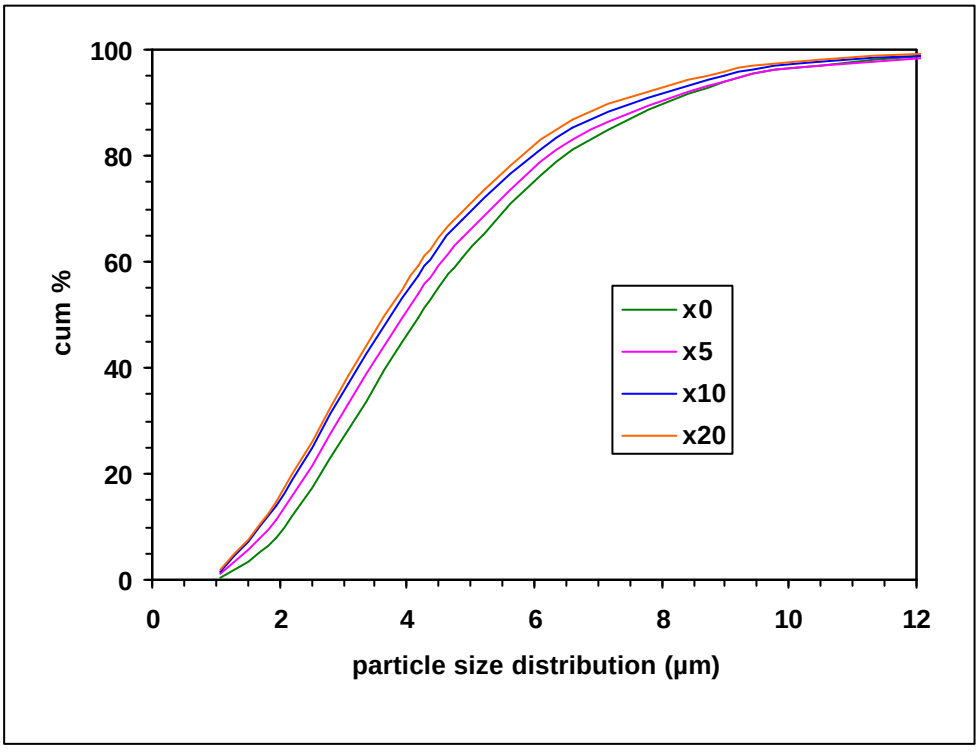

x0 :Not passed through the hammer mill
x20 :Passed 20 times through the hammer mill

The results showed a shift in the cumulative particle size distribution towards a finer particle size as the oxide is hammered. There is a negligible difference between 10 and 20 passes through the hammer mill indicating that the shift in particle size distribution becomes smaller as the sample is repeatedly hammered. This limiting effect is more clearly seen in figure 7, where a 3D representation of the cumulative % particle size distribution is shown.

Figure 7: Cumulative % particle size distribution – 3D view

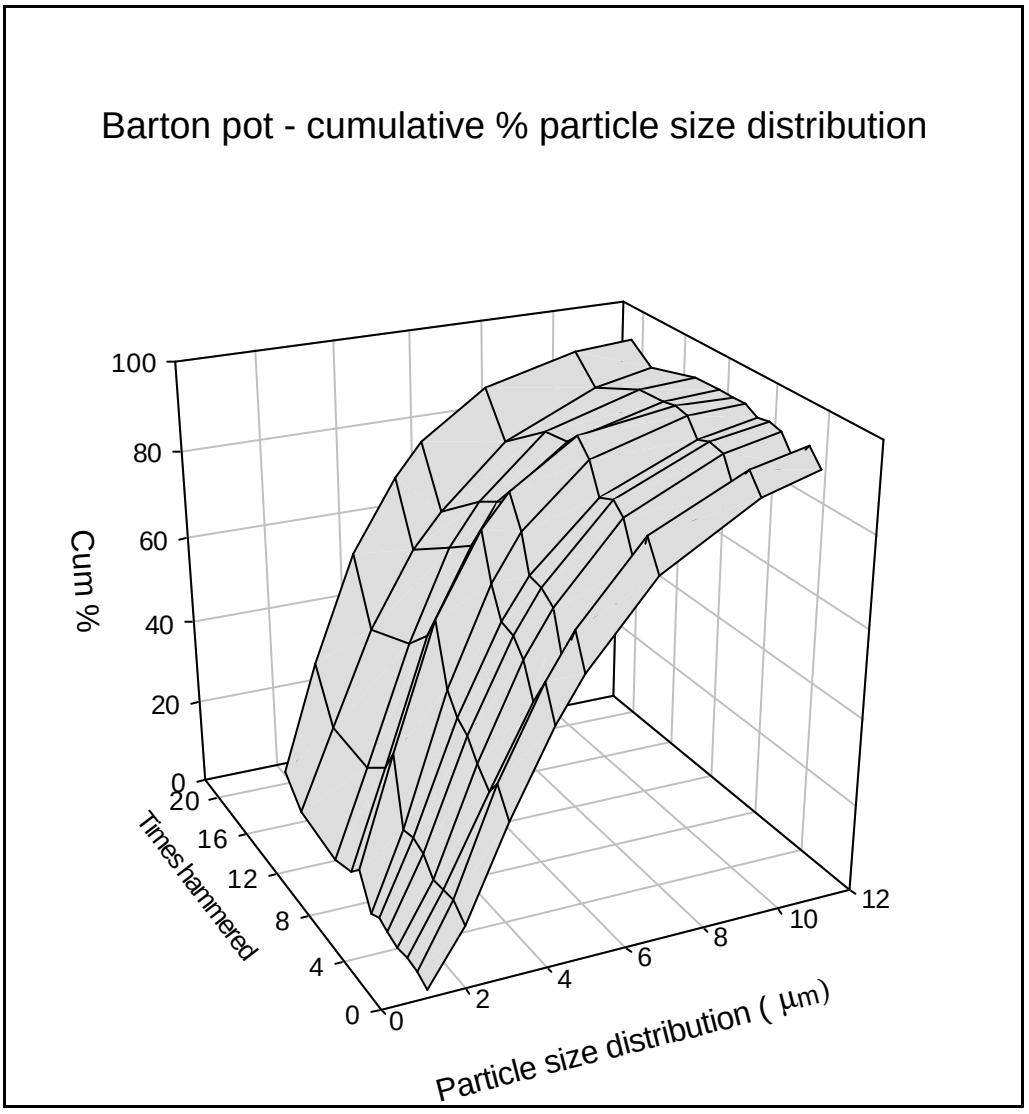

5.2.2 Ball mill process

The effect of repeatedly passing a sample of Ball mill lead oxide through the hammer mill and its influence on the particle size distribution is shown in figure 8.

Figure 8: Particle size distribution of Ball mill oxide

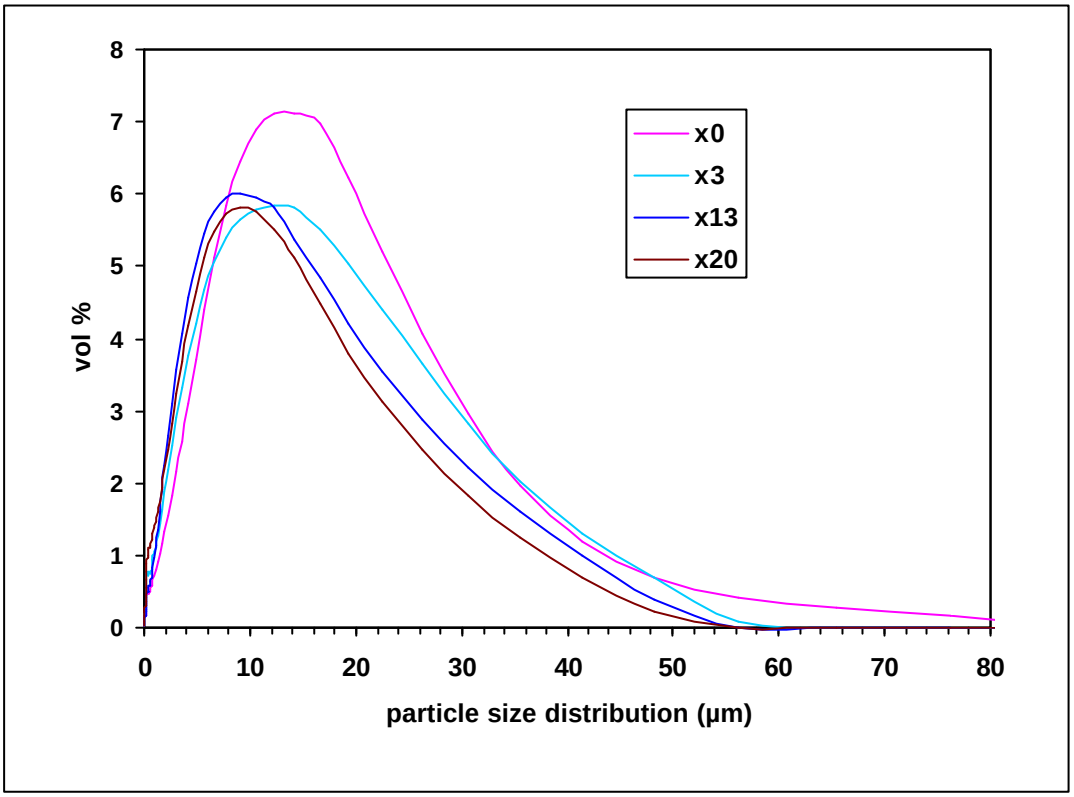

x0 :Not passed through the hammer mill
x20 :Passed 20 times through the hammer mill

The results showed that the Ball mill oxide had a fairly wide range of particle sizes. The sample, as received from the manufacturer, before being subjected to the hammer milling process, had a modal diameter of 14 µm. After 20 passes through the hammer mill this diameter was reduced to 9 µm. There was also a decrease in the % of the modal diameter as the sample was repeatedly hammered, where the extent of the shift was reduced as the sample was continually hammered. Since the distribution of the particles would always sum to 100% (figure 10), it

is the fraction of the various particle sizes that have changed during the hammer milling process.

The 3D effect of the particle size distribution curve is shown in figure 9.

Figure 9: Ball mill particle size distribution

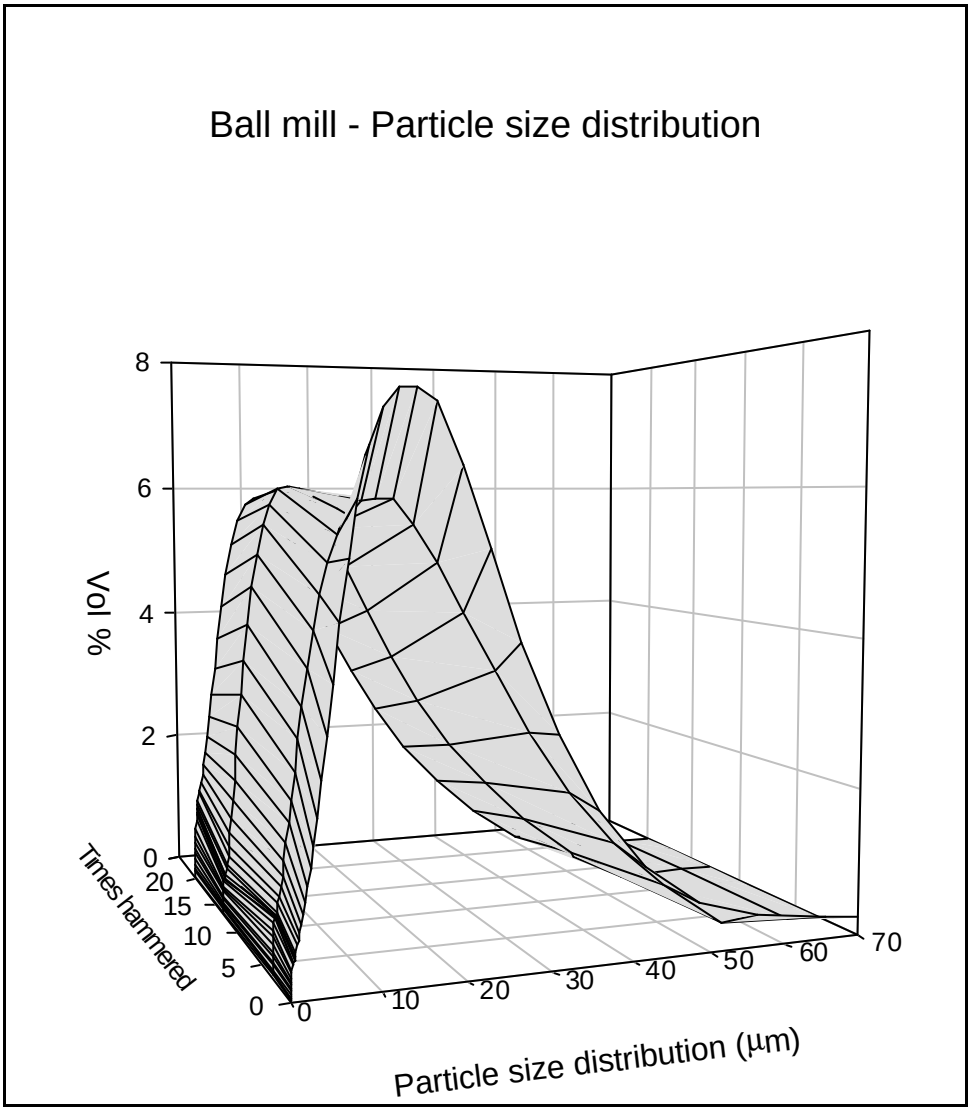

The statistics of the particle size distribution is shown in table 6. The explanations of the terms are in section 5.1.2.

Table 6: Calculated statistics of the particle size distribution for Ball mill oxide

	No of times through the hammer mill			
	0	**3**	**13**	**20**
Volume mean diameter D[4,3] (µm)	12.35	10.05	9.09	8.32
Surface area mean diameter D[3,2] (µm)	4.21	1.84	2.10	1.33
Mass mean diameter (MMD) D(v,0.5) (µm)	9.60	7.43	6.59	5.70
10% of particles < this size D(v,0.1) (µm)	1.88	0.91	1.20	0.51
90% of particles < this size D(v,0.1) (µm)	25.04	22.97	20.64	19.94
Specific surface area SSA (m^2/g)	0.143	0.326	0.286	0.451
Span (µm)	2.421	2.969	2.950	3.409

The results showed that there was a decrease in the mean diameters as the lead oxide was repeatedly passed through the hammer mill. The particle size at which 10% and 90% of the sample was smaller than this size also decreased. There was an increase in the specific surface area and the span as the sample was repeatedly hammered. The result of the hammering process on the Ball mill oxide similarly showed a decrease in the particle size mean diameters with an increase in the specific surface area. A statistical analysis of the variance (ANOVA) of the

various means is shown in appendix V (tables 17,18). The results showed that the variation seen in the particle sizes during the hammer milling process was statistically significant and not due to experimental error.

The cumulative % of the particles that are smaller than a given size is shown in figure 10.

Figure 10: Effect on cumulative % of passing Ball mill oxide through the hammer mill

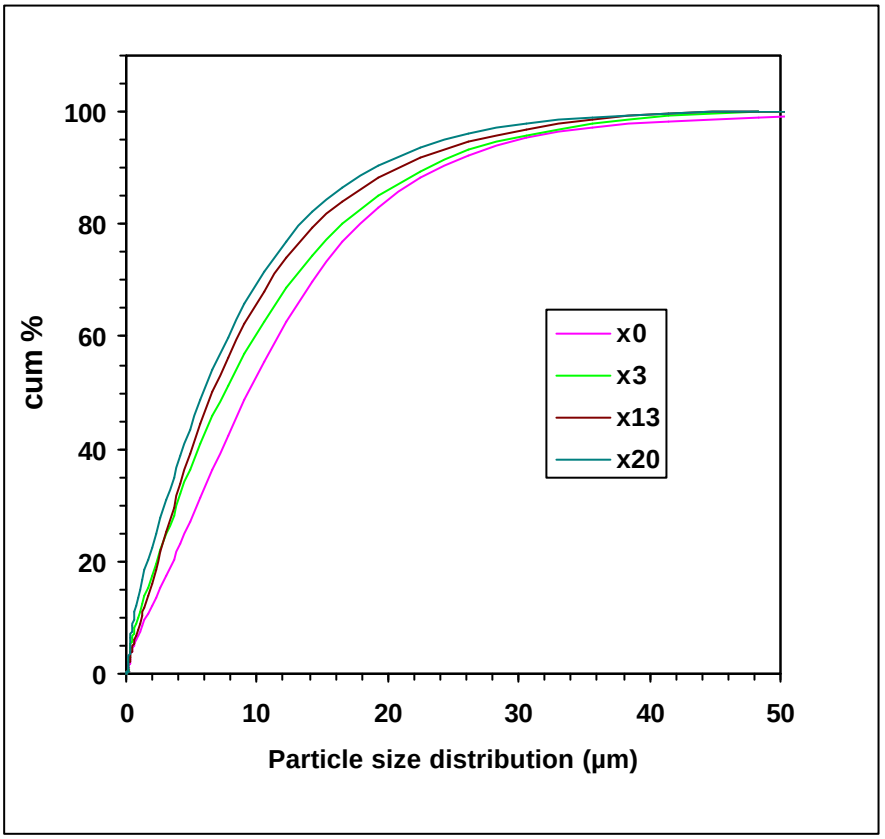

x0 :Not passed through the hammer mill
x20 :Passed 20 times through the hammer mill

The results showed a shift in the cumulative particle size distribution towards a finer particle size as the oxide is hammered. The shift to the finer particle sizes became smaller as the oxide was continually hammered. This is more clearly shown in the 3D graph in figure 11.

Figure 11: Cumulative % particle size distribution – 3D view

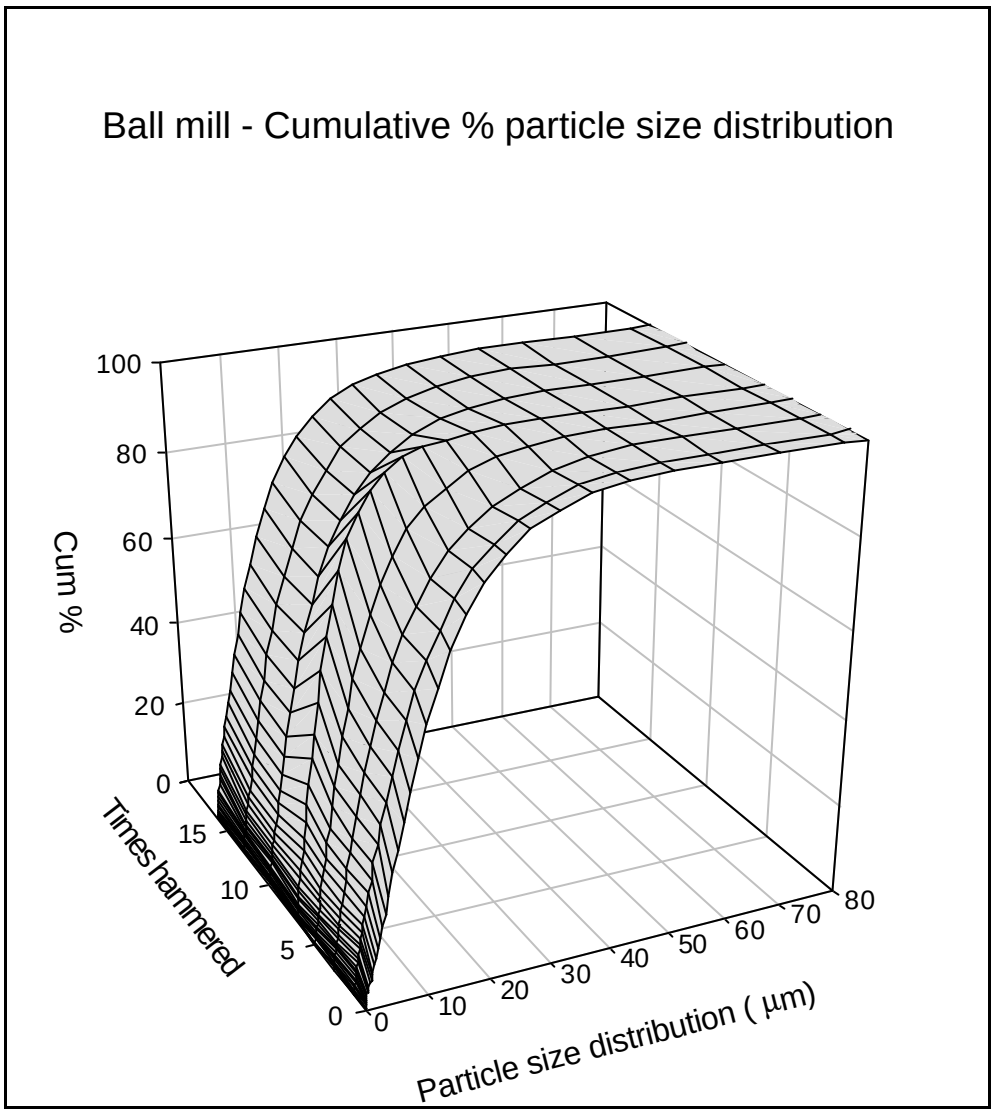

5.2.3 Summary – Barton pot and Ball mill particle size analysis

The results showed that the Ball mill sample was a much courser oxide with a larger range in particle sizes. The mean particle size of the Ball mill oxide was 12 µm when compared with 5 µm for the Barton pot oxide. This is different to what is often referred to in the literature where average Ball mill particle sizes of 2-3 µm are generally reported[2,19].

However, a comparison of Ball mill oxides from various battery plants showed a wide range of particle size means from this process[25]. The Barton pot oxide had a negligible number of particles greater than 15 µm whereas the Ball mill oxide had particles as large as 70 µm.

The wide particle size distribution of this Ball mill sample may be due to a poor process control in the manufacturing of the oxide where the age and process control ability of the equipment may have contributed to the wide range of particles produced.

Since the particles of the Ball mill are flatter in shape[19], the laser diffraction system would have determined on average a larger particle if viewed from its larger side when compared with its narrower side. This would have changed the particle size distribution spectrum slightly since the algorithm used to determine the particle size assumed that the shape of the particle was spherical. The particle shape will be discussed in more detail in section 5.4.

Passing the Ball mill oxide through the hammer mill produced a much larger reduction in the particle size distribution range. This was most likely due to the flat shaped nature of the starting material.

In the Barton pot oxide more than 90% of the particles were less than 10 µm when compared with the ball mill process where 50% of the particles were < 10 µm before being passed through the hammer mill. Hammer milling the Ball mill oxide 20 times improved this percentage to 80%.

The hammer milling of both types of lead oxide showed a similar trend in the reduction of the particle size distribution range with the improvements becoming smaller as the number of times passed through the hammer mill increased. Even though the process of hammer milling Ball mill oxide was not the primary aim of this study, the results showed that a significant reduction in the particle size distribution could be

achieved. This was most likely due to the much courser nature of the Ball mill oxide before the start of the hammer milling process.

5.3 BET surface area analysis and acid absorption number

The BET surface area analysis and acid absorption number determination are different methods that relate to the surface area of the oxide. While the BET method requires expensive equipment, the acid absorption method is quick and inexpensive, and can be readily used in the factory environment.

5.3.1 Barton pot lead oxide

The BET surface area analysis of the Barton pot lead oxide after it was repeatedly passed through the hammer mill is shown in figure 12.

Figure 12: BET surface area of Barton pot lead oxide

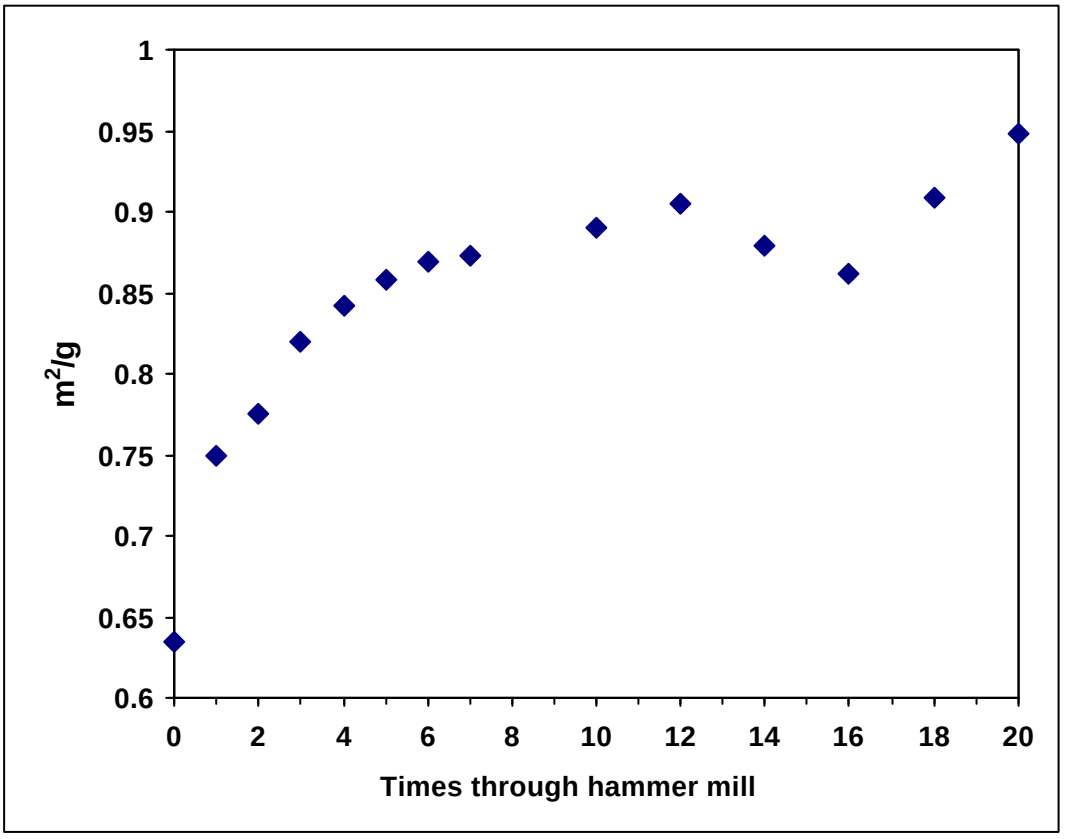

A similar trend to the results of the particle size analysis was observed with the BET surface area analysis. Initially, after a few hammer milling cycles the surface area increased, but after about 8 passes through the hammer mill, the increase in surface area with subsequent hammering was reduced. The lower values obtained after 14 and 16 passes through the hammer mill was most likely due to experimental error as the results of additional experiments (appendix III fig 44) confirmed.

The acid absorption number, which relates to the surface area of the particle showed a slight increase after 12 passes through the hammer mill. Thereafter there was no significant change in the acid absorption number. This is shown in figure 13.

Figure 13: Acid Absorption number of Barton pot oxide

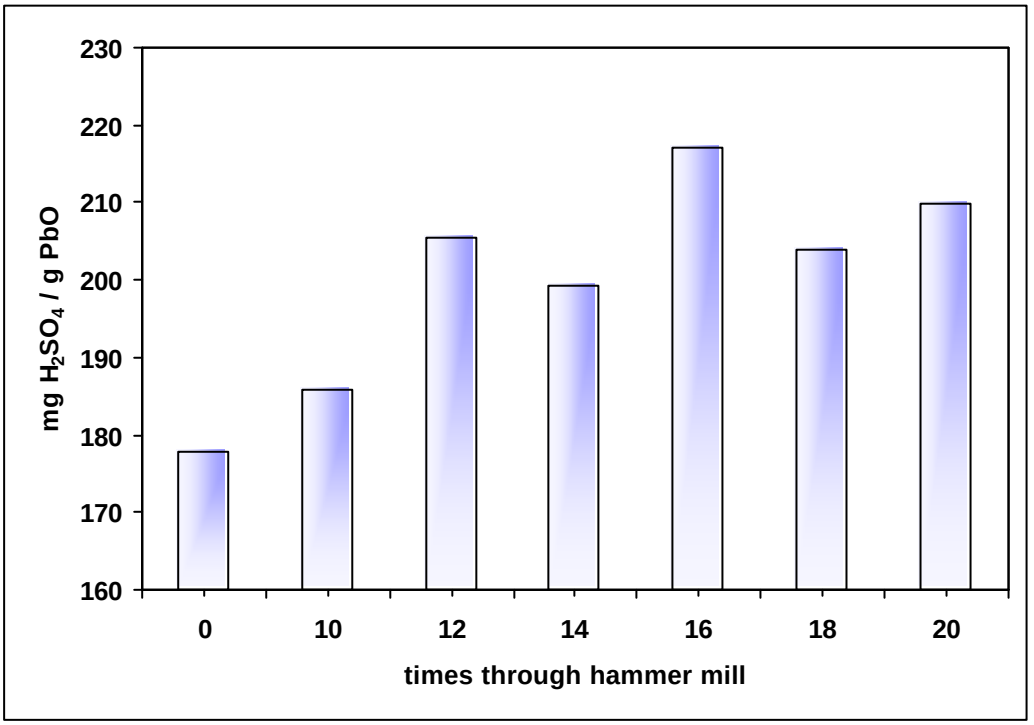

5.3.2 Ball mill lead oxide

The BET surface area analysis of the Ball mill lead oxide after it was repeatedly passed through the hammer mill is shown in figure 14.

Figure 14: BET surface area of Ball mill lead oxide

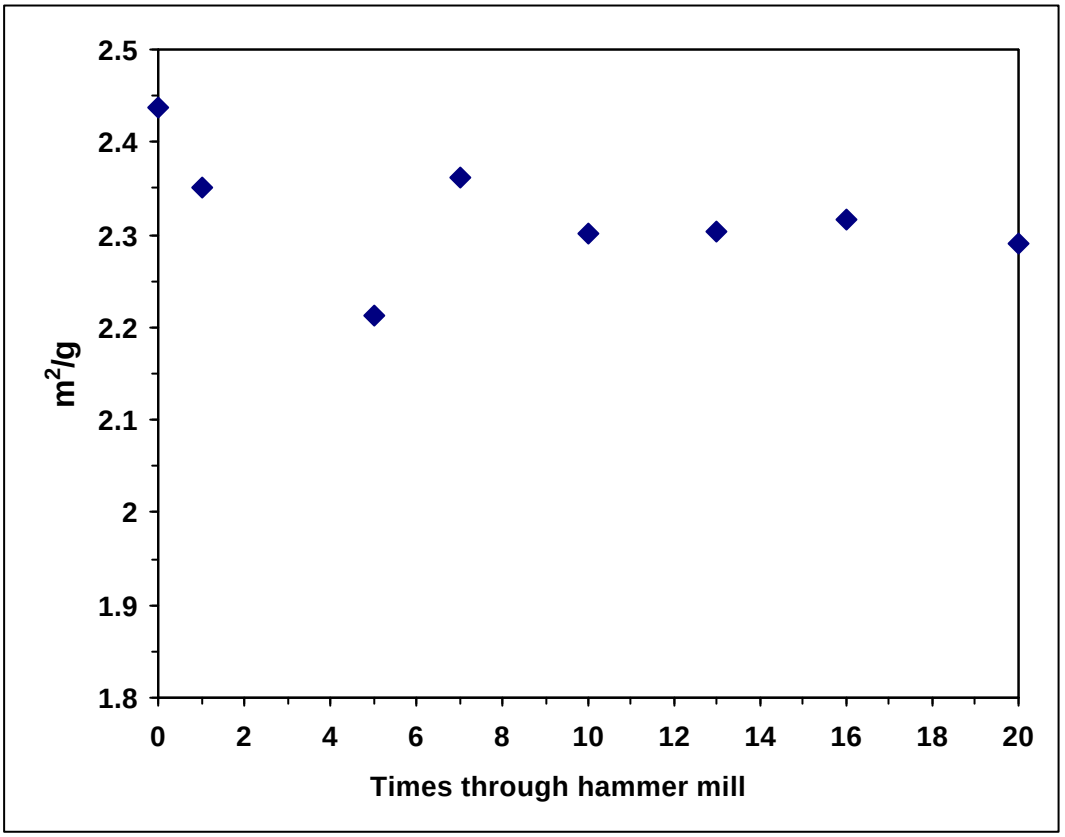

The results showed that repeatedly hammering the Ball mill sample produced no significant change in the surface area of the oxide. There was an initial slight decrease in the surface area after the hammer milling process had started and no subsequent change after about 20 passes through the hammer mill.

The acid absorption number results of the Ball mill lead oxide after it was repeatedly passed through the hammer mill are shown in figure 15.

Figure 15: Acid Absorption number of Ball mill oxide

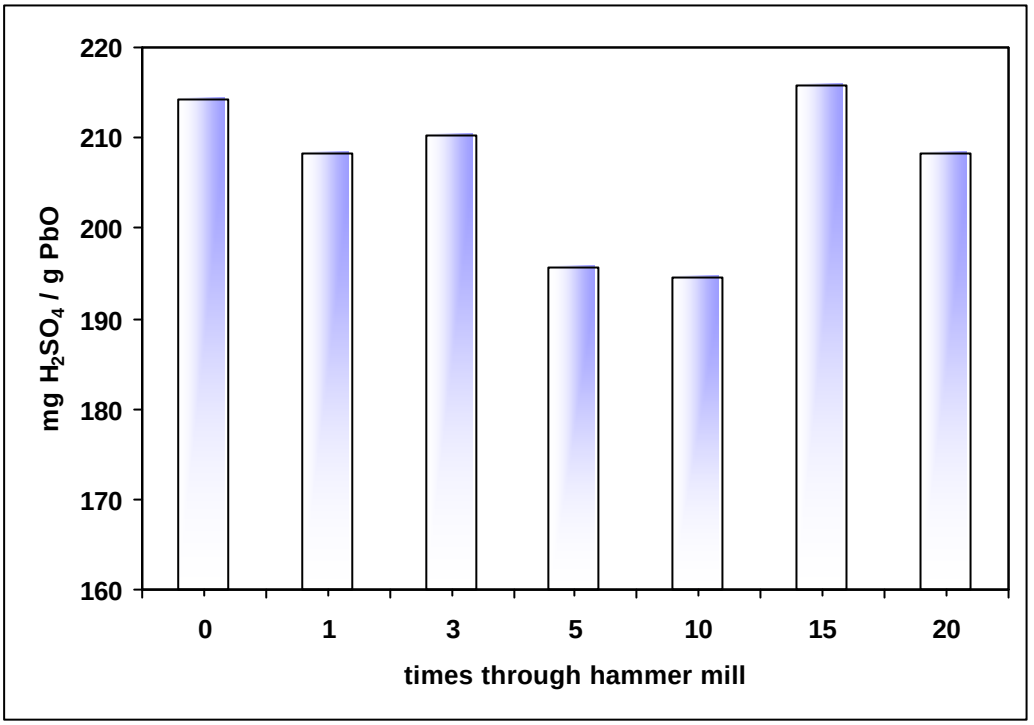

The results showed that there was initially a slight decrease and then an increase in the acid absorption number which was similar to the trend shown in the BET surface area results. However, there was no significant difference in the results between the oxide that was not hammered and that that had been passed through the hammer mill 20 times.

5.3.3 Summary - BET surface area and acid absorption number

The BET surface area analysis and the acid absorption number of the Barton pot and Ball mill oxides did not show the same trend as with the particle size distribution. The Barton pot sample showed an initial increase in the BET surface area and acid absorption number, and then

tended to show a negligible variation as the oxide was continually passed through the hammer mill.
The Ball mill oxide showed a slight decrease in the BET surface area and acid absorption number initially, however, there was no significant difference between the non-hammered oxide and the one that was hammered 20 times.

The cause of this is most likely related to the shape of the Ball mill particles which are flatter in shape as compared with the more rounded Barton pot particles. The particle size distribution analysis showed that there was a reduction in the size of the oxide grains as the sample was passed through the hammer mill. The BET surface area results of the Ball mill oxide would suggest that the particles are broken up along the larger surface plane. The results also suggest that the surface area of the flatter side of the grain is much larger than the narrower side. The surface area of a flatter particle that is ground or broken would not change as much as a more rounded particle that is broken.

In order to compare the particle shapes of the two different oxides, a shape factor was determined by dividing the results obtained from the BET surface area (fig 12, 14) by the SSA (table 4, 5) obtained from the laser diffraction technique. The SSA values are calculated by the instrumental software by assuming that the particles are spherical. A change in the BET/SSA relationship would suggest that the particle shape had changed as a result of the hammer milling process. This would be an important factor especially in the Ball mill process since the oxide particles are flatter in shape[2]. The resultant graph is shown in figure 16.

Figure 16: Particle shape factor

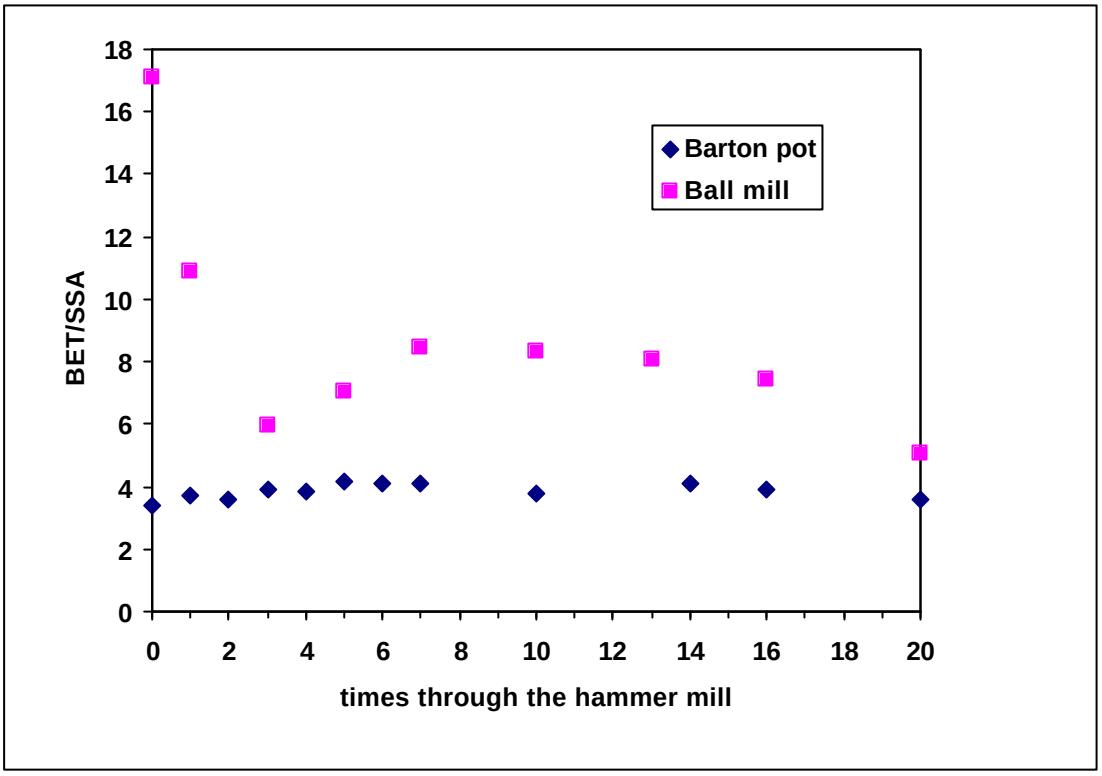

The results showed that there was no significant difference in the BET/SSA values for the Barton pot oxide as the sample was repeatedly passed through the hammer mill. However, the Ball mill oxide showed a significant decrease after the first few passes through the hammer mill, followed by a gradual decrease as the sample was repeatedly hammered. This suggests that the shape of the Ball mill particles had changed during the hammer milling process whereas for the Barton pot process the shape of the particles remained the same. Further evidence of this is shown in the SEM studies in section 5.4.

5.4 Free lead percentage

The free lead content of the lead oxide is an important parameter in the lead acid manufacturing process since it is necessary in the high humidity curing process.

5.4.1 Barton pot process

The effect of the hammer milling process on the free lead content of Barton pot oxide is shown in figure 17.

Figure 17: Free lead % of Barton pot lead oxide

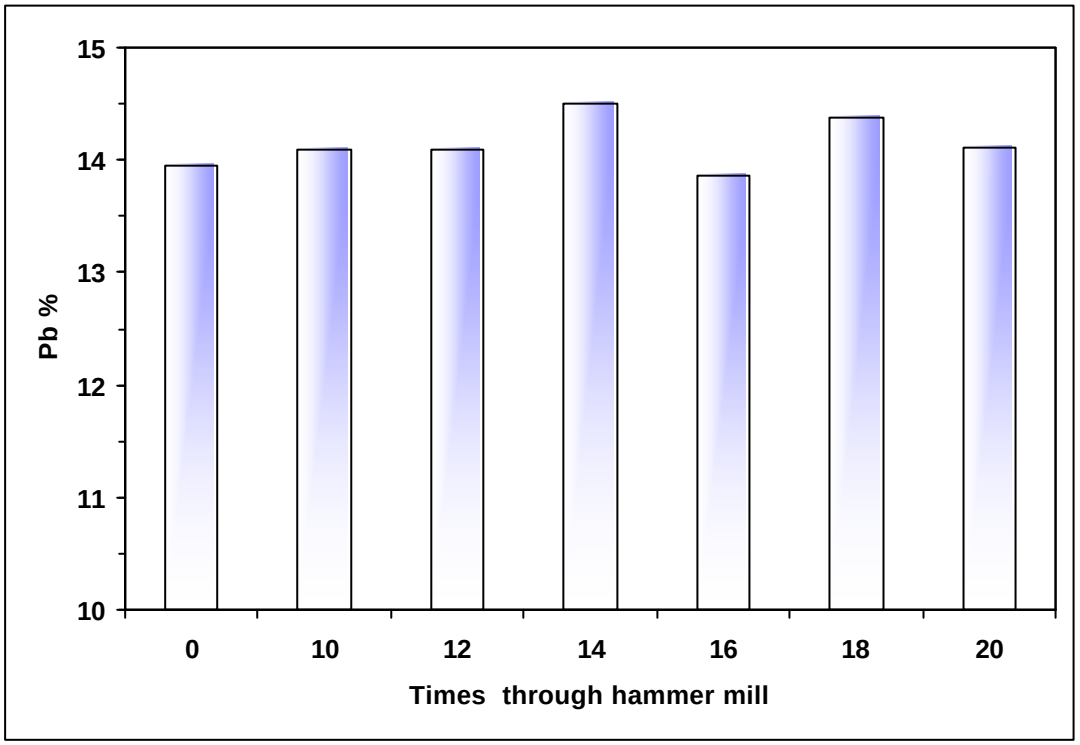

The results showed that the free lead content of the lead oxide remained relatively consistent after each repeating step of the hammer milling process. This would imply that the hammer milling process does not influence the free lead content.

5.4.2 Ball mill process

The effect on the free lead content when Ball mill lead oxide was repeatedly passed through the hammer milling process is shown in figure 18.

Figure 18: Free lead % of Ball mill lead oxide

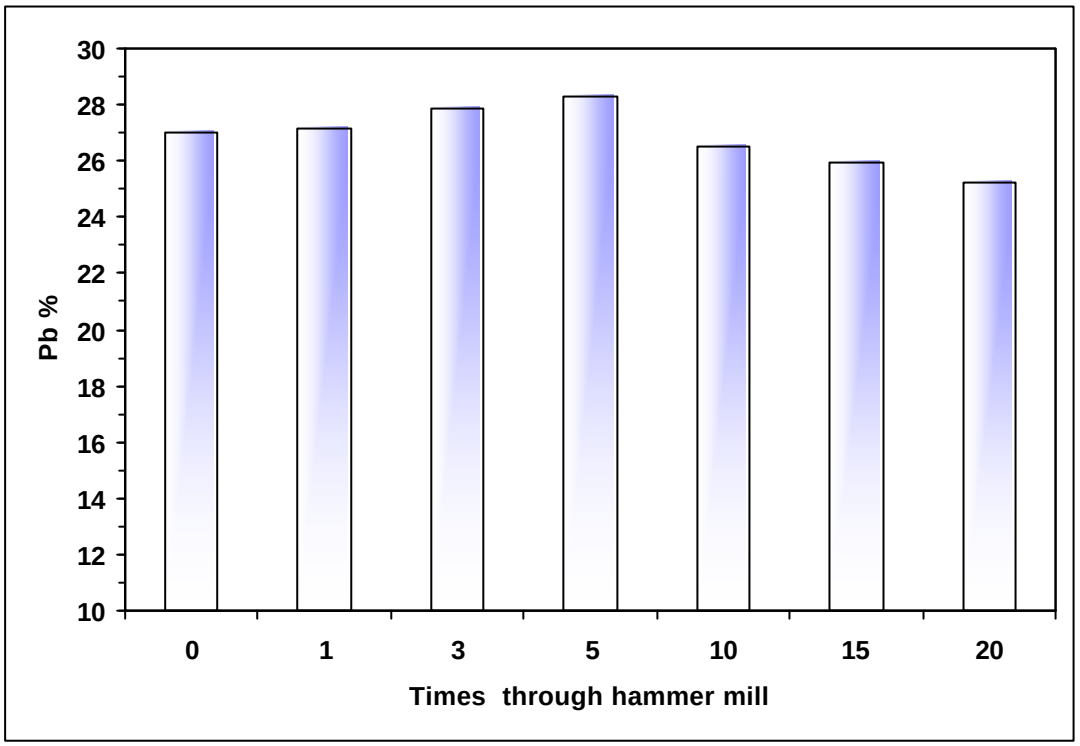

The results showed no significant variation in the free lead as a result of repeatedly passing the oxide through the hammer milling process except for a slight decrease after the 10^{th}, 15^{th} and 20^{th} cycle.

5.4.3 Summary – Free lead % in Barton pot and Ball mill oxide

For both the Barton pot and Ball mill oxides there was no significant variation in the free lead due to the hammer milling process. This implies that for both types of lead oxide the hammer milling process does not cause the free lead in the oxide to oxidise further. The free lead % in the Ball mill oxide was greater than the Barton pot oxide. This

is a function of the oxide manufacturing process and is similar to the values reported in the literature (table 2).

5.5 SEM and optical microscope studies of lead oxide

5.5.1 Barton pot oxide

Selected Barton pot samples were studied using SEM to determine if there was any visual variation in particle shape and size when the oxide was repeatedly passed through the hammer mill. The results are shown in figures 19-21.

Figure 19: Barton pot oxide before the hammer milling process

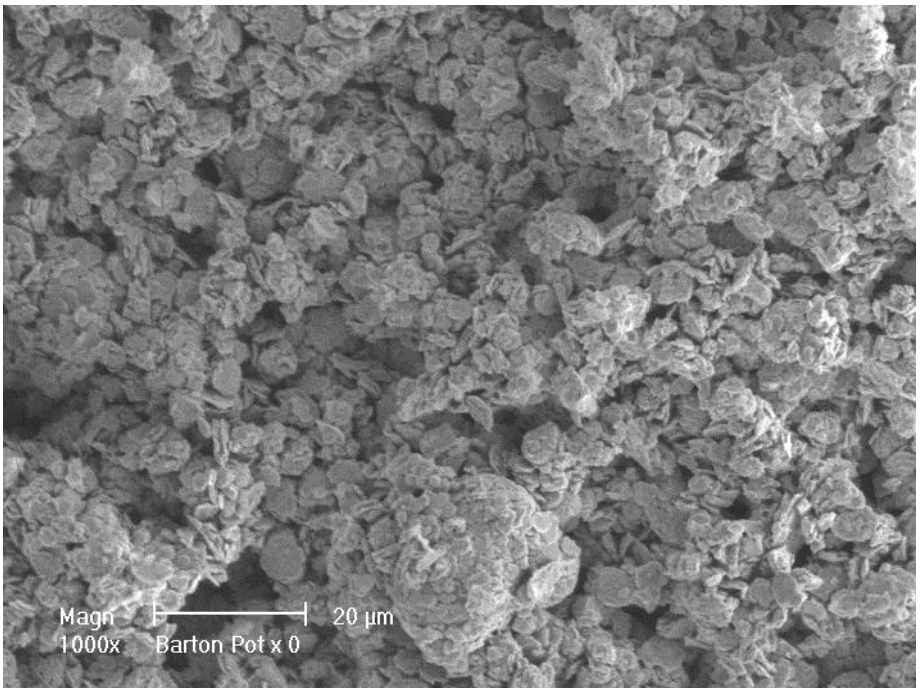

Figure 20: Barton pot oxide after 10 passes through hammer mill

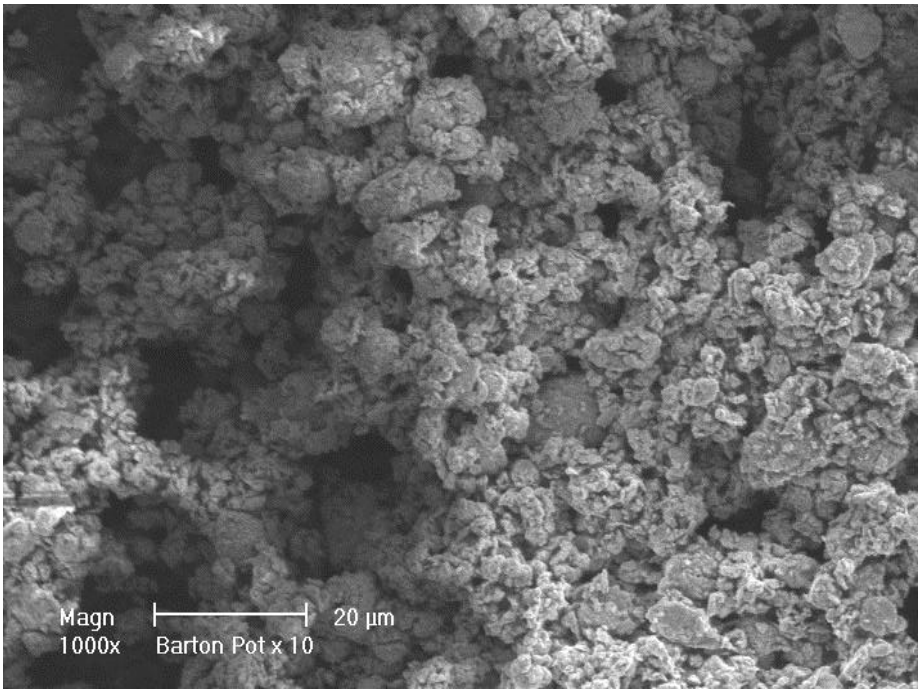

Figure 21: Barton pot oxide after 20 passes through hammer mill

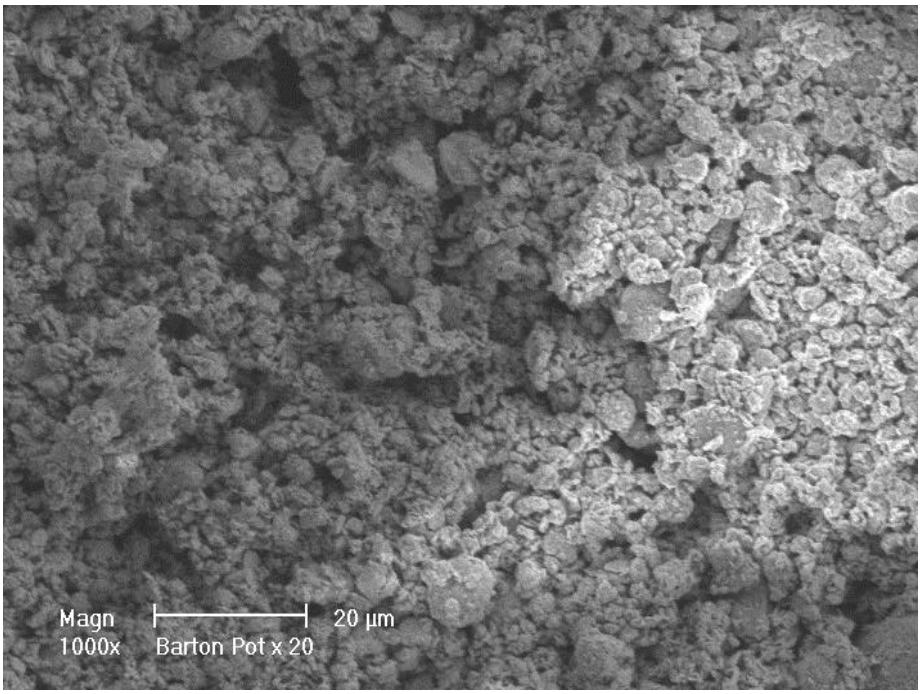

Selected Barton pot oxide samples were studied using an optical microscope to determine the effects of the hammer milling process on the Barton pot oxide. The results are shown in figures 22 – 24.

Figure 22: Barton pot oxide before the hammer mill process

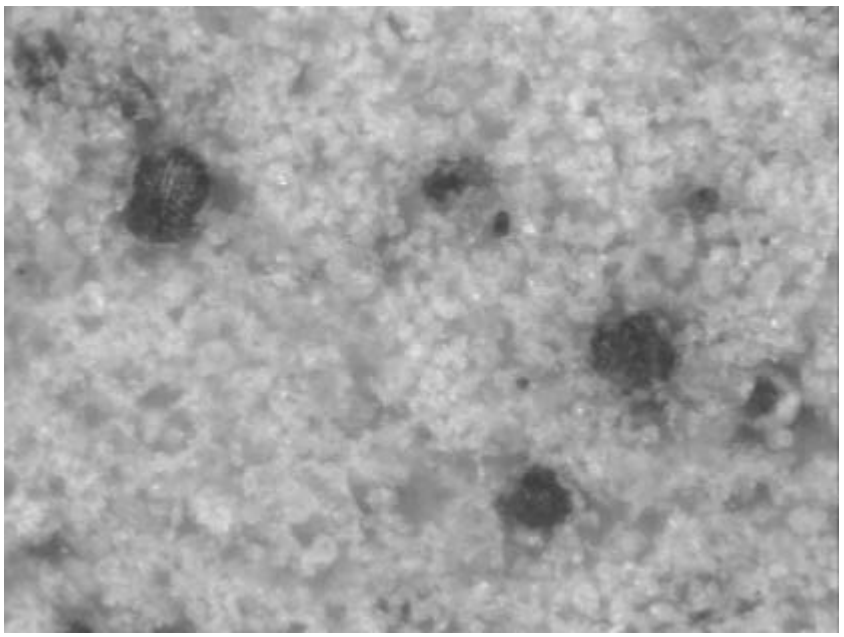

50X magnification

Figure 23: Barton pot oxide after 10 times through the hammer mill

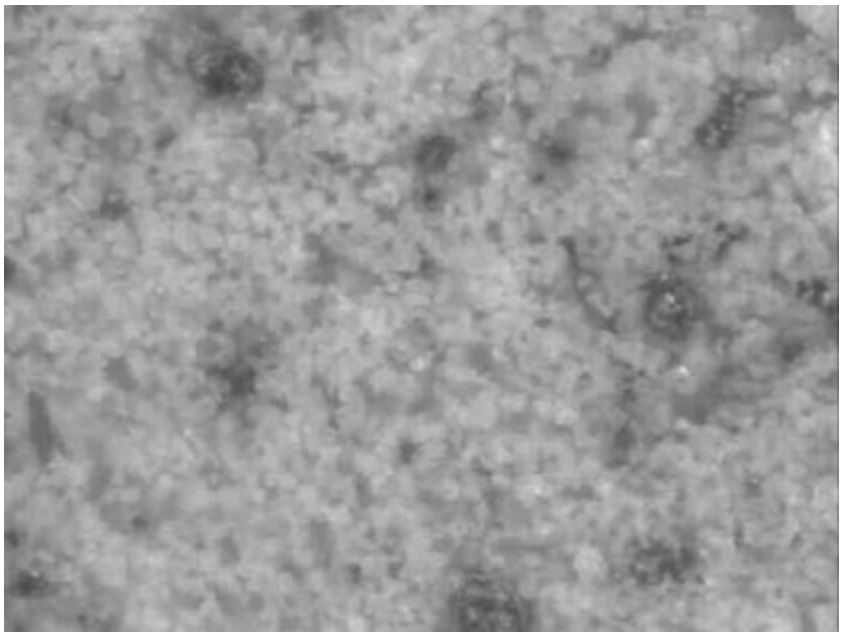

50X magnification

Figure 24: Barton pot oxide after 20 times through the hammer mill

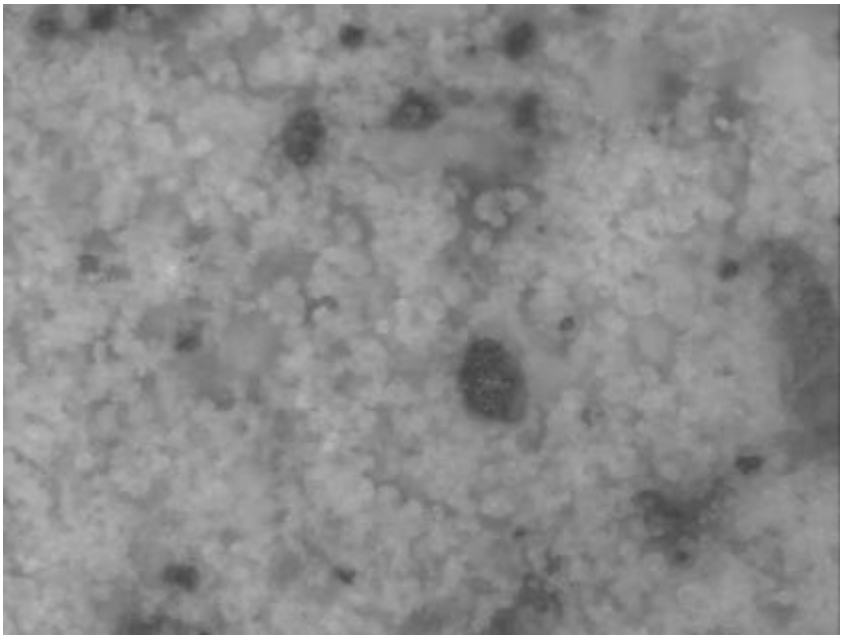

50X magnification

The SEM photograph of the Barton pot oxide before the hammer milling process (fig 19), showed that the oxide particles were relatively rounded in shape with some larger particles > 10 µm clearly visible. After 10 passes through the hammer mill (fig 20) a finer range of particles could be seen. A more uniform and finer range of particles could be seen after 20 passes through the hammer milling process (fig 21).

The optical micrograph of the Barton pot sample, before the hammer milling process (fig 22), showed that the free lead particles (dark spots) and the lead oxide particles were more rounded in shape. After being passed through the hammer mill (fig 23,24) the lead oxide tended to have a more consistent appearance in terms of its particle size.

5.5.2 Ball mill oxide

Selected Ball mill samples were studied using the SEM to determine if there was any variation in particle shape and size when the oxide was repeatedly passed through the hammer mill. The results are shown in figures 25-27.

Figure 25: Ball mill oxide before the hammer milling process

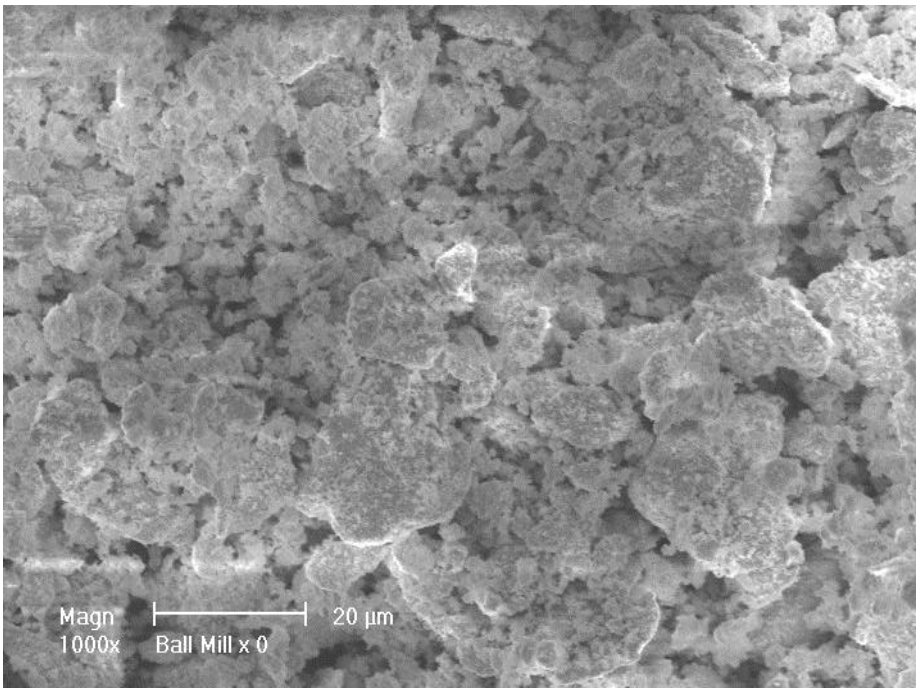

Figure 26: Ball mill oxide after 10 passes through hammer mill

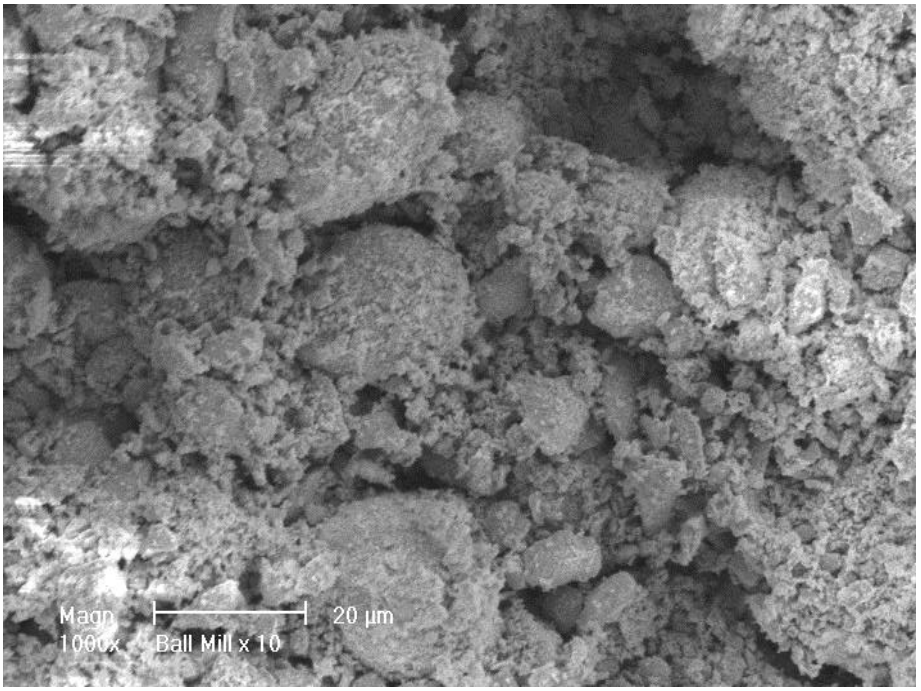

Figure 27: Ball mill oxide after 20 passes through hammer mill

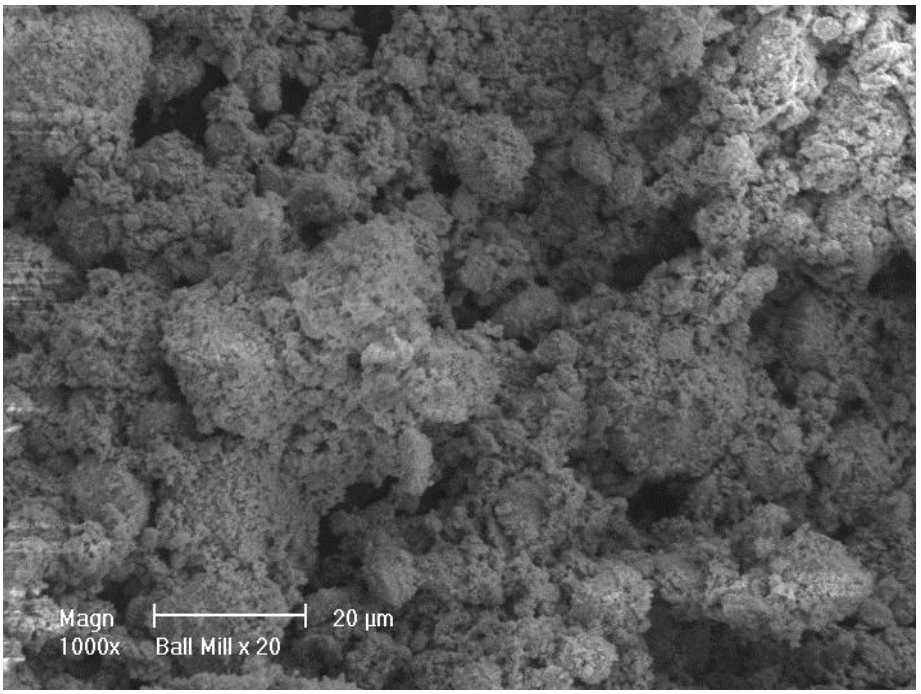

Selected Ball mill oxide samples were studied using an optical microscope to determine the effects of the hammer milling process on the Ball mill oxide. The results are shown in figures 28 – 30.

Figure 28: Ball mill before the hammer milling process

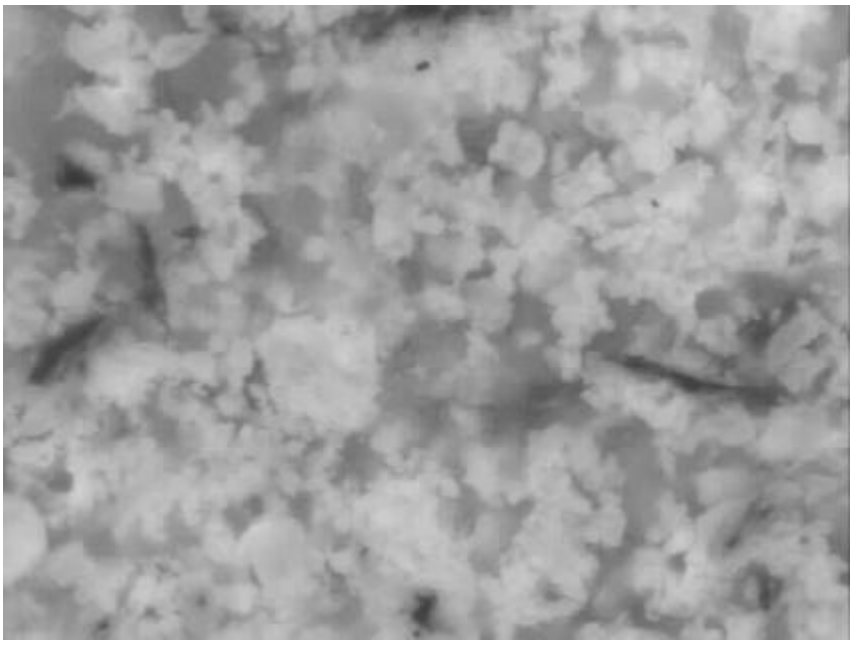

50X magnification

Figure 29: Ball mill oxide after 10 passes through the hammer mill

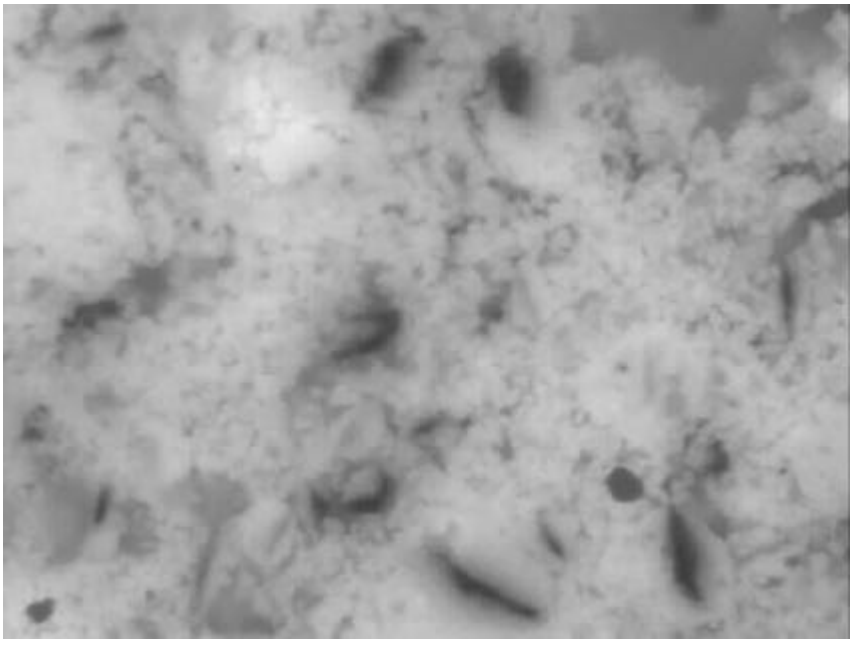

50X magnification

Figure 30: Ball mill oxide after 20 passes through the hammer mill

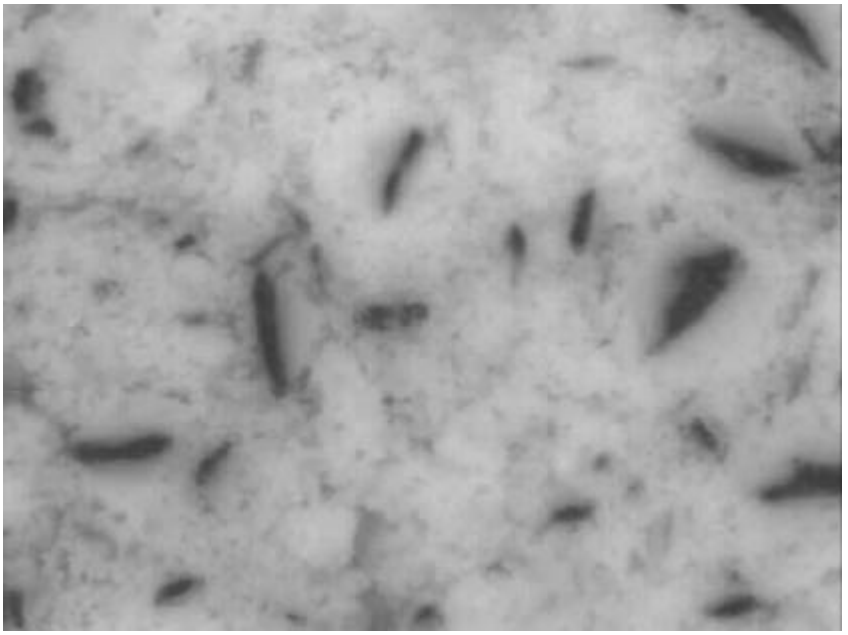

50X magnification

The SEM micrograph of the Ball mill oxide, before the hammer milling process (fig 25), showed very large irregular particles > 20 µm. The shape of the particles appeared to be flatter and irregular in shape. After 10 passes through the hammer mill (fig 26) the size of these particles was reduced and the shape of the particles became less irregular. After 20 passes through the hammer mill (fig 27) the shape of the particles appeared more rounded.

The optical micrograph of the Ball mill oxide, before the hammer milling process (fig 28) showed that the free lead particles (dark areas) were elongated and almost needle-like in shape. The lead oxide particles were more irregular in shape. After the hammer milling process (fig 29, 30) the oxide tended to have a more consistent appearance with the oxide particles having a similar particle size.

5.5.3 Summary – SEM and optical microscope study of Barton pot and Ball mill lead oxide

The SEM study of the Barton pot and Ball mill oxides before the hammer milling process showed that there was a distinct difference in the particle shape and size. The Barton pot particles were more rounded whereas the Ball mill particles were more irregular and flatter in shape. During the hammer milling process the Barton pot oxide maintained the rounded particle shape whereas the Ball mill oxide, which had a flatter shaped particle would break up and become more rounded in shape. This supports the change in shape factor BET/SSA discussed previously (fig 16).

The optical micrographs showed that the Barton pot and Ball mill oxides had a distinct difference in the shape of the free lead and lead oxide particles. The Barton pot oxide and free lead particles were more rounded in shape, whereas the Ball mill had more irregular shaped oxide particles and needle-like lead particles.

Chapter 6

Electrochemical evaluation of the positive electrode made by using Barton pot lead oxide

6.1 Cured positive electrode

6.1.1 XRD phase analysis

The XRD phase analysis results of the cured plates made using Barton pot lead oxide that was passed through the hammer mill 0, 3, 10 and 20 times respectively is shown in table 7.

Table 7: XRD phase analysis of cured electrodes

	No of times passed through the hammer mill			
	0	**3**	**10**	**20**
a -PbO (%)	24.6	37.0	29.2	40.9
T3 (%)	27.3	38.6	36.2	33.8
MBS (%)	47.2	23.3	33.6	24.2

T3 :Tri-basic lead sulphate

MBS :Mono-basic lead sulphate

The results showed that predominantly T3 crystals were produced in the cured active material. The variation in T3 can be attributed to sample analysis where only a small sample from an entire plate was taken, and not due to the grinding process.

6.1.2 BET surface area analysis of the cured electrodes

The BET surface area analysis results of the cured positive electrodes, made using Barton pot oxide are shown in figure 31.

Figure 31: BET surface area of cured positive plates

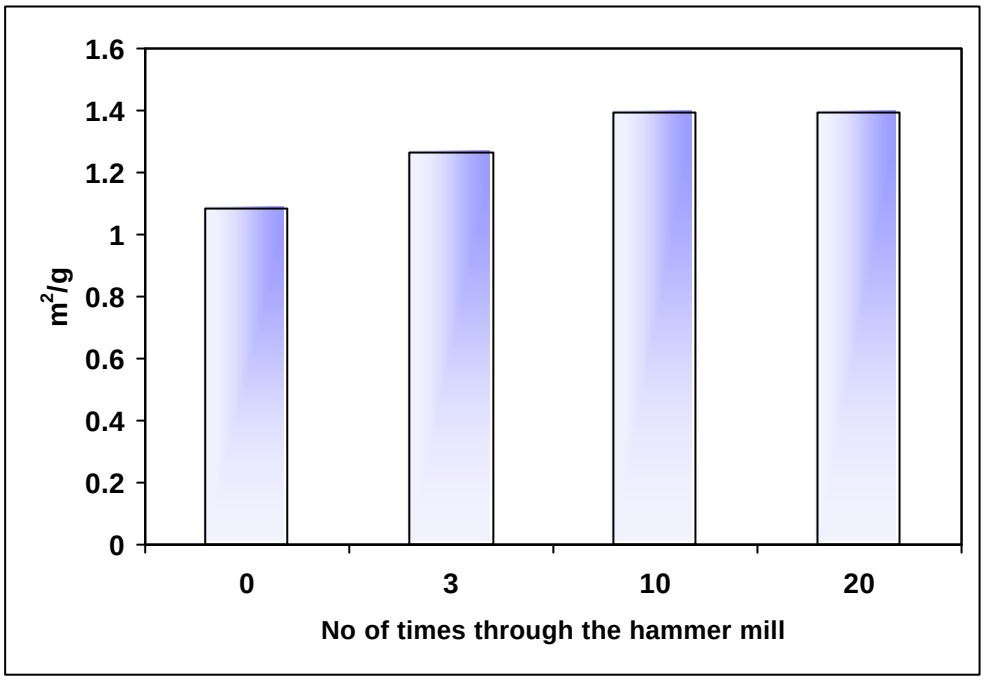

The results showed that there was a slight increase in the surface area of the cured positive electrode once the oxide had been passed through the hammer mill. This change was not significant, but a finer oxide could influence the paste mixing process due to the greater reactivity of the finer oxide with the H_2SO_4 used in this process. The slightly higher surface area of the cured electrodes that were made using hammer milled oxide may result in a slightly more reactive electrode when H_2SO_4 is added to the battery cell at the start of the formation process.

6.2 Cell Formation

The formation voltage profiles of the cells prepared using Barton pot lead oxide that was passed through the hammer mill is shown in figure 32.

Figure 32: Formation voltage profiles

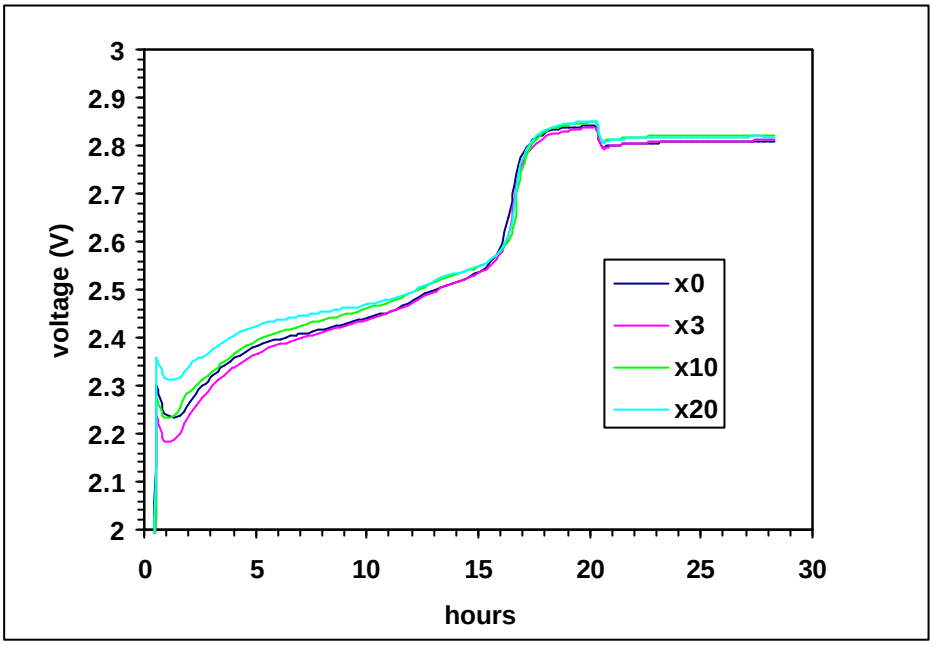

x0 :Not passed through the hammer mill
x20 :Passed 20 times through the hammer mill

The results showed that there were small voltage differences during the first 5 hours of the formation process, after which the voltage profiles were very similar. The slight variation of the voltage profiles at the start of the formation process could be explained by the variation in the reaction of the H_2SO_4 with the active material when the acid was added to the cell.

$$3PbO.\ PbSO_4 + 3\ H_2SO_4 \ ?\ 4\ PbSO_4 + 3\ H_2O \qquad (9)$$

This would result in slight variations in the cell resistance which would result in a voltage variation at the start of the formation process

according to Ohm's law (V = IR). Since batteries are formed using a constant current, a higher voltage would indicate a higher resistance to accepting the charge and result in a reduced active material conversion efficiency during formation.

6.3 Analysis of the formed plates

6.3.1 XRD phase analysis

The XRD phase analysis results of the formed positive electrodes that were made using Barton pot oxide that was passed through the hammer mill is shown in table 8.

Table 8: XRD phase analysis of formed positive electrodes

	No of times passed through the hammer mill			
	0	**3**	**10**	**20**
aPbO_2 (%)	13.8	14.0	10.7	17.8
ßPbO_2 (%)	45.8	66.8	66.8	59.1
$PbSO_4$ (%)	40.4	19.3	22.5	23.1

The results showed similar levels of a-PbO_2 in the formed active material. A lower level of ß-PbO_2 and more $PbSO_4$ was found in the plate made using oxide that had not been passed through the hammer mill.

6.3.2 BET surface area analysis

The BET surface area analysis results of the formed positive electrodes made using Barton pot oxide that was passed through the hammer mill is shown in figure 33.

Figure 33: BET surface area of formed positive electrodes

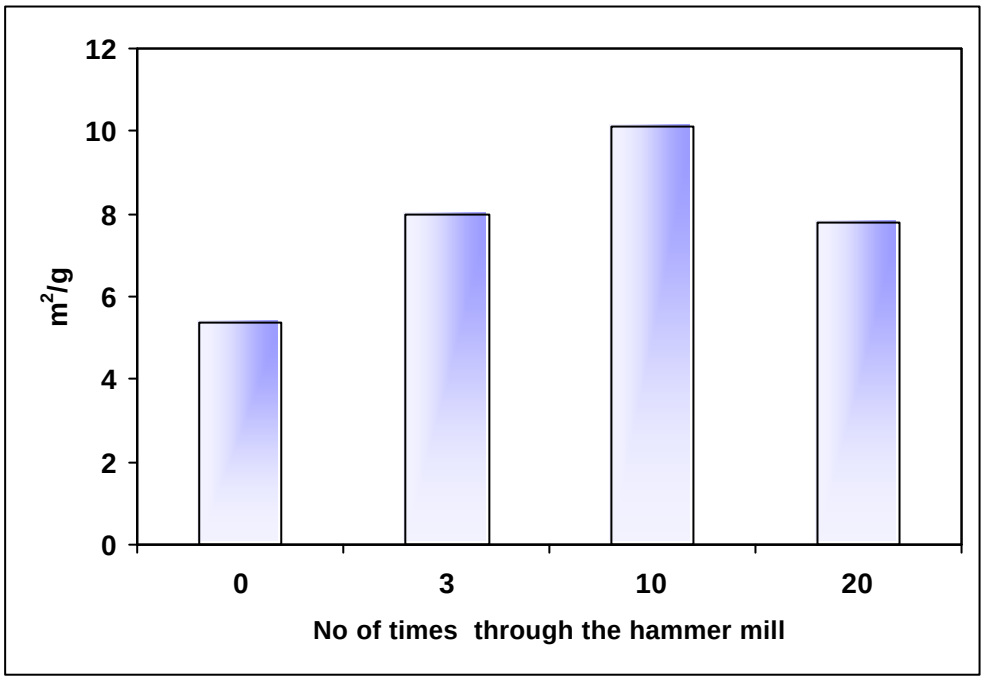

The results showed that there was an increase in the surface area of the positive electrodes that were made using Barton pot oxide that had been passed through the hammer mill 3 and 10 times, followed by a decrease in surface area for the active material made with oxide that had been hammered 20 times. This change in surface area may be related to the differences observed in the formation voltage profiles (fig 32) where the electrodes made using oxide that had been passed through the hammer mill three times showed a reduced resistance during the initial stages of formation while the 20 times electrode showed an increased resistance. This may have resulted in the variation of the surface area in the formed active material.

6.4 C20 capacity tests

6.4.1 Initial capacity testing

The results of the first 20 h capacity test at the rated capacity of 9Ah at ambient temperature are shown in figure 34.

Figure 34: Initial C20 capacity tests

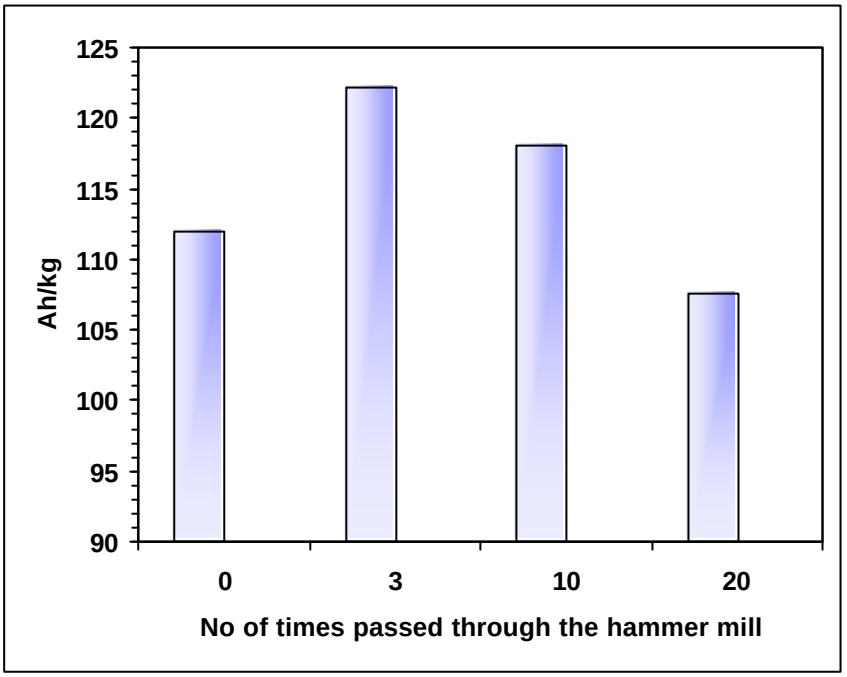

The results showed that the performance of the cells improved after 3 passes through the hammer mill, and then started to decline in the cells made with oxide that had been passed though the hammer mill 10 and 20 times. The 10 passes cell was still better than the 0 passes cell, while the performance of the 20 passes cell was worst than the cell made with oxide that had not been passed through the hammer mill. A similar trend was observed when the experiments were repeated. This is shown in appendix IV (fig 45, 48).

The trend shown in the results tends to suggest that the hammer milling process of oxide does improve the initial performance of the cell, but that further hammer milling results in a deterioration of the cell performance.

6.4.2 Capacity cycles

The results of the C_{20} capacity cycling tests on the cells made using Barton pot oxide that had been passed through the hammer mill is shown in figure 35.

Figure 35: Capacity cycling tests

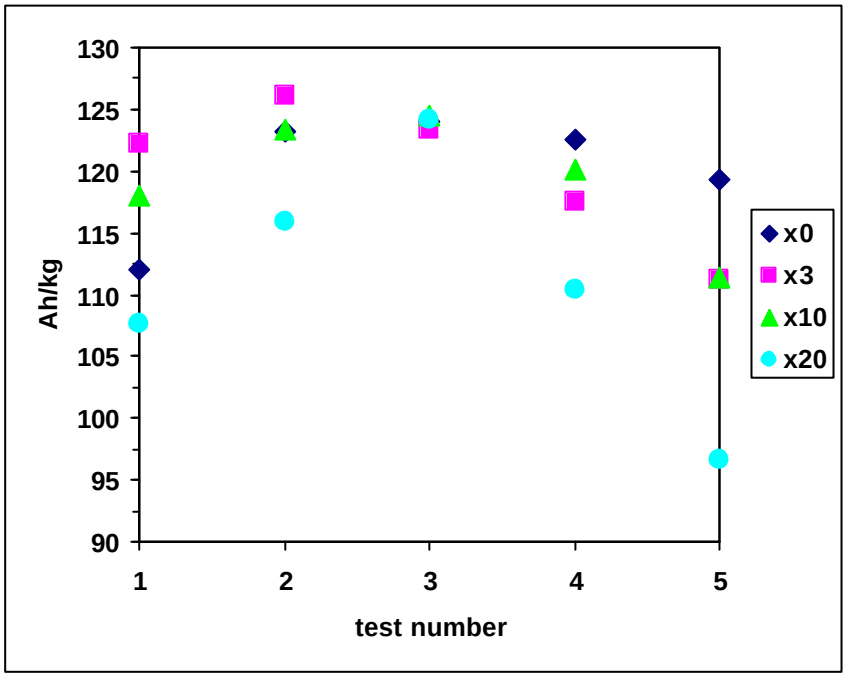

x0 :Not passed through the hammer mill
x20 :Passed 20 times through the hammer mill

The results showed that all the cells achieved a similar capacity value after 3 capacity cycles. After the third cycle there was a decrease in the capacity values, with the 20 times sample showing the largest decay in performance and the 0 times sample the smallest.

It would seem that grinding the oxide to remove the course particles is beneficial to cell performance, but too much grinding can lead to a decrease in the electrochemical performance of the cells. Additional experiments showing a similar trend is shown in appendix IV (fig 46, 49).

6.5 Power density determination using high currents

The high current performance of the cells made using Barton pot oxide that had been passed through the hammer mill is shown in figure 36. The tests were done at 10 A, 20 A and 40 A respectively at ambient temperature.

Figure 36: High current discharge tests

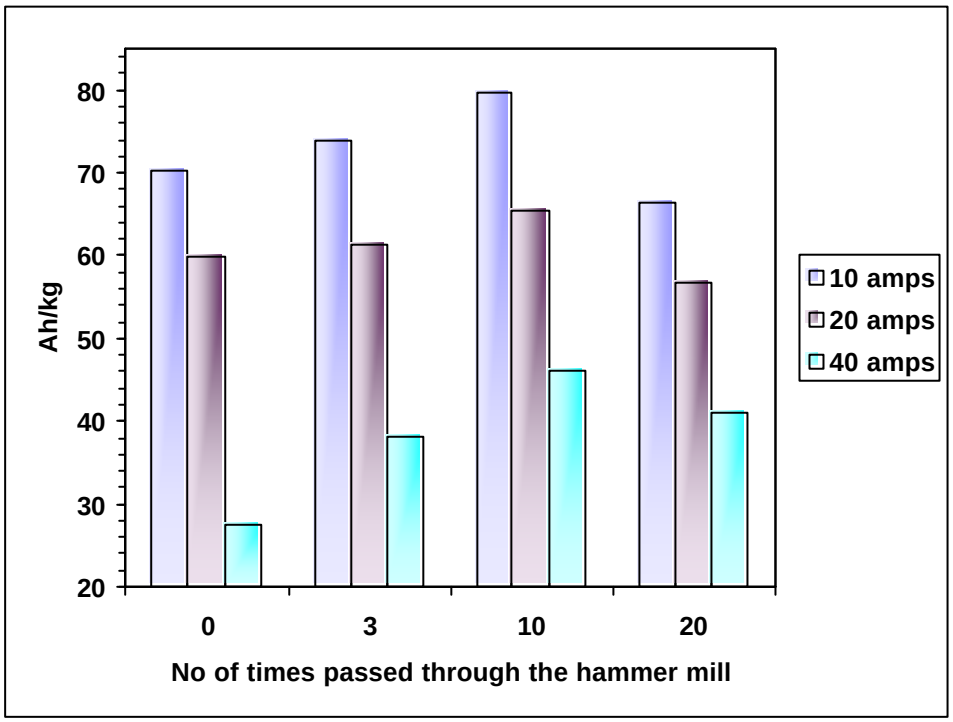

The results in figure 36 showed a similar trend to the C_{20} capacity testing with an improvement in performance up to 10 passes, followed by a decrease in the performance of the cell with the 20 passes oxide sample. There was a slight difference in the trend observed, in that the

sample with 10 passes showed a slightly higher current density to the one seen in the low current tests where there was only an improvement in performance up to the 3 passes sample.

The biggest improvement was seen at the higher current of 40 A where the percentage increase in the performance was 48% compared with 14% and 8% for the 10 A and 20 A discharges respectively. This is most likely related to the reaction kinetics during the discharge reaction at higher currents, where the reaction is more dependant on the active material surface area exposed to the acid and the diffusion rate of the acid becomes a limiting factor. Evidence of this can be seen in the BET surface area results (fig 33) which showed an increase in the active material surface area of the electrodes made using the hammer milled oxide.

The results showed that the hammer milling process improved the high rate performance of the cells, but that there was a limit after which no improvement and a decrease in the performance was observed.

The trend observed during the high current tests was similar to that of the BET surface area results (fig 33). This is most likely due to the fact that at high currents the performance is more dependent on surface area due to the short duration of the discharge period. Additional experiments showing a similar trend is shown in appendix IV (fig 47, 50). The analysis of variance in appendix V (table 20) showed that the variation in performance from 1 to 20 hammer milling steps was not significant. However, the variation from 1-10 milling steps (table 21) was statistically significant. This confirmed the observation that continued hammer milling of the oxide produced a reduced improvement in electrical performance.

6.6 Evaluation of the “float” current

The recharge current profile towards the end of the recharge period after the 5th C_{20} capacity test is shown in figure 37. This was done to determine if the hammer milling process had any effect on the “float current” as this would give an indication of the water loss properties of a cell. The water loss characteristics of a battery are affected mainly by the purity of the lead used to manufacture the lead oxide and by the choice of lead alloy for the grid. While it was not expected for the hammer milling process to affect the water loss characteristics of the battery, this test was performed as it is an important parameter that is monitored by battery manufacturers. The recharge was done at a constant voltage of 2.67 V with a maximum current of 2 A.

Figure 37: Recharge current profile

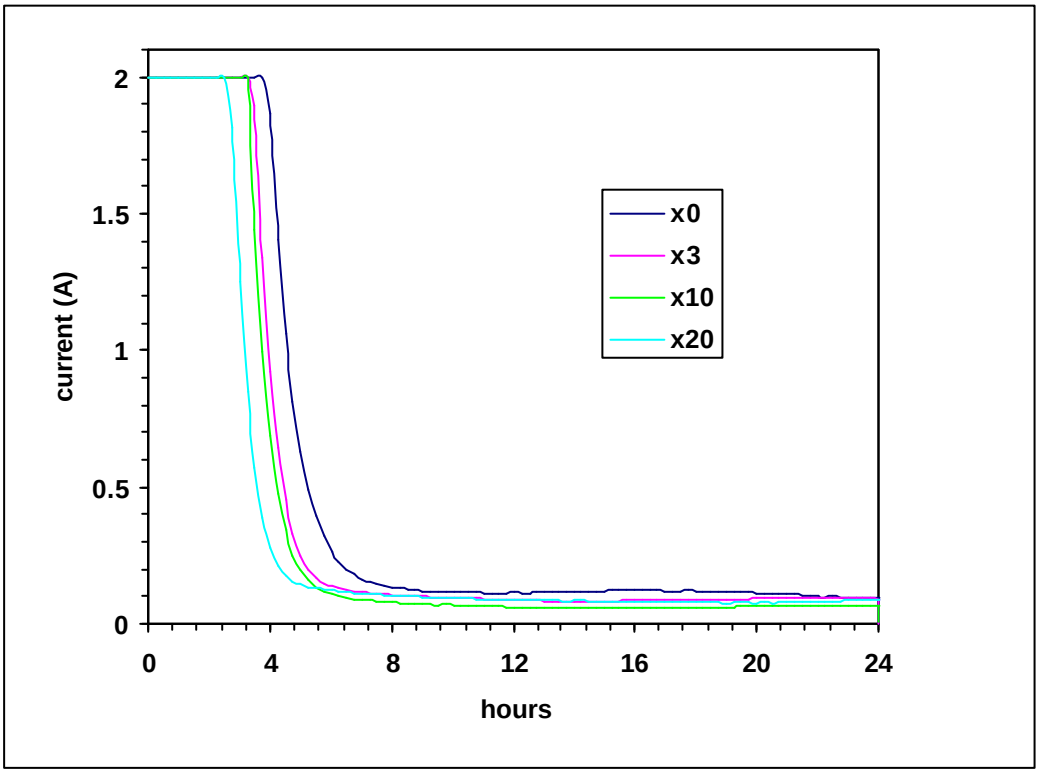

x0 : Not passed through the hammer mill
x20 : Passed through the hammer mill 20 times

The results showed that the cells reached the 2.67 V charge level in the order of its capacity achieved (the lower capacity cells reached 2.67 V first). The current then rapidly decreased to the float current level and, towards the end of the recharge process, the currents in all the cells was similar. This showed that the hammer milling process on the oxide had no effect on the recharge current at the end of the recharge process and would not affect the water loss characteristics of the cells.

Chapter 7
Conclusions

1. The effect of passing Barton pot oxide repeatedly through a hammer mill reduced the mean particle size from 5 to 3µm. The effect was more pronounced during the first few passes through the hammer mill. With repeated passes the effectiveness of the particle size reduction diminished and there was very little difference between 10 and 20 passes through the hammer mill. The optimum number of passes through the hammer mill was found to be 6-8 times after which continued grinding produced negligible improvements.

   A similar trend was seen when the ball mill oxide was repeatedly passed through the hammer mill. Since the starting material of the ball mill oxide had a larger particle size distribution, the initial improvements were better with the tendency to approach a limit after about 8 passes through the hammer mill.

2. Repeatedly passing the Barton pot oxide through the hammer mill resulted in an increase in the BET surface area of the oxide. The trend was similar to the particle size distribution where there was an initial increase which levelled out after about 8 passes through the hammer mill. A similar effect was observed with the acid absorption number which relates to the surface area.

   A similar trend was not seen when the Ball mill oxide was repeatedly passed through the hammer mill. The Ball mill oxide had a larger surface area of 2.3 m^2/g, which did not change appreciably during the hammer milling process. This was attributed to the fact that the Ball mill particles had a flatter shape and when the hammer milling process split up the particles, the surface area did not change appreciably. The breaking of the particles resulted in a change in the

particle shape, which can be related to the shape factor. The shape factor is a comparison between the results of the surface area obtained by two different techniques.

3. The hammer milling process did not appreciably change the free lead percentage in either the Barton pot or the Ball mill samples. This is an important parameter in the lead acid battery process as a loss of free lead in the oxide would result in processing problems during the electrode preparation.

4. When the Barton pot and Ball mill oxides were compared using optical and scanning electron microscopy it was found that the Barton pot oxide particles were more rounded in shape whereas the Ball mill oxide particles had a flatter and more irregular shape. The free lead particles were more rounded in the Barton pot oxide and were needle like in shape in the Ball mill oxide. During the hammer milling process, the Barton pot particles were reduced in size, but maintained their almost rounded shape. However, the Ball mill particles were reduced in size and the irregular shapes became more rounded.

5. The hammer milling of Barton pot oxide showed improvements in the electrical performance of the positive electrode at both low (capacity tests) and high (HRD tests) current rates to a certain limit. At low rates improvements were observed with 3 passes through the hammer mill whereas at high current rates the improvement was observed up to 10 passes through the hammer mill. Thereafter the electrical performance would tend to decrease. Repetitive grinding of the oxide also resulted in a faster decay of the energy density during the capacity cycling.

6. Since the greatest effect in the first few passes through the hammer mill was the removal of the very course particles >15 μm, it would

seem that the removal of the course particles results in the improvement in electrical performance. Further refining of the oxide through additional grinding did not result in further improvements in the electrical performance of the positive electrode. The requirement for a fine particle lead oxide for battery manufacturing should not only be limited in terms of an upper limit, but as the study showed, also be limited to a lower limit in size. Barton pot oxide with a mean particle size of 4-5 µm and with a negligible number of particles above 15 µm seems to be preferred.

7. It has been shown that the hammer milling of Barton pot oxide has an important role to play in producing a lead oxide capable of producing electrodes with better electrical performance. It may also provide battery companies with an opportunity to increase lead oxide production rates by making a courser oxide and then removing to course particles using a hammer mill without having to invest in an additional costly lead oxide production plant.

   Since most battery companies have more than one oxide mill that may produce a variation in oxide quality, the hammer milling process may be useful to stabilise the particle size distribution of the oxide from the various sources in order to produce electrodes that can deliver a more consistent electrical performance.

   It has been shown that the hammer milling of Barton pot lead oxide can improve the electrode performance, especially the high rate performance. It is recommended to the manufacturer to scale up the process where a larger hammer mill capable of processing 1000 kg of oxide would be used. The oxide can then be processed through the system in the normal way and complete batteries can be assembled for evaluation.
   It is recommended that the hammer mill be positioned between the oxide storage silos and the paste mixing process. This would allow

for only stabilised or aged oxide and not hot, freshly made oxide to be passed through the hammer milling process.

While it may not be feasible to have multiple passes through the hammer mill at an industrial level, the design of the hammer mill should be such that the oxide flow rate and grinding speed can be adjusted to provide a similar oxide in a single pass to the ones obtained with multiple passes in the laboratory hammer mill.

References

1 D. A. Rand, Background aspects of leady oxide production, *J. Power Sources*, **28**, (1989), 107-111

2 T. L. Blair, Lead oxide technology – Past, present, and future, *J. Power Sources*, **73**, (1998), 47-55

3 G. L. Corino, R. J. Hill, A. M. Jessel, D. A. Rand, J. A. Wunderlich, A study of the phase composition, crystallinity, morphology, porosity and surface area of leady oxides used in lead/acid battery plates, *J. Power Sources*, **16**, (1985), 141-168

4 G. W. Vinal, *Storage Batteries*, 4th edition, J. Wiley and sons, 1955

5 J.A Orsino, Lead oxide as used in lead/acid storage batteries, part 1, *Battery Man*, May 1986, 15-20

6 J.A Orsino, Lead oxide as used in lead/acid storage batteries, part 2*, Battery Man*, June 1986, 24-26

7 Mike Weighhall and Bob Nelson, A guide to VRLA battery formation techniques, Digatron firing circuits, U.S.A., 2001

8 D.A. Rand, R.J. Hill, M. McDonagh, Improving the curing of positive plates for lead/acid batteries, *J. Power Sources*, **31**, (1990), 203-215

9 S. Grugeon-Dewaele, J.B. Leriche, J.M. Tarascon, A. Delahaye-Vidal, L. Torcheux, J.P. Vaurijoux, F. Henn, A. de Guibert, Soaking and formation of tetra-basic lead sulphate, *J. Power Sources*, **64** (1997) , 71-80

10 D. Linden, *Handbook of batteries*, 2nd edition, McGraw-Hill, Inc, 1995

11 H.A. Keihne, *Batteries,* Expert verlag, 1989

12 H. Bode, *Lead Acid Batteries*, J. Wiley & sons Inc, 1977

13 ESB incorporated – International group production process specifications, Willard Batteries archives

14 Daramic separator specifications, BS-P-3000-1, BS-P-3500-2, 1998

15 Willard Batteries Materials specifications, WMS001,rev 1 1996, Willard Batteries Materials specifications, WMS008, rev 2, 1996

16 Willard Batteries, Endurance testing of Calcium batteries, project No 158, 1997- 2000

17 M Barak, *Electrochemical Power sources*, The institute of Electrical Engineers, London and New York, 1980

18 Ford battery specification, ES-F4SF-10655-AA, 1999, Volkswagen battery specification, VWTL75073, 1998

19 T. Blair, Crystals hold the key for perfect pastes, *Batteries International*, Jan 1997, 37-42

20 L.T. Lam, O.V Lim, N.P. Haigh, D.J. Rand, J.E. Manders, D.M. Rice, Oxide for valve regulated lead-acid batteries, *J. Power Sources*, **73**, (1998), 36-46

21 L. Prout, Aspects of lead/acid battery technology 3, *J. Power Sources*, **41**, (1993), 185-193

22 N. E. Hehner, E. J. Ritchie, *Lead Oxides*, IBMA Inc, 1974

23 L.T. Lam, I.G. Mawston, D. Pavlov, D.A.J. Rand, Aspects of lead/acid battery manufacture and performance, *J. Power Sources*, **48** (1994) 257-268

24 K. H. Brockmann, Modern technology for leady oxide production, *J. Power Sources*, **28**, (1989), 121-125

25 D. Hardy, R. Marx, New developments in battery oxide production, *J. Power Sources*, **38**, (1992), 75-85

26 D. P. Boden, Improved oxides for production of lead/acid battery plates, *J. Power Sources*, **73**, (1998), 56-59

27 Malvern Instruments Ltd, MAN 0101, Issue 1.3, August 1997

28 B. Zeelie, Experimental design and analysis for scientists and engineers, P E Technikon, 2003

Appendix I

Hammer Mill Specifications

Appendix II

Test methods

Free lead %

Acid absorption number

C20 capacity and cranking test

Apparent density apparatus

Fischer particle size apparatus

WILLARD CHEMICAL METHODS

Subject : **Test for free lead content of oxide**

WCM: **1.20**

Issue date: **January 2000**

Method

Gravimetric

Apparatus

100 ml acetic acid

Reagent

% % acetic acid – add 100 ml acetic acid to 1800 ml of deionised water and mix.

Procedure

Weigh out accurately 2.5 g of oxide into a 100 ml beaker.

Add 60 ml of 5 % acetic acid and heat to boil

When solution is clear, remove from the hot plate.

Pour off the solution and wash the residual lead three times with tap water.

Place in a drying oven for one hour at 105 – 120 ^{o}C.

Remove from the oven and allow to cool to room temperature.

Determine the mass of the residual lead.

Calculation

$$\% \text{ free lead} = \frac{\text{Mass of residual lead}}{\text{Mass of oxide sample}} * 100$$

WILLARD CHEMICAL METHODS

Subject : **Determination of acid absorption in lead oxide**
WCM: **1.21**
Issue date: **September 1999**

Specification (General)

150 -200 mg sulphuric acid reacted per gram of grey oxide

Reagents

Sulphuric acid S.G. 1.095 – 1.105
Sodium hydroxide 1N
Phenolphthalein indicator (1% solution in ethanol or for 100 ml 1.0 g phenolphthalein in 50 ml alcohol, dissolve, add 50 ml water, then mix)

Apparatus

Flask shaker
100 ml and 25 ml pipettes
500 ml round bottom flasks with stoppers
250 ml beakers
Filter funnels and stands
Filter paper 542

Method

Preheat about 120 ml of sulphuric acid S.G. 1.100 for each sample to be determined to 34 ^{o}C. The grey oxide sample size should always be adjusted to consist of 35.0 g lead oxide (PbO). Thus the free lead of the grey oxide must be determined first.
Grey oxide sample size = (35/(100 - % free lead)) x 100
Accurately weigh out the sample onto a piece of paper
Pipette 100 ml of the pre-heated sulphuric acid into a dry 500 ml round bottom flask
Add the grey oxide while swirling the flask

Stopper the flask and clamp on the shaker
Adjust flask shaker to 20 rpm. Set the timer for 10 minutes and switch the shaker on. After 10 minutes remove the flask from the shaker and allow to stand for 5 minutes.
Filter the acid into a 250 ml beaker through filter paper 542. Allow the filtrate to cool.
Pipette 25 ml of the filtrate into a 250 ml Erlenmeyer flask.
Add about 50 ml de-ionised water and a few drops of phenolphthalein indicator solution and then titrate with 1N sodium hydroxide solution.
Record the result

For the blank determination pipette 25 ml of the sulphuric acid S.G. 1.100 used into a 250 ml Erlenmeyer flask and titrate with 1N sodium hydroxide solution using phenolphthalein indicator solution as indicator.
Record the result

Colour change with titration is from colourless to pink.

Calculation

$$\text{Acid absorption} = \frac{(\text{blank reading} - \text{sample reading}) \times 4 \times 49.03)}{\text{Sample mass}}$$

Acid absorption units = mg sulphuric acid per gram of grey oxide

IEC 95-1 test method for lead acid batteries

Capacity check C_e

Throughout the duration of the tests, the battery shall be placed in a water-bath at a temperature of 25 ± 2°C. The upper surface of the battery shall be at least 15 mm but no more than 25 mm above the level of the water. If several batteries are in the same water-bath then the distance between them and also the distance to the walls of the bath shall be at least 25 mm.

The battery shall be discharged with a current I_h (rated capacity/20) kept constant at ± 2% of the nominal value until the terminal voltage falls to 10.5 ± 0.05 V. The duration t (h) of this discharge shall be recorded. The beginning of the discharge shall take place from 1 h to 5 h from the time of the end of charging.

The capacity C_e is: $C_e = t \cdot I_n$ (Ah)

Cranking performance test

After a rest period of 1 h to 5 h after preparation according to Clause 4.2 the battery shall be placed in a cooling chamber with (forced) air circulation at a temperature of -18 ± 1$_o$C for a minimum of 20 h or until the temperature of one of the middle cells has reached -18 ± 1$_o$C.

The battery shall then be discharged – either within or outside the cooling chamber within 2 min after the end of the cooling period with a current I (rated current). This current shall be kept constant to within ± 0.5% during the discharge.
After 60 s discharge, the terminal voltage shall be recorded. It shall be no less than 8.4 V.

Figure 38: Apparatus used to determine the apparent density of lead oxide

Figure 39: Apparatus used to determine the Fischer particle size of lead oxide

Appendix III

Additional experimental results – Lead oxide

Particle size analysis

BET surface area

Figure 40: Barton pot oxide particle size distribution (exp 2)

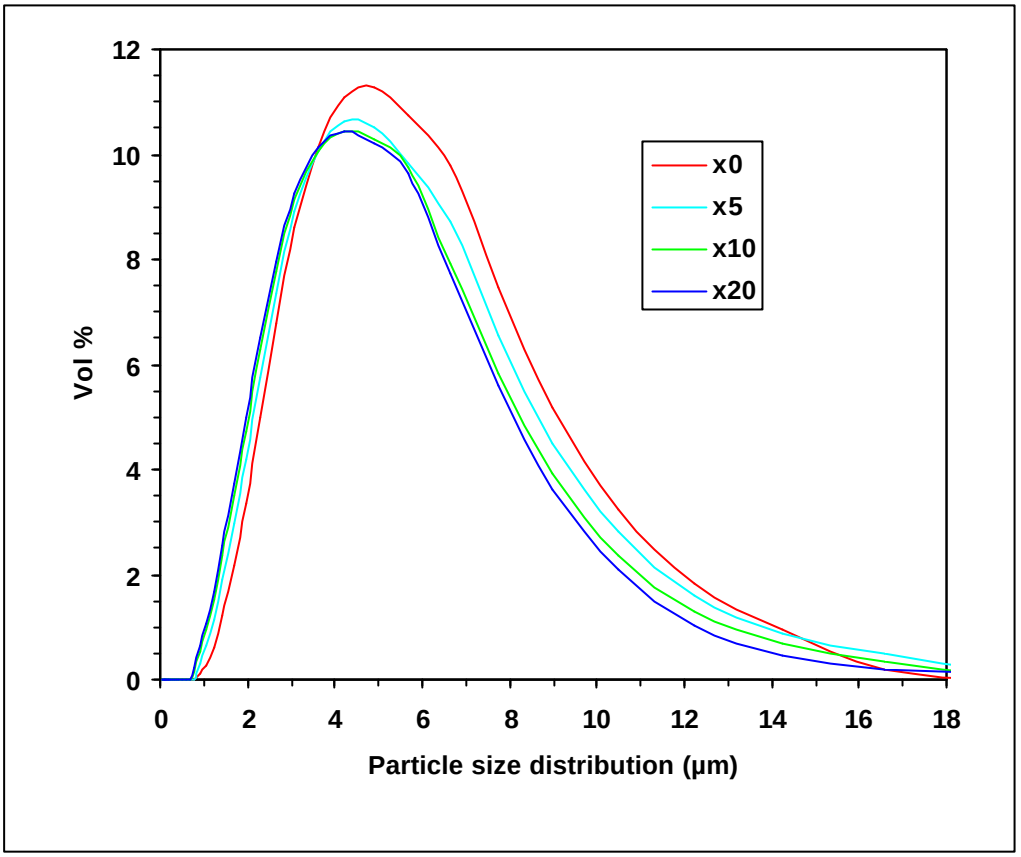

Figure 41: Cum% - Barton pot oxide (exp 2)

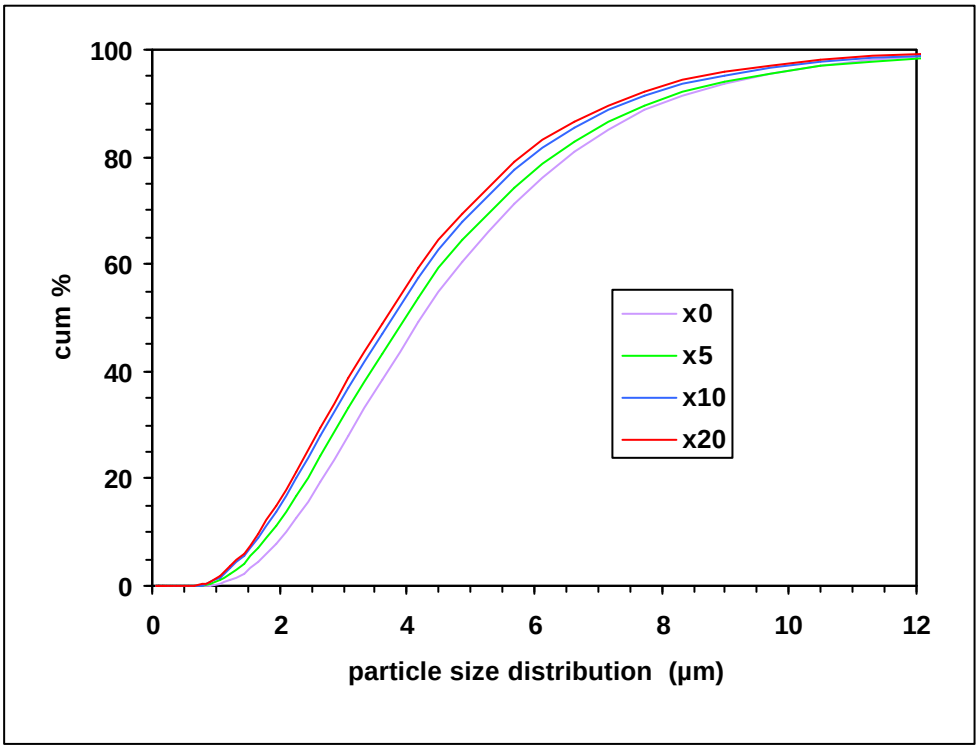

Figure 42: Barton pot particle size distribution (exp 3)

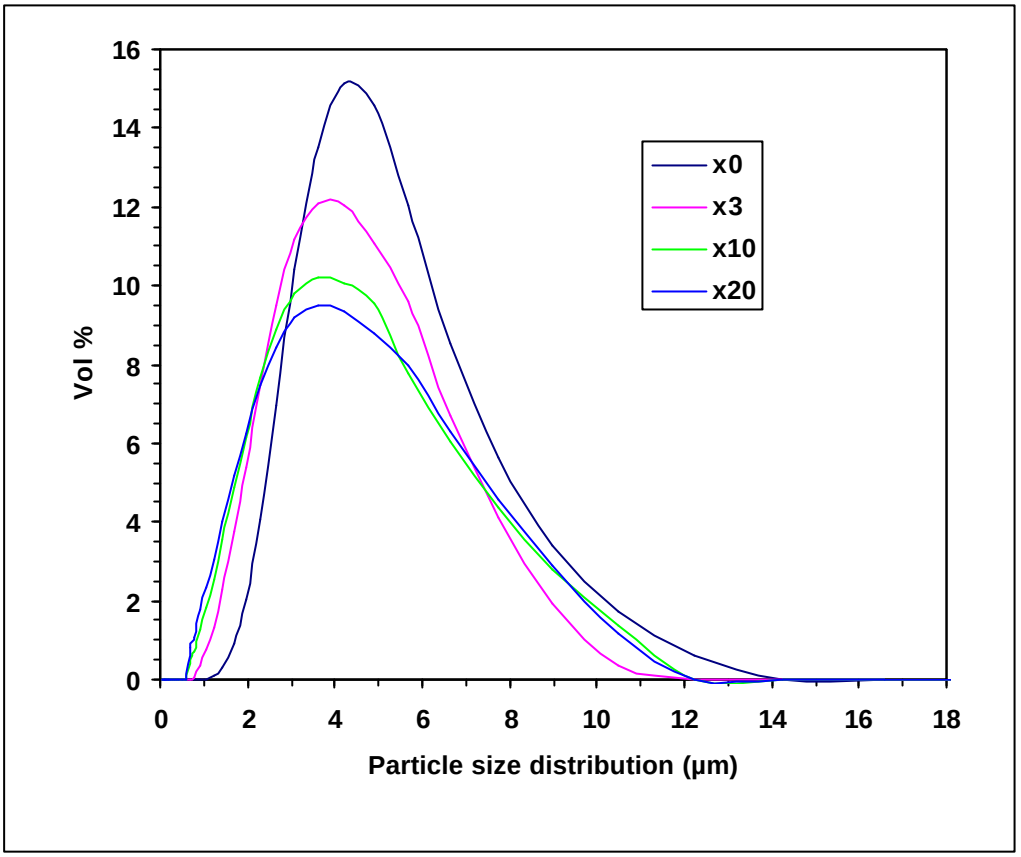

Figure 43: Cum % - Barton pot oxide (exp 3)

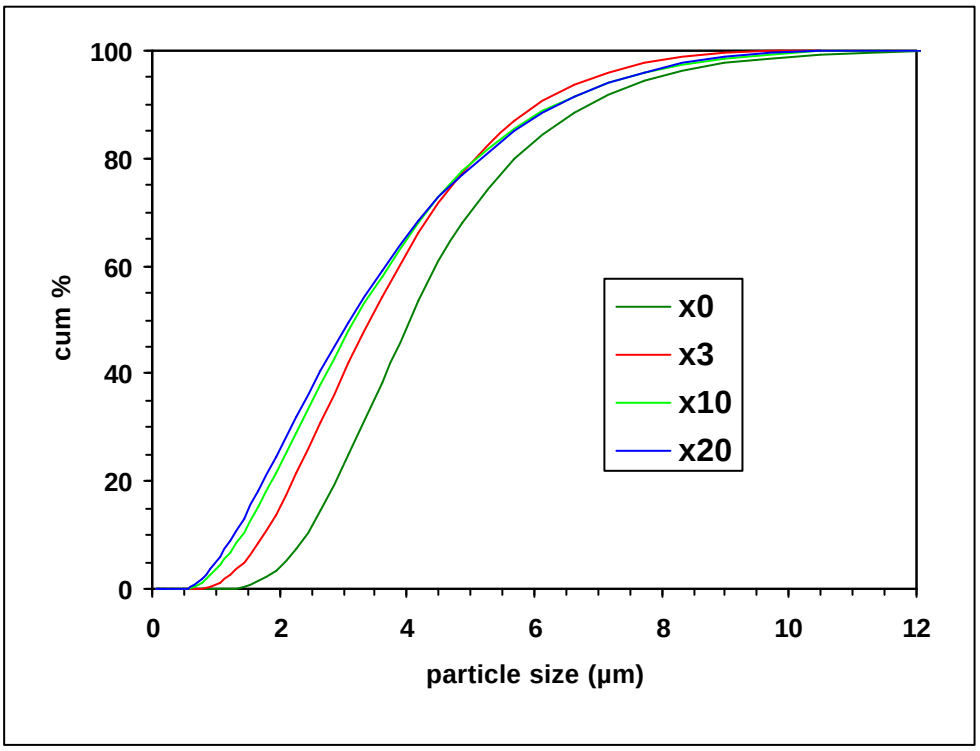

Table 9: Barton pot particle size distribution before hammer milling

Result: Histogram Table

ID: mtr4 x0	Run No: 97	Measured: 11/18/02 10:52AM
File: LAURANCE	Rec. No: 598	Analysed: 11/26/03 3:02PM
Path: C:\SIZERS\DATA\		Source: Analysed

Range: 300RF mm Beam: 2.40 mm Sampler: MS17		Obs': 34.6 %
Presentation: 3THD	Analysis: Polydisperse	Residual: 2.945 %
Modifications: None		

Conc. = 0.0166 %Vol	Density = 9.980 g/cm^3	S.S.A.= 0.1853 m^2/g
Distribution: Volume	D[4, 3] = 4.47 um	D[3, 2] = 3.24 um
D(v, 0.1) = 1.77 um	D(v, 0.5) = 3.93 um	D(v, 0.9) = 7.99 um
Span = 1.584E+00	Uniformity = 4.878E-01	

Size (um)	Volume Under %	Size (um)	Volume Under %	Size (um)	Volume Under %	Size (um)	Volume Under %
0.055	0.00	0.635	0.00	7.31	86.44	84.15	100.00
0.061	0.00	0.700	0.01	8.06	90.30	92.79	100.00
0.067	0.00	0.772	0.04	8.89	93.48	102.3	100.00
0.074	0.00	0.851	0.22	9.80	95.98	112.8	100.00
0.082	0.00	0.938	0.63	10.81	97.85	124.4	100.00
0.090	0.00	1.03	1.19	11.91	99.11	137.2	100.00
0.099	0.00	1.14	1.98	13.14	99.81	151.3	100.00
0.109	0.00	1.26	3.06	14.49	100.00	166.8	100.00
0.121	0.00	1.39	4.47	15.97	100.00	183.9	100.00
0.133	0.00	1.53	6.33	17.62	100.00	202.8	100.00
0.147	0.00	1.69	8.66	19.42	100.00	223.6	100.00
0.162	0.00	1.86	11.44	21.42	100.00	246.6	100.00
0.178	0.00	2.05	14.79	23.62	100.00	271.9	100.00
0.196	0.00	2.26	18.74	26.04	100.00	299.8	100.00
0.217	0.00	2.49	23.24	28.72	100.00	330.6	100.00
0.239	0.00	2.75	28.28	31.66	100.00	364.6	100.00
0.263	0.00	3.03	33.80	34.92	100.00	402.0	100.00
0.290	0.00	3.34	39.72	38.50	100.00	443.3	100.00
0.320	0.00	3.69	45.91	42.45	100.00	488.8	100.00
0.353	0.00	4.07	52.25	46.81	100.00	539.0	100.00
0.389	0.00	4.48	58.59	51.62	100.00	594.3	100.00
0.429	0.00	4.94	64.81	56.92	100.00	655.4	100.00
0.473	0.00	5.45	70.80	62.76	100.00	722.7	100.00
0.522	0.00	6.01	76.54	69.21	100.00	796.9	100.00
0.576	0.00	6.63	81.85	76.32	100.00	878.7	100.00

Table 10: Barton pot particle size distribution after 5 passes through the hammer mill

Result: Histogram Table

ID: mtr4 x5	Run No: 175	Measured: 11/19/02 10:00AM
File: LAURANCE	Rec. No: 716	Analysed: 11/26/03 3:13PM
Path: C:\SIZERS\DATA\		Source: Analysed

Range: 300RF mm	Beam: 2.40 mm	Sampler: MS17 Obs': 23.7 %
Presentation: 3THD	Analysis: Polydisperse	Residual: 3.417 %
Modifications: None		

Conc. = 0.0096 %Vol	Density = 9.980 g/cm^3	S.S.A.= 0.2031 m^2/g
Distribution: Volume	D[4, 3] = 4.20 um	D[3, 2] = 2.96 um
D(v, 0.1) = 1.59 um	D(v, 0.5) = 3.71 um	D(v, 0.9) = 7.54 um
Span = 1.606E+00	Uniformity = 4.969E-01	

Size (um)	Volume Under %	Size (um)	Volume Under %	Size (um)	Volume Under %	Size (um)	Volume Under %
0.055	0.00	0.635	0.14	7.31	88.77	84.15	100.00
0.061	0.00	0.700	0.38	8.06	92.32	92.79	100.00
0.067	0.00	0.772	0.68	8.89	95.15	102.3	100.00
0.074	0.00	0.851	1.17	9.80	97.28	112.8	100.00
0.082	0.00	0.938	1.85	10.81	98.82	124.4	100.00
0.090	0.00	1.03	2.71	11.91	99.73	137.2	100.00
0.099	0.00	1.14	3.81	13.14	99.94	151.3	100.00
0.109	0.00	1.26	5.19	14.49	100.00	166.8	100.00
0.121	0.00	1.39	6.91	15.97	100.00	183.9	100.00
0.133	0.00	1.53	9.05	17.62	100.00	202.8	100.00
0.147	0.00	1.69	11.65	19.42	100.00	223.6	100.00
0.162	0.00	1.86	14.68	21.42	100.00	246.6	100.00
0.178	0.00	2.05	18.23	23.62	100.00	271.9	100.00
0.196	0.00	2.26	22.34	26.04	100.00	299.8	100.00
0.217	0.00	2.49	26.96	28.72	100.00	330.6	100.00
0.239	0.00	2.75	32.07	31.66	100.00	364.6	100.00
0.263	0.00	3.03	37.62	34.92	100.00	402.0	100.00
0.290	0.00	3.34	43.51	38.50	100.00	443.3	100.00
0.320	0.00	3.69	49.64	42.45	100.00	488.8	100.00
0.353	0.00	4.07	55.87	46.81	100.00	539.0	100.00
0.389	0.00	4.48	62.09	51.62	100.00	594.3	100.00
0.429	0.00	4.94	68.14	56.92	100.00	655.4	100.00
0.473	0.00	5.45	73.93	62.76	100.00	722.7	100.00
0.522	0.00	6.01	79.44	69.21	100.00	796.9	100.00
0.576	0.00	6.63	84.49	76.32	100.00	878.7	100.00

Table 11: Barton pot particle size distribution after 10 passes through the hammer mill

Result: Histogram Table

ID: mtr4 x10	Run No: 157	Measured: 11/18/02 1:18PM
File: LAURANCE	Rec. No: 694	Analysed: 11/26/03 3:10PM
Path: C:\SIZERS\DATA\		Source: Analysed

Range: 300RF mm	Beam: 2.40 mm	Sampler: MS17 Obs': 27.8 %
Presentation: 3THD	Analysis: Polydisperse	Residual: 3.495 %
Modifications: None		

Conc. = 0.0099 %Vol	Density = 9.980 g/cm^3	S.S.A.= 0.2338 m^2/g
Distribution: Volume	D[4, 3] = 3.72 um	D[3, 2] = 2.57 um
D(v, 0.1) = 1.37 um	D(v, 0.5) = 3.25 um	D(v, 0.9) = 6.79 um
Span = 1.668E+00	Uniformity = 5.144E-01	

Size (um)	Volume Under %	Size (um)	Volume Under %	Size (um)	Volume Under %	Size (um)	Volume Under %
0.055	0.00	0.635	0.70	7.31	92.46	84.15	100.00
0.061	0.00	0.700	1.04	8.06	95.16	92.79	100.00
0.067	0.00	0.772	1.56	8.89	97.23	102.3	100.00
0.074	0.00	0.851	2.33	9.80	98.69	112.8	100.00
0.082	0.00	0.938	3.35	10.81	99.59	124.4	100.00
0.090	0.00	1.03	4.61	11.91	99.98	137.2	100.00
0.099	0.00	1.14	6.17	13.14	100.00	151.3	100.00
0.109	0.00	1.26	8.07	14.49	100.00	166.8	100.00
0.121	0.00	1.39	10.37	15.97	100.00	183.9	100.00
0.133	0.00	1.53	13.16	17.62	100.00	202.8	100.00
0.147	0.00	1.69	16.43	19.42	100.00	223.6	100.00
0.162	0.00	1.86	20.15	21.42	100.00	246.6	100.00
0.178	0.00	2.05	24.38	23.62	100.00	271.9	100.00
0.196	0.00	2.26	29.12	26.04	100.00	299.8	100.00
0.217	0.00	2.49	34.30	28.72	100.00	330.6	100.00
0.239	0.00	2.75	39.85	31.66	100.00	364.6	100.00
0.263	0.00	3.03	45.70	34.92	100.00	402.0	100.00
0.290	0.00	3.34	51.73	38.50	100.00	443.3	100.00
0.320	0.00	3.69	57.82	42.45	100.00	488.8	100.00
0.353	0.00	4.07	63.86	46.81	100.00	539.0	100.00
0.389	0.00	4.48	69.70	51.62	100.00	594.3	100.00
0.429	0.00	4.94	75.23	56.92	100.00	655.4	100.00
0.473	0.00	5.45	80.34	62.76	100.00	722.7	100.00
0.522	0.08	6.01	85.00	69.21	100.00	796.9	100.00
0.576	0.41	6.63	89.09	76.32	100.00	878.7	100.00

Table 12: Barton pot particle size distribution after 20 passes through the hammer mill

Result: Histogram Table

ID: mtr4 x20	Run No: 94	Measured: 11/18/02 10:41AM
File: LAURANCE	Rec. No: 592	Analysed: 11/26/03 3:01PM
Path: C:\SIZERS\DATA\		Source: Analysed

Range: 300RF mm Beam: 2.40 mm Sampler: MS17		Obs': 39.9 %
Presentation: 3THD	Analysis: Polydisperse	Residual: 3.133 %
Modifications: None		

Conc. = 0.0129 %Vol	Density = 9.980 g/cm^3	S.S.A.= 0.2748 m^2/g
Distribution: Volume	D[4, 3] = 3.46 um	D[3, 2] = 2.19 um
D(v, 0.1) = 1.07 um	D(v, 0.5) = 2.91 um	D(v, 0.9) = 6.70 um
Span = 1.931E+00	Uniformity = 5.927E-01	

Size (um)	Volume Under %	Size (um)	Volume Under %	Size (um)	Volume Under %	Size (um)	Volume Under %
0.055	0.00	0.635	1.99	7.31	92.66	84.15	100.00
0.061	0.00	0.700	2.87	8.06	95.16	92.79	100.00
0.067	0.00	0.772	4.05	8.89	97.14	102.3	100.00
0.074	0.00	0.851	5.51	9.80	98.60	112.8	100.00
0.082	0.00	0.938	7.23	10.81	99.55	124.4	100.00
0.090	0.00	1.03	9.18	11.91	99.98	137.2	100.00
0.099	0.00	1.14	11.43	13.14	100.00	151.3	100.00
0.109	0.00	1.26	13.99	14.49	100.00	166.8	100.00
0.121	0.00	1.39	16.90	15.97	100.00	183.9	100.00
0.133	0.00	1.53	20.21	17.62	100.00	202.8	100.00
0.147	0.00	1.69	23.89	19.42	100.00	223.6	100.00
0.162	0.00	1.86	27.89	21.42	100.00	246.6	100.00
0.178	0.00	2.05	32.23	23.62	100.00	271.9	100.00
0.196	0.00	2.26	36.90	26.04	100.00	299.8	100.00
0.217	0.00	2.49	41.82	28.72	100.00	330.6	100.00
0.239	0.00	2.75	46.93	31.66	100.00	364.6	100.00
0.263	0.00	3.03	52.18	34.92	100.00	402.0	100.00
0.290	0.00	3.34	57.47	38.50	100.00	443.3	100.00
0.320	0.00	3.69	62.73	42.45	100.00	488.8	100.00
0.353	0.00	4.07	67.88	46.81	100.00	539.0	100.00
0.389	0.00	4.48	72.84	51.62	100.00	594.3	100.00
0.429	0.00	4.94	77.58	56.92	100.00	655.4	100.00
0.473	0.00	5.45	82.07	62.76	100.00	722.7	100.00
0.522	0.25	6.01	86.13	69.21	100.00	796.9	100.00
0.576	1.17	6.63	89.66	76.32	100.00	878.7	100.00

Table 13: Ball mill particle size distribution before passing through the hammer mill

Result: Histogram Table

ID: BM 0103 X0 31-03-03	Run No: 218	Measured: 3/31/03 11:31AM
File: LAURANCE	Rec. No: 761	Analysed: 11/26/03 3:19PM
Path: C:\SIZERS\DATA\		Source: Analysed

Range: 300RF mm	Beam: 2.40 mm	Sampler: MS17 Obs': 29.7 %
Presentation: 3THD	Analysis: Polydisperse	Residual: 1.299 %
Modifications: None		

Conc. = 0.0164 %Vol	Density = 9.980 g/cm^3	S.S.A.= 0.1426 m^2/g
Distribution: Volume	D[4, 3] = 12.35 um	D[3, 2] = 4.21 um
D(v, 0.1) = 1.88 um	D(v, 0.5) = 9.60 um	D(v, 0.9) = 25.04 um
Span = 2.412E+00	Uniformity = 7.879E-01	

Size (um)	Volume Under %	Size (um)	Volume Under %	Size (um)	Volume Under %	Size (um)	Volume Under %
0.055	0.00	0.635	2.61	7.31	38.61	84.15	99.71
0.061	0.00	0.700	3.10	8.06	42.49	92.79	99.84
0.067	0.00	0.772	3.64	8.89	46.60	102.3	99.93
0.074	0.00	0.851	4.20	9.80	50.90	112.8	99.98
0.082	0.00	0.938	4.78	10.81	55.34	124.4	100.00
0.090	0.00	1.03	5.38	11.91	59.87	137.2	100.00
0.099	0.00	1.14	6.02	13.14	64.41	151.3	100.00
0.109	0.00	1.26	6.69	14.49	68.97	166.8	100.00
0.121	0.00	1.39	7.41	15.97	73.50	183.9	100.00
0.133	0.00	1.53	8.18	17.62	77.79	202.8	100.00
0.147	0.00	1.69	9.01	19.42	81.72	223.6	100.00
0.162	0.00	1.86	9.90	21.42	85.26	246.6	100.00
0.178	0.00	2.05	10.87	23.62	88.37	271.9	100.00
0.196	0.00	2.26	11.94	26.04	91.00	299.8	100.00
0.217	0.00	2.49	13.10	28.72	93.17	330.6	100.00
0.239	0.00	2.75	14.38	31.66	94.90	364.6	100.00
0.263	0.00	3.03	15.81	34.92	96.23	402.0	100.00
0.290	0.00	3.34	17.40	38.50	97.21	443.3	100.00
0.320	0.00	3.69	19.18	42.45	97.91	488.8	100.00
0.353	0.00	4.07	21.17	46.81	98.40	539.0	100.00
0.389	0.22	4.48	23.39	51.62	98.75	594.3	100.00
0.429	0.80	4.94	25.87	56.92	99.01	655.4	100.00
0.473	1.27	5.45	28.62	62.76	99.21	722.7	100.00
0.522	1.70	6.01	31.67	69.21	99.40	796.9	100.00
0.576	2.15	6.63	34.99	76.32	99.57	878.7	100.00

Table 14: Ball mill particle size distribution after 3 passes through the hammer mill

Result: Histogram Table

ID: BM 0103 X3 31-03-03	Run No: 236	Measured: 3/31/03 12:03PM
File: LAURANCE	Rec. No: 779	Analysed: 11/26/03 3:21PM
Path: C:\SIZERS\DATA\		Source: Analysed

Range: 300RF mm	Beam: 2.40 mm	Sampler: MS17 Obs': 26.0 %
Presentation: 3THD	Analysis: Polydisperse	Residual: 0.571 %
Modifications: None		

Conc. = 0.0072 %Vol	Density = 9.980 g/cm^3	S.S.A.= 0.3259 m^2/g
Distribution: Volume	D[4, 3] = 10.05 um	D[3, 2] = 1.84 um
D(v, 0.1) = 0.91 um	D(v, 0.5) = 7.43 um	D(v, 0.9) = 22.97 um
Span = 2.969E+00	Uniformity = 9.148E-01	

Size (um)	Volume Under %	Size (um)	Volume Under %	Size (um)	Volume Under %	Size (um)	Volume Under %
0.055	0.02	0.635	7.72	7.31	49.41	84.15	100.00
0.061	0.05	0.700	8.28	8.06	52.95	92.79	100.00
0.067	0.10	0.772	8.88	8.89	56.58	102.3	100.00
0.074	0.17	0.851	9.52	9.80	60.27	112.8	100.00
0.082	0.25	0.938	10.19	10.81	63.99	124.4	100.00
0.090	0.36	1.03	10.90	11.91	67.73	137.2	100.00
0.099	0.48	1.14	11.68	13.14	71.48	151.3	100.00
0.109	0.63	1.26	12.52	14.49	75.17	166.8	100.00
0.121	0.80	1.39	13.43	15.97	78.72	183.9	100.00
0.133	0.99	1.53	14.42	17.62	82.08	202.8	100.00
0.147	1.21	1.69	15.50	19.42	85.23	223.6	100.00
0.162	1.46	1.86	16.69	21.42	88.11	246.6	100.00
0.178	1.75	2.05	17.99	23.62	90.70	271.9	100.00
0.196	2.08	2.26	19.42	26.04	92.96	299.8	100.00
0.217	2.46	2.49	20.98	28.72	94.89	330.6	100.00
0.239	2.88	2.75	22.70	31.66	96.48	364.6	100.00
0.263	3.35	3.03	24.57	34.92	97.75	402.0	100.00
0.290	3.83	3.34	26.61	38.50	98.70	443.3	100.00
0.320	4.31	3.69	28.83	42.45	99.40	488.8	100.00
0.353	4.77	4.07	31.24	46.81	99.86	539.0	100.00
0.389	5.25	4.48	33.83	51.62	99.97	594.3	100.00
0.429	5.75	4.94	36.61	56.92	100.00	655.4	100.00
0.473	6.24	5.45	39.57	62.76	100.00	722.7	100.00
0.522	6.72	6.01	42.70	69.21	100.00	796.9	100.00
0.576	7.21	6.63	45.99	76.32	100.00	878.7	100.00

Table 15: Ball mill particle size distribution after 13 passes through the hammer mill

Result: Histogram Table

ID: BM 0103 X13 08-04-03 Run No: 247 Measured: 4/8/03 12:59PM
File: LAURANCE Rec. No: 812 Analysed: 11/26/03 3:23PM
Path: C:\SIZERS\DATA\ Source: Analysed

Range: 300RF mm Beam: 2.40 mm Sampler: MS17 Obs': 17.8 %
Presentation: 3THD Analysis: Polydisperse Residual: 0.650 %
Modifications: None

Conc. = 0.0055 %Vol Density = 9.980 g/cm^3 S.S.A.= 0.2860 m^2/g
Distribution: Volume D[4, 3] = 9.09 um D[3, 2] = 2.10 um
D(v, 0.1) = 1.20 um D(v, 0.5) = 6.59 um D(v, 0.9) = 20.64 um
Span = 2.950E+00 Uniformity = 9.076E-01

Size (um)	Volume Under %	Size (um)	Volume Under %	Size (um)	Volume Under %	Size (um)	Volume Under %
0.055	0.02	0.635	5.69	7.31	54.01	84.15	100.00
0.061	0.05	0.700	6.17	8.06	57.85	92.79	100.00
0.067	0.09	0.772	6.70	8.89	61.69	102.3	100.00
0.074	0.15	0.851	7.30	9.80	65.50	112.8	100.00
0.082	0.22	0.938	7.96	10.81	69.29	124.4	100.00
0.090	0.31	1.03	8.69	11.91	73.01	137.2	100.00
0.099	0.42	1.14	9.51	13.14	76.57	151.3	100.00
0.109	0.54	1.26	10.43	14.49	79.91	166.8	100.00
0.121	0.67	1.39	11.44	15.97	83.03	183.9	100.00
0.133	0.83	1.53	12.58	17.62	85.90	202.8	100.00
0.147	1.00	1.69	13.84	19.42	88.51	223.6	100.00
0.162	1.18	1.86	15.25	21.42	90.85	246.6	100.00
0.178	1.39	2.05	16.82	23.62	92.90	271.9	100.00
0.196	1.62	2.26	18.55	26.04	94.68	299.8	100.00
0.217	1.88	2.49	20.47	28.72	96.18	330.6	100.00
0.239	2.15	2.75	22.58	31.66	97.43	364.6	100.00
0.263	2.44	3.03	24.88	34.92	98.44	402.0	100.00
0.290	2.75	3.34	27.39	38.50	99.19	443.3	100.00
0.320	3.07	3.69	30.10	42.45	99.71	488.8	100.00
0.353	3.39	4.07	33.02	46.81	99.98	539.0	100.00
0.389	3.74	4.48	36.14	51.62	100.00	594.3	100.00
0.429	4.09	4.94	39.44	56.92	100.00	655.4	100.00
0.473	4.46	5.45	42.90	62.76	100.00	722.7	100.00
0.522	4.85	6.01	46.51	69.21	100.00	796.9	100.00
0.576	5.25	6.63	50.22	76.32	100.00	878.7	100.00

Table 16: Ball mill particle size distribution after 20 passes through the hammer mill

Result: Histogram Table

ID: BM 0103 X20 08-04-03	Run No: 253	Measured: 4/8/03 1:46PM
File: LAURANCE	Rec. No: 827	Analysed: 11/26/03 3:25PM
Path: C:\SIZERS\DATA\		Source: Analysed

Range: 300RF mm	Beam: 2.40 mm	Sampler: MS17 Obs': 31.2 %
Presentation: 3THD	Analysis: Polydisperse	Residual: 1.716 %
Modifications: None		

Conc. = 0.0067 %Vol	Density = 9.980 g/cm^3	S.S.A.= 0.4508 m^2/g
Distribution: Volume	D[4, 3] = 8.32 um	D[3, 2] = 1.33 um
D(v, 0.1) = 0.51 um	D(v, 0.5) = 5.70 um	D(v, 0.9) = 19.94 um
Span = 3.409E+00	Uniformity = 1.055E+00	

Size (um)	Volume Under %	Size (um)	Volume Under %	Size (um)	Volume Under %	Size (um)	Volume Under %
0.055	0.03	0.635	11.71	7.31	58.66	84.15	100.00
0.061	0.07	0.700	12.56	8.06	62.18	92.79	100.00
0.067	0.15	0.772	13.44	8.89	65.69	102.3	100.00
0.074	0.25	0.851	14.35	9.80	69.17	112.8	100.00
0.082	0.39	0.938	15.29	10.81	72.61	124.4	100.00
0.090	0.56	1.03	16.27	11.91	75.96	137.2	100.00
0.099	0.76	1.14	17.30	13.14	79.13	151.3	100.00
0.109	1.00	1.26	18.38	14.49	82.06	166.8	100.00
0.121	1.27	1.39	19.53	15.97	84.75	183.9	100.00
0.133	1.58	1.53	20.75	17.62	87.21	202.8	100.00
0.147	1.94	1.69	22.06	19.42	89.44	223.6	100.00
0.162	2.33	1.86	23.46	21.42	91.44	246.6	100.00
0.178	2.77	2.05	24.97	23.62	93.22	271.9	100.00
0.196	3.27	2.26	26.60	26.04	94.79	299.8	100.00
0.217	3.81	2.49	28.37	28.72	96.13	330.6	100.00
0.239	4.40	2.75	30.28	31.66	97.28	364.6	100.00
0.263	5.04	3.03	32.36	34.92	98.22	402.0	100.00
0.290	5.71	3.34	34.60	38.50	98.95	443.3	100.00
0.320	6.40	3.69	37.03	42.45	99.55	488.8	100.00
0.353	7.10	4.07	39.64	46.81	99.96	539.0	100.00
0.389	7.83	4.48	42.44	51.62	100.00	594.3	100.00
0.429	8.58	4.94	45.41	56.92	100.00	655.4	100.00
0.473	9.34	5.45	48.54	62.76	100.00	722.7	100.00
0.522	10.12	6.01	51.81	69.21	100.00	796.9	100.00
0.576	10.90	6.63	55.20	76.32	100.00	878.7	100.00

Figure 44: Barton pot oxide BET surface area (exp 2)

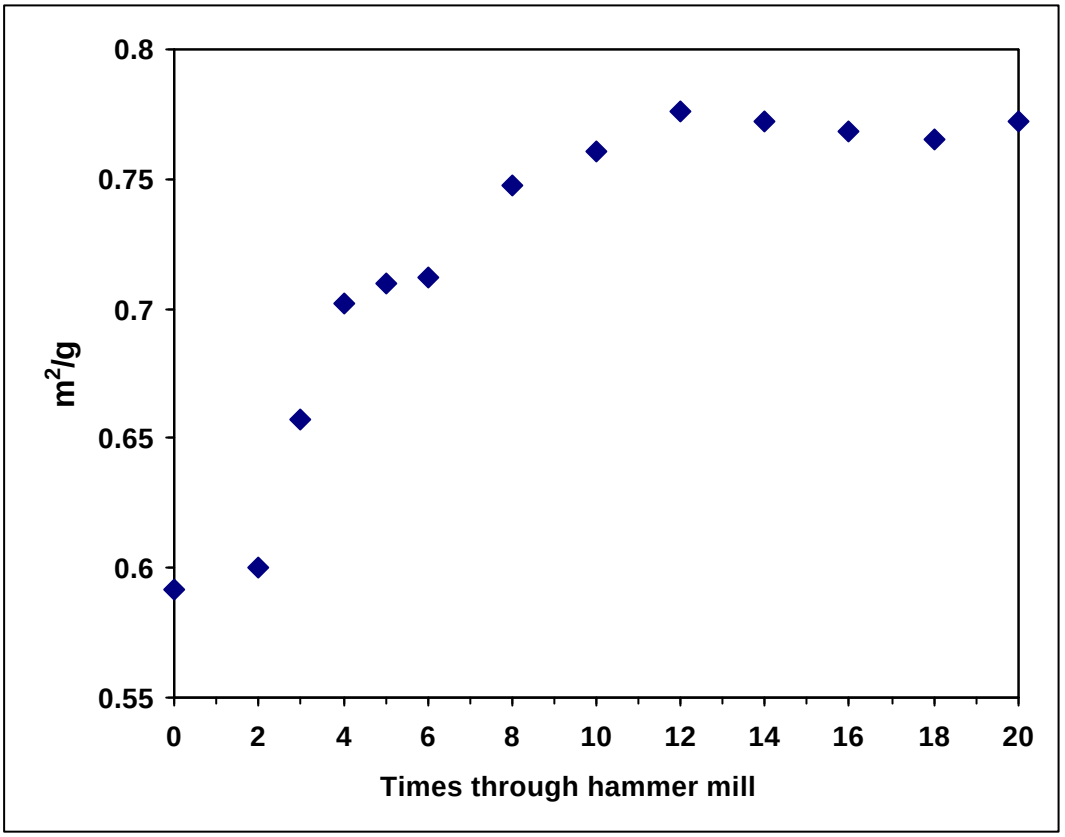

Appendix IV

Additional experimental results - electrochemical evaluation of cells

Figure 45: Initial C20 Capacity test (exp 2)

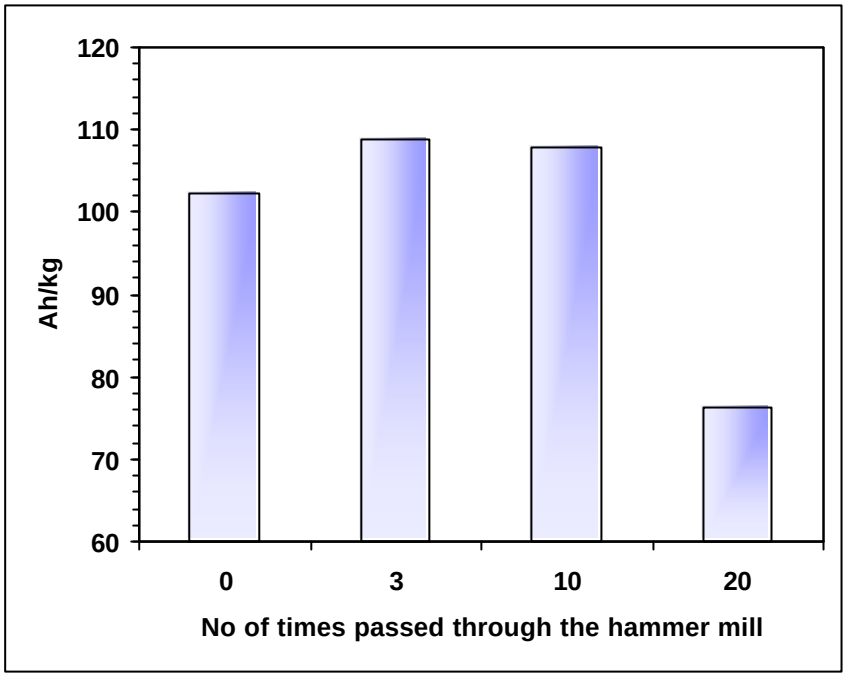

Figure 46: Capacity cycles (exp 2)

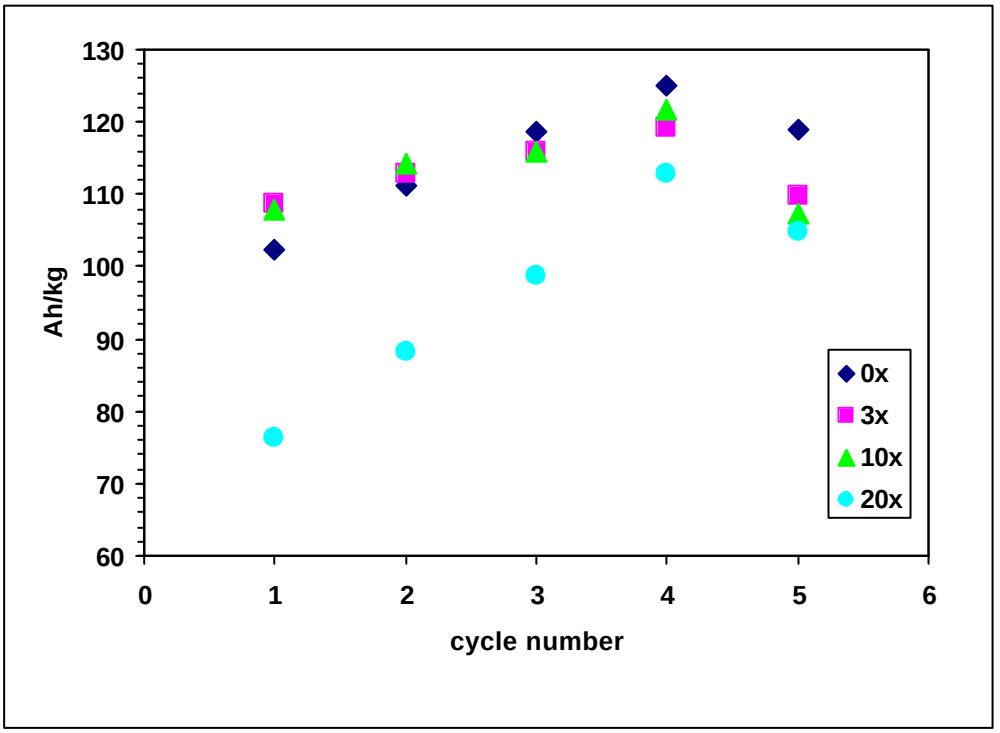

Figure 47: High current tests (exp2)

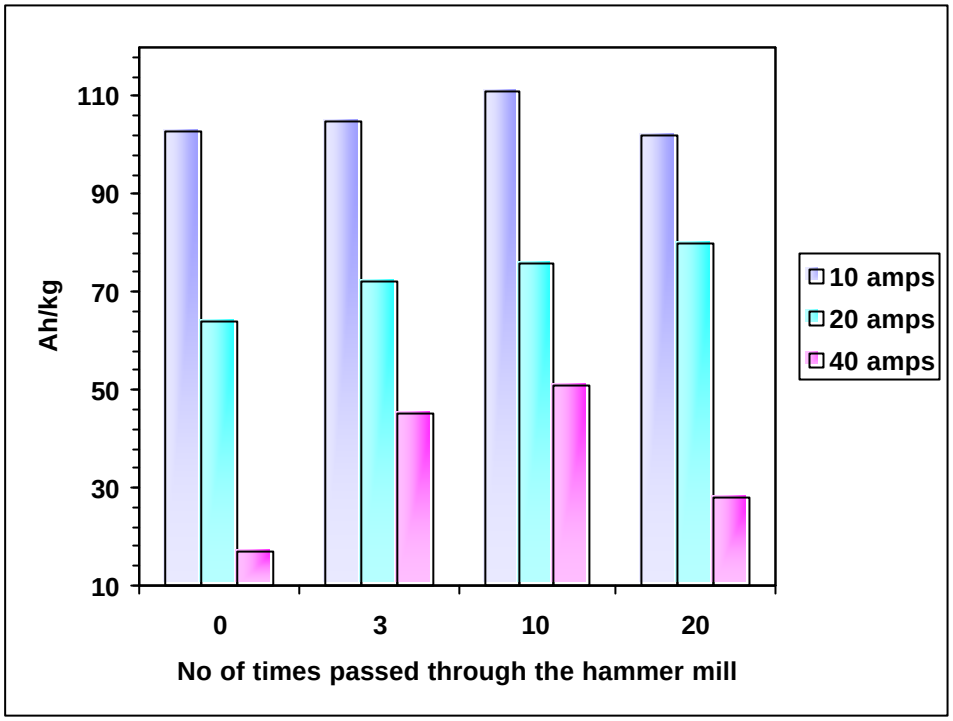

Figure 48: Initial C20 Capacity tests (exp 3)

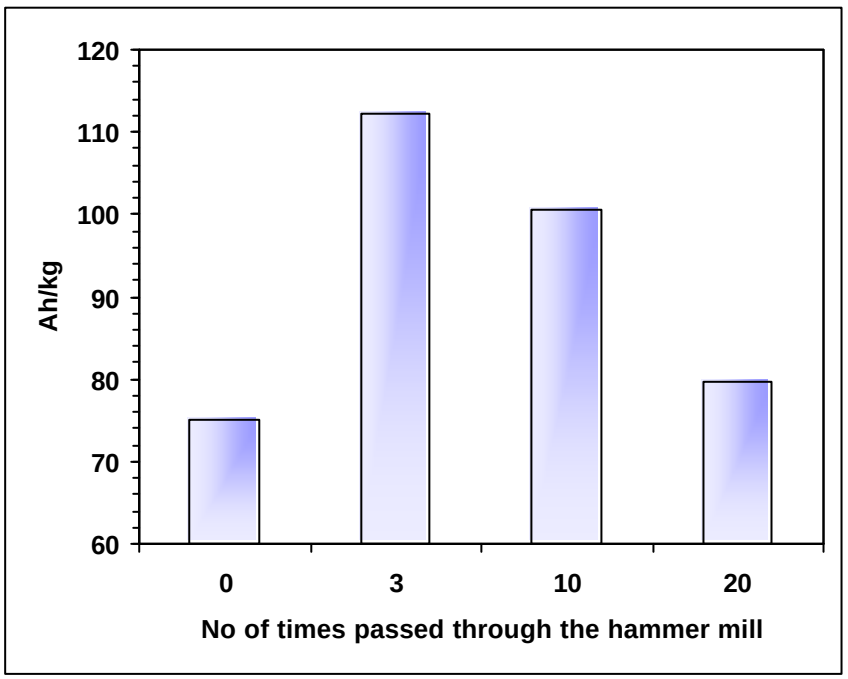

Figure 49: Capacity cycles (exp 3)

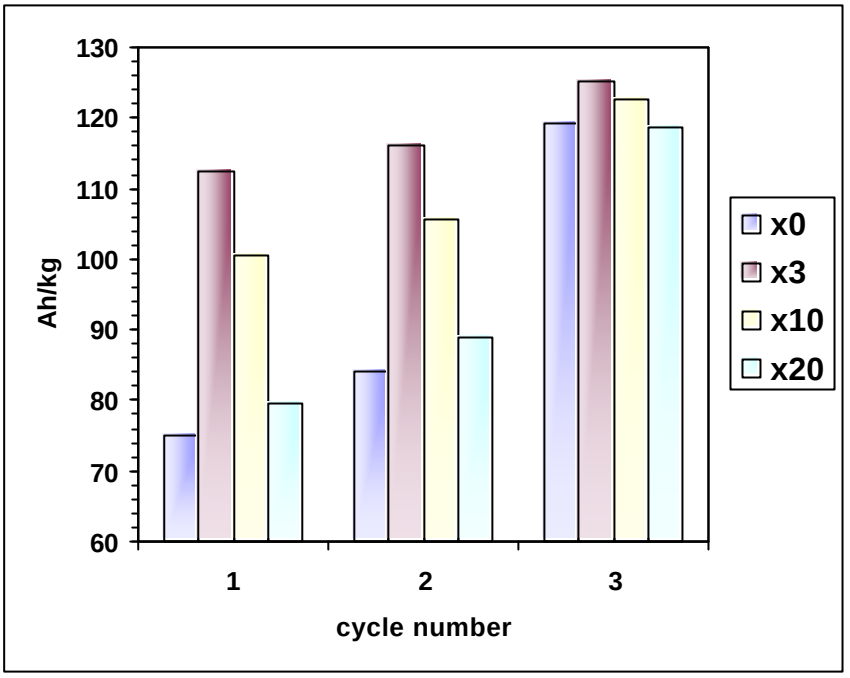

Figure 50: High current tests (exp 3)

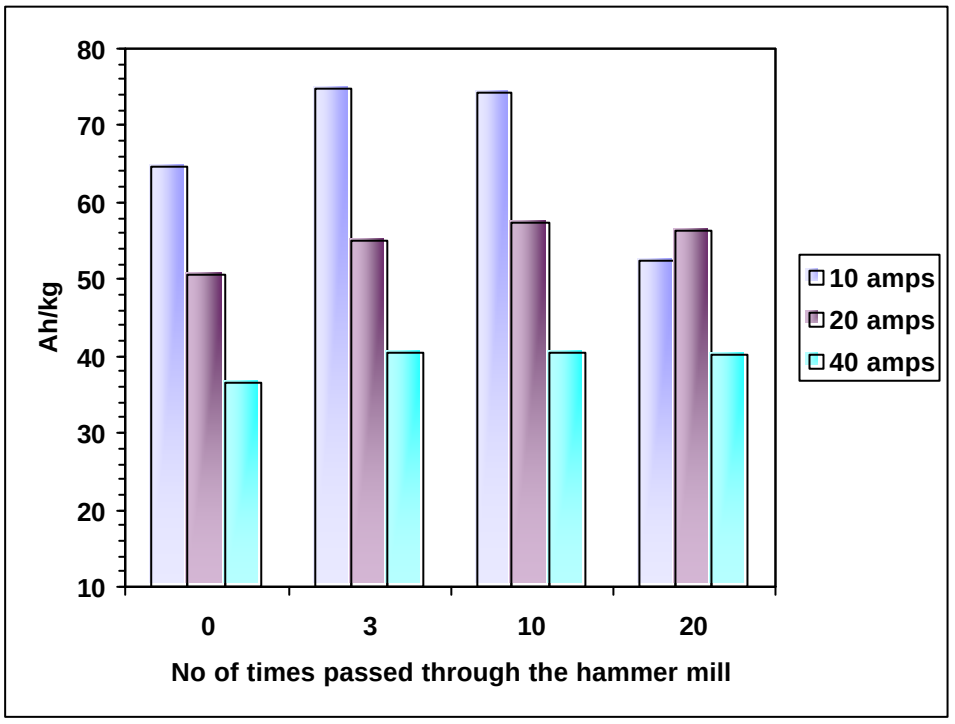

Appendix V

Statistics and experimental design

Barton pot oxide – ANOVA evaluation

The ANOVA (analysis of variance) of the various means in table 5 was performed using Microsoft Excel data analysis. The statistical formulas and definitions may be found in "Experimental design and analysis for scientists and engineers" by B Zeelie[28].

Table 17: ANOVA – Various mean diameters for Barton pot oxide

Anova: Two-Factor Without Replication

SUMMARY	*Count*	*Sum*	*Average*	*Variance*
No of times through the hammer mill				
x0	3	11.64	3.88	0.3801
x1	3	10.9	3.633333	0.387733
x2	3	10.07	3.356667	0.293733
x3	3	10.05	3.35	0.2236
x4	3	10.04	3.346667	0.340433
x5	3	10.54	3.513333	0.321633
x6	3	9.76	3.253333	0.146033
x7	3	10.33	3.443333	0.363333
x8	3	8.9	2.966667	0.322233
x10	3	9.54	3.18	0.3343
x14	3	10.34	3.446667	0.359233
x16	3	11.05	3.683333	0.848033
x20	3	9.07	3.023333	0.570233
Mass mean diameter	13	44.83	3.448462	0.067231
vol mean diameter	13	51.48	3.96	0.0995
SA mean diameter	13	35.92	2.763077	0.063823

ANOVA

Source of Variation	*SS*	*df*	*MS*	*F*	*P-value*	*F crit*
Rows (No of times hammered)	2.362923	12	0.19691	11.70566	2.8E-07	2.183377
Columns (various means)	9.377544	2	4.688772	278.732	2.44E-17	3.402832
Error	0.403723	24	0.016822			
Total	12.14419	38				

SS Sum of squares
Df Degrees of freedom
MS Mean square
F Calculated F- value
P Calculated probability value
F_{crit} $F_{critical}$ from F-tables

Since F > $F_{critical}$ for both columns and rows, it implies that the mean is changing and that the various means are different[28].

Ball mill oxide – ANOVA evaluation

The results of the Ball mill oxide (table 6) was used in a similar way to perform an ANOVA evaluation.

Table 18: ANOVA – Various mean diameters for Ball mill oxide

Anova: Two-Factor Without Replication

SUMMARY	*Count*	*Sum*	*Average*	*Variance*
No of times through the hammer mill				
x0	3	26.16	8.72	17.1457
x1	3	22.24	7.413333	17.26723
x3	3	19.32	6.44	17.5861
x5	3	19.08	6.36	16.9461
x7	3	17.18	5.726667	10.88263
x10	3	13.68	4.56	4.7812
x13	3	17.78	5.926667	12.54503
x16	3	17.44	5.813333	12.98143
x20	3	15.35	5.116667	12.47023
vol mean diameter	9	84.83	9.425556	2.752253
SA mean diameter	9	20.43	2.27	0.673575
Mass mean diameter	9	62.97	6.996667	2.0128

ANOVA

Source of Variation	*SS*	*df*	*MS*	*F*	*P-value*	*F crit*
Rows (times hammered)	36.62625	8	4.578281	10.64288	4.11E-05	2.591094
Columns (various means)	238.3286	2	119.1643	277.0147	3.85E-13	3.633716
Error	6.88277	16	0.430173			
Total	281.8376	26				

SS Sum of squares
Df Degrees of freedom
MS Mean square
F Calculated F- value
P Calculated probability value
F_{crit} $F_{critical}$ from F-tables

F > $F_{critical}$ for both columns and rows which implies that the mean is changing and that the various means are different[28].

High current discharge tests – ANOVA evaluation

The results of the high current discharge tests in figure 50 were used to perform an ANOVA evaluation. The Ah/kg results at various current rates are shown in table 19.

Table 19: ANOVA – High rate discharge tests

	Times hammered			
Discharge current (A)	**0**	**x3**	**x10**	**x20**
10 amps	70.23	73.95	79.64	66.38
20 amps	59.95	61.32	65.40	56.64
40 amps	27.57	38.03	46.03	40.96

The results of the ANOVA evaluation by considering the results of 0 to 20 passes through the hammer mil is shown in table 20.

Table 20: ANOVA – 0-20 passes through the hammer mill

Anova: Two-Factor Without Replication

SUMMARY	*Count*	*Sum*	*Average*	*Variance*
10 amps	4	290.2068	72.55171	31.86643
20 amps	4	243.3131	60.82827	13.17638
40 amps	4	152.5837	38.14591	60.60329
x0	3	157.7503	52.58345	495.6398
x3	3	173.309	57.76967	332.1263
x10	3	191.0674	63.68912	284.6313
x20	3	163.9769	54.65895	164.5625

ANOVA

Source of Variation	*SS*	*df*	*MS*	*F*	*P-value*	*F crit*
Rows (current)	2447.583	2	1223.791	69.05143	7.22E-05	5.143249
Columns (times hammered	210.6009	3	70.2003	3.960995	0.071407	4.757055
Error	106.3374	6	17.7229			
Total	2764.521	11				

The results showed that the number of times that the oxide was hammered was not a significant factor and that only the discharge current was significant since $F > F_{crit}$ only for the current.

The results of the ANOVA evaluation by considering the results of 0 to 10 passes through the hammer mil is shown in table 21.

Table 21: ANOVA – 0-10 passes through the hammer mill

Anova: Two-Factor Without Replication

SUMMARY	*Count*	*Sum*	*Average*	*Variance*
10 amps	3	223.8244	74.60812	22.42657
20 amps	3	186.6749	62.22495	8.060337
40 amps	3	111.6275	37.20917	85.63998
x0	3	157.7503	52.58345	495.6398
x3	3	173.309	57.76967	332.1263
x10	3	191.0674	63.68912	284.6313

ANOVA

Source of Variation	*SS*	*df*	*MS*	*F*	*P-value*	*F crit*
Rows (current)	2177.814	2	1088.907	92.71069	0.000446	6.944276
Columns (times hammered)	185.2729	2	92.63645	7.887164	0.040918	6.944276
Error	46.98087	4	11.74522			
Total	2410.068	8				

The results showed that both the discharge current and the number of hammering steps was significant since $F > F_{crit}$. This implied that the continued hammer milling of the oxide reduced the significance of the hammer milling process. It suggests that some hammer milling of the oxide is beneficial, but subsequent hammer milling has a reduced effect.